OFFICE OF NAVAL RESEARCH

Contract N00014-NAonr 18-76

Task No. NR 056-573

TECHNICAL REPORT NO. 5

Catalysis by Solid Surfaces

by

T. E. Madey, J. T. Yates, Jr., D. R. Sandstrom*
and R.J.H. Voorhoeve (Bell Laboratories
Murray Hill, NJ)

Reprint of Publication

from

Treatise on Solid State Chemistry
Vol. 6B, Surfaces II,
Ed. by N. B. Hannay
(Plenum, New York, 1976)

National Bureau of Standards
Surface Processes and Catalysis Section
Washington, DC 20234

October 6, 1976

*NBS Guest Worker; on leave from Washington State University, Pullman, Washington

Reprinted from: TREATISE ON SOLID STATE CHEMISTRY, Vol. 6B (1976)
Edited by N. B. Hannay
Book available from: Plenum Publishing Corporation
227 West 17th Street, New York, N.Y. 10011

Catalysis by Solid Surfaces

*T. E. Madey, J. T. Yates, Jr., and D. R. Sandstrom**
Surface Processes and Catalysis Section
National Bureau of Standards
Washington, D.C.

and

R. J. H. Voorhoeve
Bell Laboratories
Murray Hill, New Jersey

This chapter gives an overview of current concepts in catalysis of predominantly simple reactions. Catalysts covered are metals, semiconducting oxides, and sulfides. The emphasis is on the connections between solid-state chemistry/physics, spectroscopy, and surface physics in ultrahigh vacuum on the one hand and catalysis on the other hand. For physicists and materials scientists of various plumage, the chapter is expected to serve as a concise (but not oversimplified) primer.

1. Introduction

We are on the threshold of new insight into the fundamental nature of heterogeneous catalytic processes. This is partly due to recent advances in our ability to accurately and reproducibly measure phenomena at the atomic level on surfaces using modern tools.[1],†

* NBS Guest Worker; on leave from Washington State University, Pullman, Washington.
† See also the April 1975 issue of *Physics Today*, which contains several articles on modern surface measurement techniques.

In addition, however, the entry of solid-state and molecular orbital theorists into the catalytic field is just beginning to have a major effect in defining the fundamental features of catalytic processes in terms which may eventually enhance our ability to predict catalytic behavior and to design optimal catalysts on the basis of well-founded principles.

"Heterogeneous catalysis" comprises the phenomena of the enhancement of the rates of chemical conversions in fluids by the presence of solid surfaces, which are called "catalysts." It is evident that heterogeneous catalysis is essentially a problem in chemical kinetics and that theoretical efforts must come to grips with factors affecting the *rates* of reactions—not just with the states of adsorbed species that exist in stable forms under nonreactive conditions. It is the focus on reaction rates which is missing from most theoretical work at present, and it is here that major conceptual advances can now be expected to occur.

This chapter will emphasize certain aspects of experimental catalytic research which have supplied reliable data of use in formulating both general and specific concepts of major importance in heterogeneous catalysis. In addition, theoretical concepts are discussed where it seems clear that the particular concept is verified by sound experimental observations.

The field of catalysis is vast and in this short review it was necessary to pick certain topics while excluding others. We have endeavored to communicate the essence of a variety of topics relevant to the understanding of the field of heterogeneous catalysis, but the reader is referred to the original literature for detailed treatments, which are beyond the scope of this chapter. The reader is particularly directed to the excellent series of reviews appearing each year in *Advances in Catalysis* and in *Catalysis Reviews*. It is hoped that in this review the combination of ideas derived from classical experiments with ideas based on more recent work will help to form a fresh impression of the frontiers of this exciting field.

2. Historical Development of the Understanding of Catalysis

2.1. A Chronology

The development of modern concepts in heterogeneous catalysis began in 1913 with Sabatier, who was the first to suggest that catalysis proceeds through the formation of an intermediate compound on the catalyst surface.[2] This idea was not extensively developed at the

time, largely due to the fact that the molecular organometallic compounds which were candidates as catalytic intermediates were unknown to chemists of that era. As will be discussed, the concept of the surface intermediate in catalysis plays a very important role in present-day thinking. This is partially a result of the success of inorganic chemists (since 1950) in the synthesis of analogous molecular compounds of organometallic species.

The concept of "active centers" in catalysis was introduced in 1925 by Taylor,[3] who reasoned that catalytic activity on a solid was restricted to a distribution of specific sites on the surface rather than to all available sites. Since that time, a number of attempts to identify lattice imperfections (such as dislocations and point defects) with catalytically active centers have been made. Although some illuminating facts suggesting a relationship between lattice imperfections and catalysis are available, it is still not possible to formulate a generally satisfactory theory to account for such relationships.[4,5] Many apparent experimental correlations between catalytic activity and lattice imperfections are suspect due to the possible influence of impurities and other interferences. This is particularly so in metals. In compounds such as oxides, sulfides, and halides, point defects are more easily identified as the catalytic sites.[4] One instance of the participation of point defects which appears to be well documented is in Ziegler–Natta catalysis (polymerization of olefin monomers), as will be discussed in Section 6.3.

Historically, catalytic chemists have distinguished between the geometric and the electronic factors in catalysis. This somewhat artificial separation of solid-state properties has resulted in correlations between catalytic activity and lattice spacing on the one hand, and between catalytic activity and electronic character on the other hand.[6] It is now widely recognized that geometric properties of a solid are intimately related to the electronic properties, and that attempts to separate the two can be misleading.

In the 1930's, Balandin developed his multiplet theory of catalysis, which stressed the importance of surface geometry.[7] He reasoned that the activity of a catalyst depends on the presence in the surface lattice of a correctly spaced array of atoms ("multiplet") to interact with the reactive group of atoms in the reactant molecules ("the index"). In addition, the importance of energetic factors was recognized in the later developments of the theory. A priori, the theory needs a rather detailed mechanistic model of the reaction. Since the theory is generally tested by comparing various catalysts with

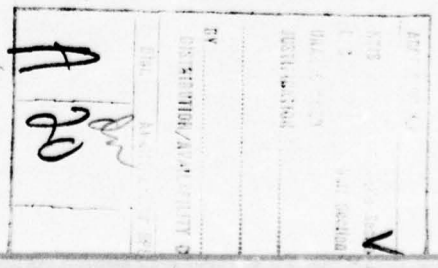

different lattice spacings or different crystal structure, a requirement for such tests is that the mechanism of the reaction is the same on all catalysts compared. For example, according to this theory, the dehydrogenation of cyclohexane and the hydrogenation of benzene by the sextet mechanism should proceed if a suitably spaced hexagonal array of atoms is present in the surface. Therefore, metals and alloys having hcp and fcc structures should be more active than those having bcc structures. Although there is considerable evidence to support this tenet,[7] many counterexamples cast serious doubt on the general validity of Balandin's ideas. For instance, evaporated films of bcc W and Fe are highly active for hydrogenation of benzene, whereas fcc Cu and Ag are inactive.[6] Balandin,[7] recognizing the difficulty, has allowed of the possibility that benzene hydrogenation would also occur through intermediate steps involving only two metal atoms (doublet mechanism). Indeed, Boudart[8] has pointed out that the interconversion of benzene and cyclohexane can be classified as "structure-insensitive" reactions on Pt and Ni catalysts, and such reactions can of course not be used as a test for surface geometry! Here, as elsewhere in the theory of catalysis, concepts which appear to have basic validity can only be tested and applied within a framework of sufficient knowledge regarding the mechanisms of the reactions and the energetics of the intermediate surface complexes. Modern work in catalysis is much more apprehensive about these factors and hence tends to study the examples of template effects in much more detail. Along these lines, Somorjai[9] has provided recent evidence that the surface structure may have a specific influence on certain reactions. He has reported that high-index planes of Pt containing steps and terraces play a special role in the dehydrocyclization of *n*-heptane to toluene; the activity for this reaction is higher on certain stepped surfaces than on the smooth Pt(111) plane. Conversion of neopentane has been shown to require a triplet of Pt sites.[8] In another example where geometry is important, template effects appear to be well established in the catalytic reactions of enzymes[10] but these have to remain outside the scope of this chapter.

The electronic approach to the understanding of catalysis on metals, developed in the late 1940's and 1950's, seeks a relationship between the *bulk* electronic properties of a solid and its catalytic activity. Boudart[11] and Beeck[12] recognized in 1949 that the catalytic activity of a number of transition metals for the hydrogenation of ethylene ($H_2 + C_2H_4 \rightarrow C_2H_6$) could be expressed as plots of the logarithm of the rate constant for the reaction as a function of

the percentage *d* character of the catalyst. (In Pauling's theory of bonding in solids,[13] the cohesive energy of transition metals is attributed to the formation of *dsp* orbitals; percentage *d* character is a measure of the extent to which *d* electrons participate in the bonding *dsp* orbitals). As will be discussed below, Sinfelt[14] has recently attempted to correlate activities for ethane hydrogenolysis (to produce methane) with percentage *d* character. As he points out, "while there is a degree of correlation between hydrogenolysis activity and percentage *d*-character, this parameter alone is not adequate for characterizing the catalytic activity of transition metals for hydrogenolysis."

There are several basic limitations to the electronic approach to the catalysis by metals as outlined above. First, there is no simple correlation between the bonding between metal atoms in the bulk and the electronic properties of the surface. In particular, the atomic orbitals available for bonding at the surface will depend on the crystal face. The catalytic activity of a particular solid is, in many cases, dependent on the exposed crystal faces. For example, Gwathmey and

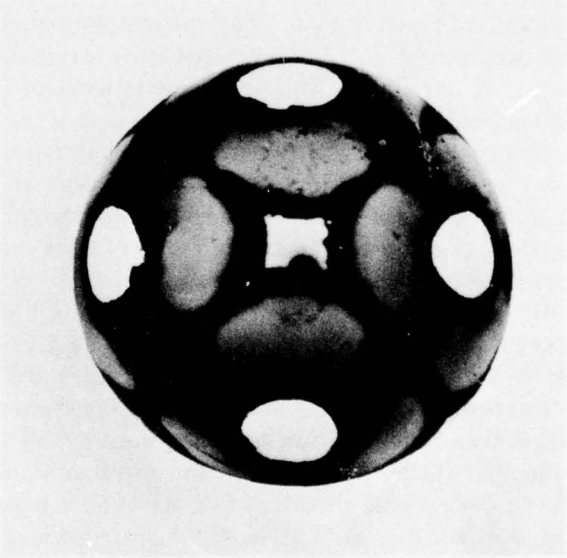

Fig. 1. Crystallographic decoration of a nickel single-crystal sphere by the deposition of carbon in the catalytic decomposition of ethylene. (From the work of Cunningham and Gwathmey,[15] courtesy K. Lawless.)

Cunningham[15] demonstrated the specificity of different Ni crystal planes for decomposition of C_2H_4 and CO (Figure 1), Van Hardeveld and Hartog[16] showed that chemisorption of N_2 on Ni, Pd, Pt, and Ir and H–D exchange into benzene over Ni occurred on sites where the adsorbate would have 5-coordination, and Boudart[8] has discussed several structure-sensitive reactions. Another basic objection to the oversimplified electronic approach given above is that the catalytic process often constitutes a major perturbation to the metal, to the point where metal salts are formed as intermediates. Such was the case in the decomposition of formic acid on a series of metals studied by Fahrenfort *et al.*[17] The electronic properties of the metal might be expected to be of limited relevance in such cases which involve "corrosive chemisorption."[18]

The successes of the theory of semiconductors led in the 1940's and 1950's to the development of an electronic theory of catalysis on semiconductors by Wolkenstein,[19,20] Hauffe,[21,22] Weisz[23] and others. It had been known for some time that chemisorption on semiconductors changed their conductivity.[24] The new theories were based on the concept that if chemisorption changed the number of charge carriers in the semiconductor, then it should be possible to influence the rate of reaction by varying the concentration of charge carriers whenever the charge transfer entered into the rate-determining step of the catalytic process. This idea was reinforced by initially successful attempts by Stone[25] to correlate the activity of a series of oxides for the decomposition of N_2O with their electrical transport properties (*n*- or *p*-type conductors and insulators). It had been established that the rate-determining step for this reaction involves the uptake of an electron by the lattice.[26,27] Further support was derived from the experiments by Parravano[28] and by Schwab and Block,[29] who showed that doping of NiO with Li or Ga would have dramatic effects on the activation energies for the CO oxidation. Enthusiasm was hardly tempered by the fact that the effects in Parravano's experiments[30] had the opposite sign from the effects found by Schwab and Block. However, discussions by Garrett[31] and Garcia-Moliner[32] have clearly shown the extreme simplifications involved in these electronic theories of catalysis on semiconductors. Among these were the complete neglect of intrinsic surface states, the frequent assumption of complete ionization of the surface states induced by adsorption, and the assumption that these states are always to be found in the forbidden gap between valence and conduction bands. As more of these simplifications are removed, more

detailed knowledge of the semiconductor is necessary for a quantitative test of the theory. Even the simplest quantitative test, measuring the reaction rate as a function of doping level, requires the knowledge of a multitude of semiconductor parameters unknown for any of the catalysts concerned.[31] In the absence of such tests, qualitative confirmation of the relation between reaction rate and conductivity has been extensively pursued. As will be discussed below, Chon and Prater[33] have related measurements of the rate of CO oxidation with measurements of the carrier concentration for ZnO. Quantitative confirmations may become possible with the use of single crystals for catalytic rate measurements coupled with measurements of the electronic properties of the surface. The ambiguities introduced by the use of polycrystalline samples, such as surface segregation, spurious electric fields, intergranular resistance, and shape effects, would then be removed.

Recent developments in catalysis seem to be returning to the concept originally introduced by Sabatier: Rather than concentrating on the general electronic and geometric properties of the solid, theoretical and experimental work is concerned with the properties of atoms and complexes at surfaces. Among the catalytic chemists, Dowden[34,35] had stressed this viewpoint as early as 1956. However, since then much more comprehensive treatments of the surface complex have become possible. The concepts of coordination chemistry and the local site approach are dominating present thinking concerning catalytic mechanisms.

2.2. The Steady-State Surface of the Catalyst

At this point, it is important to focus attention on the differences between the state of the catalyst per se and the steady state of the catalyst in situ. The catalyst per se can be studied in some experimental atmosphere (e.g., air for microscopy, N_2 for surface area determination, ultrahigh vacuum for surface physics measurements), but the state of its surface is then in general not representative for the catalytically active state. For instance, in air or N_2, it is likely to be covered with oxygen, CO, hydrocarbons, sulfur compounds, and the like. Catalysts prepared in ultrahigh vacuum (UHV) are probably highly unsaturated and in the process of being covered with carbon, oxygen, or hydrogen from residual gases. In contrast, in the catalytic reactor, under the influence of the reaction partners, bonds with the catalyst are continuously made and broken, resulting in a dynamic steady

state of the surface. The nature of this state is dependent on the reaction conditions. From the selectivity of the reduction of NO to NH_3 or N_2, as many as five reproducible states have been deduced for Ru supported on Al_2O_3.[36] Few steady-state surfaces have been studied by UHV surface techniques and perhaps not many are amenable to such study. In one notable exception, Joyner *et al.*[37] have found that the Pt surface active for hydrogenation was an ordered carbonaceous overlayer.

For steady-state surfaces, a further distinction is appropriate between catalytic processes in which the intermediates are short-lived and those in which fairly stable surface compounds are formed or, more generally, in which atoms cease to belong to the catalyst and transfer to the surface compound or even to the product. An example is the participation of lattice oxygen in oxidation reactions catalyzed by oxides. The former type is characterized by sufficiently weak interaction between the catalyst and the reacting species that the atoms forming the catalyst surface remain fixed in their lattice positions. At all times, an imaginary plane separates the catalyst and the reacting species. This type of catalytic process has therefore been called *suprafacial catalysis* by Voorhoeve *et al.*[38] It includes catalytic reaction involving extralattice oxygen[30] for the low-temperature oxidation of CO. Another example is the olefin disproportionation reaction,[39] which was discussed by Mango and Schachtschneider[40,41] in terms of a cyclobutane intermediate. The catalyst in the suprafacial catalytic processes primarily provides the electronic bridge for electron flow between the reaction species. It is in these cases that (cooperative) electronic properties of the catalyst are expected to have the most clear-cut influence on the catalytic rate parameters.

There are a large class of catalytic processes in which atoms belonging to the catalyst surface leave their lattice positions and become part of the surface compound or of the product molecules, their place in the lattice being taken by reactant atoms. These types of catalytic systems, in which the separation between catalyst surface and reacting layer becomes diffuse, have therefore been called *intrafacial catalysis*.[38] Corrosive chemisorption is often a forerunner of this type. An example of intrafacial catalysis is the decomposition of formic acid on metal catalysts. Sachtler and Fahrenfort[17] have identified metal formates as the intermediates in this process. Many selective oxidations over metal oxides belong to this class also, since lattice oxygen becomes part of the product. This so-called Mars–Van

Krevelen mechanism, originally proposed for the oxidation of xylene to phthalic anhydride,[42] has been shown to apply for oxidation of propylene and CO over bismuth molybdate at 425°C by Keulks[43] and for many selective oxidation processes[44] (see Section 5.4). In these intrafacial catalytic processes, the kinetic parameters are frequently linked more significantly to the chemical stability of the solid, i.e., to the heat of formation of the metal oxide[45,46] or the heat of formation of the metal formate,[17] rather than to "electronic" properties.

2.3. The Surface Complex: Relation of Heterogeneous Catalysis to Coordination Chemistry

The categories of elementary processes customarily used to analyze heterogeneous catalysis have been listed as follows:[47,48]

(1) Diffusion of reactants to the surface.
(2) Chemisorption of at least one of the reactants on the surface.
(3) Surface diffusion of chemisorbed reactants and subsequent surface reaction.
(4) Desorption of products from the surface.
(5) Diffusion of products from the surface.

Steps 1 and 5 involve transport of material through a gaseous or liquid medium, and need not concern us for the moment. Adsorption and desorption processes are discussed at some length in other chapters of this volume, and will only be discussed here as is necessary to understand catalytic mechanisms. The key step for many catalytic processes is step 3, which is generally believed to involve the formation of surface intermediates which decompose to yield the desired product(s). Surface intermediates or complexes are frequently short-lived compounds whose existence is often inferred from more or less indirect evidence.

A basis for thought about the nature of surface complexes is provided by organic and inorganic chemists, who have identified a wide variety of molecular coordination complexes formed from transition metal atoms, ranging from metal carbonyls $[M_x(CO)_y]$ to complex organometallic compounds. There is abundant evidence from recent experimental studies of chemisorption and catalysis that similar compounds can exist on the surfaces of transition metals. Infrared spectroscopy has been used to demonstrate that a formate (HCOO) is formed when formic acid (HCOOH) is adsorbed on a number of different metallic catalysts; a further conclusion is that

decomposition proceeds via the formate intermediate on all of the metals studied.[17] Ultraviolet photoemission spectroscopy has been applied by Demuth and Eastman[49] in studies of the decomposition of C_2H_4 and C_2H_2 on Ni. This work demonstrates convincingly that dehydrogenation of C_2H_4 leads to formation of a chemisorbed acetylenic intermediate, which undergoes further decomposition at elevated temperatures. Burwell[2] has cited extensive work based largely on kinetics and the use of isotope tracers which supports the existence of a veritable "organometallic zoo" of surface organometallic intermediates in reactions involving hydrogen and hydrocarbons over transition metal catalysts.

The ability to directly detect a catalytic intermediate in high concentration on a surface implies that its decomposition to yield the catalytic products is a rate-controlling process. Unfortunately, the direct detection of the elusive surface catalytic intermediate is frequently hampered by its low concentration under reaction conditions. If the rate-controlling step involves formation of the intermediate via adsorption and/or diffusion, then rapid decomposition of the intermediate may result in a steady-state concentration so low as to be undetectable using presently available techniques.

In any event, it appears that an understanding of the fundamental basis of catalytic activity will involve an understanding of the physics underlying the coordination chemistry of organic and inorganic transition metal complexes. This philosophy is the basis for the recent theoretical work of Johnson, Slater, and Messmer,[50,51] who have applied the self-consistent field, X-alpha scattered wave approach to the investigation of catalytic problems. Their calculation of energy level schemes and orbital "maps" for small metallic clusters and organometallic compounds are providing new insights into the electronic structure of potential catalytic intermediates.

2.4. The Role of *d* Electrons in Catalysis

It has long been recognized that the most active catalysts for many reactions are transition metals. (There are notable exceptions. For example, Ag is highly efficient in catalyzing the oxidation of ethylene). Also, as indicated in Table 1, transition metals are more active in chemisorption than the non-transition metals. The basic questions concerning the preeminence of transition metals are: What, if anything, is unique about unfilled *d* orbitals and catalysis? Can we identify the catalytic activity of transition metals with *d* orbitals per se,

TABLE 1
The Activities of Metal Films in Chemisorption*

Metals	Gases					
	N_2	H_2	CO	C_2H_4	C_2H_2	O_2
W, Ta, Mo, Ti, Zr, Fe, Ca, Ba	+	+	+	+	+	+
Ni, Pt, Rh, Pd	−	+	+	+	+	+
Cu, Al	−	−	+	+	+	+
K	−	−	−	−	+	+
Zn, Cd, In, Sn, Pb, Ag	−	−	−	−	−	+
Au	−	−	+	+	+	−

* Table taken from Ref. 194, p. 231; data based on adsorption studies on metal films. (+) Gas chemisorbed. Chemisorption takes place over a large part of the surface with great rapidity. (−) Gas not chemisorbed. Little or no adsorption observed between 0°C and temperatures at which physical adsorption occurs.

or are there simply coincidental geometric and electronic factors in "good" catalysts which influence those kinetic and thermodynamic properties of species that are involved in catalytic reactions (stability of intermediates, heats of adsorption of reactants and products, etc)?

It is helpful to consider the differences between *s* orbitals and *d* orbitals in metals. Clearly, *s* orbitals in free atoms are spherically symmetric; an *s* band in a solid has a broad, free-electron-like density of states without a high density of localized electronic states anywhere within a few volts above or below the Fermi level E_F. In an isolated atom, completely filled *d* orbitals also result in a spherically symmetric charge shell. Partially filled *d* orbitals exhibit a localization in space and energy which promotes electronic overlap with ligands of a reacting molecule. In contrast to the broad, sparsely populated density of states of *s* bands in solids, the density of states of *d* electrons in the valence band of transition metals is usually narrow and dense. This localization in energy and space can result in a strong "mixing" between metal surface orbitals and the orbitals of an adsorbing atom or molecule. Whether or not such mixing results in strong bond formation and/or catalytic reaction depends on the details of the positions of the energy levels of molecular orbitals of adsorbed intermediates with respect to the Fermi level.

It is interesting to note that transition metals exhibit a rich coordination chemistry with molecules such as CO and the other

π-electron molecules. As discussed in Mango and Schachtschneider's[40,41] treatments of organometallic coordination complex chemistry, *d* orbitals are spatially localized to overlap effectively with ligand orbitals. In addition, the correspondence between *d*-orbital energies and ligand molecular orbital energies makes possible a strong interaction in which electron transfer between ligand and metal and also between various *d* levels in the metal atom can occur. This property of the transition metal atom can promote catalytic processes in the ligands which would be strongly symmetry-forbidden in the absence of the transition metal atom, i.e., an activation barrier is lowered by the action of the transition metal atom.

One may conclude that the spatial and energy localization of *d* electrons in transition metals is related to the unique catalytic activity of these metals, although other geometric and electronic factors have a major influence on reaction kinetics also.

Many of the topics which have been briefly treated in this historical survey will be discussed in more depth in the following sections.

3. The Nature of Heterogeneous Catalysts

3.1. Character and Use of Catalysts

It is appropriate to indicate in general terms the character of practical heterogeneous catalysts so that the reader will have some feeling of the technological aspects of catalytic chemistry. Catalysts are typically prepared in forms dictated by the type of reactor in which they will be used, among other factors.[52] Fundamental to any catalytic process is provision for reactant and product transport to and away from the active area of the catalyst. Since high surface area is desirable in order to increase the activity per unit quantity of catalyst, some of the active area will usually be inside the catalyst particle, and the problem of transport through narrow pores becomes a factor of kinetic importance, as discussed in detail by Weisz and Prater.[53]

A wide variety of processes use metals as catalysts, including hydrogenation–dehydrogenation, reforming of hydrocarbon molecules, ammonia synthesis, etc.[54] Platinum is a particularly important catalyst in petroleum processing, nickel in hydrogenation of fatty oils, and iron in the ammonia synthesis. A large-volume use of catalysts has recently developed in the catalytic treatment of automotive exhaust to remove carbon monoxide and unburned hydrocarbons. The extremes of temperature and contamination met in this

environment have resulted in an intense effort to develop metallic catalysts and new ceramic supports.[55] Among the more unusual applications of metal catalysts in large-scale chemical manufacture is the use of copper catalysts to accelerate a gas–solid reaction, i.e., the reaction of organic halides with silicon to form the precursors for silicones.[56,57]

To obtain high specific area, metal catalysts are usually present in highly dispersed form, either as a powder, or more commonly as particles supported in a nonmetallic matrix. Supported metal catalyst particles are typically prepared on high-area silica or alumina powders by reduction of metal salts deposited by drying and calcining (i.e., high-temperature heating in a controlled atmosphere) the salt-impregnated support material. Metal content may range up to 50% by weight, but values in the 1% range or lower are common for noble metal catalysts.

Catalyst manufacture is best described as an art and few standard procedures are available, according to Ciapetta and Plank,[58] who have listed a number of useful preparative methods for various technically important catalysts.

Other forms of metal catalysts include high-area metals and alloys bonded to screens, tubes, or other structures for support and heat transfer. An example is Raney nickel catalyst, which is prepared by NaOH treatment of nickel–aluminum alloys; this alkali leaching process increases the active surface area of the Raney nickel by dissolution of aluminum from the alloy.[59]

Often, metals are supported on active insulator supports in order to achieve a dual function catalyst, in which different classes of reactions are performed successively on different catalyst sites, as discussed in an excellent general review by Haensel and Burwell.[60]

Oxide catalysts play an exceedingly important role in the refining of petroleum products.[52] An example is the catalytic cracking of petroleum distillate fractions, for which natural aluminosilicates, amorphous synthetic silica–alumina combinations, and crystalline, synthetic silica–alumina compounds (synthetic zeolites) exhibit catalytic activity attributed to acid sites.[61] Some chemicals manufactured on a very large scale, such as butadiene, acrylonitrile, and ethylene oxide, are produced by selective oxidation over metal oxide catalysts, one of the most popular being bismuth molybdenum oxide. Similar selective oxidation catalysts play an important role in the manufacture of pharmaceuticals.

Sulfides such as cobalt molybdenum sulfide and nickel tungsten sulfide are extensively used for partial hydrogenation of sulfur-containing feedstocks in the petroleum industry to remove sulfur as H_2S and in hydrocracking of heavy distillates.[62]

Chlorides are extensively used as polymerization catalysts, e.g., $TiCl_3$ for polypropylene.[63] Another important use is that of a CuCl catalyst in the recovery of Cl_2 from HCl.[64]

Catalytic reactors take many forms, dictated by the nature of the catalytic process as well as the manufacturing process desired. Commonly employed for gaseous reactants with solid catalysts are "fixed-bed" reactors, in which the reactant gases flow through a packed bed of pellets, spheres, or coarse grains. However, these are impractical where continuous movement of the solid is required for cooling of an exothermic reaction or for transport of the solid to a regenerator in order to restore the catalyst to useful activity. In such cases fluid bed reactors are common,[65] in which the gas or liquid flows upward through the particulate solid at a sufficient velocity to suspend the catalyst particles in the fluid phase. For hydrogenation reactions of heavy distillates, trickle reactors are used to effect two-phase flow of gas and liquid through a fixed, packed catalyst bed. For some processes, such as polymerizations, fine catalyst particles are suspended in a stirred liquid and the reactions occur at the liquid–solid interface. Laboratory as well as commercial versions of these and other reactor designs are widely used.[66,67]

The design of a commercial catalyst has as its central factors high rate of conversion for reactants (activity); preferential or exclusive formation of desired products rather than side or waste products (selectivity); stability of both activity and selectivity under the conditions of the process, including impurities in the reagents; and mechanical strength. The latter is crucial for fixed-bed reactors to withstand the hydrostatic pressure of the self-supporting catalyst bed and also for fluid beds, where attrition of the suspended particles would otherwise lead to excessive losses of catalyst blown out of the reactors.

In the following sections, more details concerning the nature of finely divided catalysts will be discussed.

3.2. Catalyst Characterization: Surface Area and Dispersion Measurements

For the comparison of the catalytic activity of different high-area catalysts, it is desirable to separate the two factors involved, namely

the available surface area of the active phase and its activity normalized per unit of surface area. The determination of the surface area of the catalysts may be done indirectly using a number of physical techniques, such as X-ray or electron diffraction line broadening, low-angle scattering of X-rays, and electron microscopy.[68] The average particle size as determined in this manner may then be related to catalyst surface area. However, to do this with acceptable accuracy, the distribution of particle sizes is required.

A more direct method involves measuring the adsorptive properties of the catalyst, where the quantity of gas adsorbed per unit mass of active catalyst is measured. This may be done in several ways, as follows.

(a) For unsupported catalysts, such as high-area Pt black, the surface area may be determined by the physical adsorption of a gas that is not chemisorbed by the catalyst. The adsorption isotherm is fitted to some model (such as the BET or Brunauer–Emmett–Teller model),[69] and the adsorbate surface area is determined directly, using well-known areas for the physically adsorbed molecule.[70,71]

(b) For supported catalysts, it is often possible to selectively chemisorb molecules such as O_2, CO, H_2, or NO on the catalytic material. These measurements, carried out to saturation of the monolayer, are often directly reported (as μmoles/g of catalytic component). Assumptions about the monolayer capacity (molecules adsorbate/surface atom) can be made so that the number of surface atoms in the catalyst may be estimated.[72]

(c) For supported catalysts, where interference in chemisorption measurements occurs due to support adsorption, or to absorption in the bulk of the catalyst, it is often possible to titrate a chemisorbed layer on the catalytic surface with a second gas. This has been done for O(ads) on supported Pd[73] and Pt[70] using H_2(g).

Methods (a), (b), and (c) have been intercompared with each other.[74] An example of this may be found in the work of Sinfelt, who compared H_2 and CO chemisorption results for a number of different supported metals at different degrees of metal dispersion.[72] The ratio of hydrogen chemisorption per metal atom was found to be equal to the ratio of CO chemisorption per metal atom over a wide range of dispersion of the metal. In the limit of highest dispersion every metal atom was able to adsorb either one H or one CO.

The observation that for a given catalyst the monolayer capacity for H and CO chemisorption agrees with fair accuracy may imply a simple stoichiometric relation between the number of atoms or molecules in the monolayer and the number of surface metal atoms.

This has, in fact, been checked for Pt by comparing the BET surface area with oxygen chemisorptive uptake.[70] There is, of course, some uncertainty about the correct average Pt site density to assume for the catalyst; choosing the average of the site densities for Pt(100), Pt(110), and Pt(111) as 8.4 $Å^2$/site, an O/Pt ratio of 1.1 was obtained for Pt surface atoms. It was found by titration that 2.16 H reacted with 1 O(ads) in this experiment, in agreement with the stoichiometry of H_2O product as well as with calorimetric measurements made on Pt black.[75]

For the characterization of oxides, volumetric measurements of the chemisorption of NO coupled with infrared absorption measurements are good techniques for the determination of the number of oxygen vacancies and their coordination. For example,[76] on chromia, NO can be adsorbed on a single oxygen vacancy as an NO_2 chelate and on a double vacancy as a *cis*-dimer:

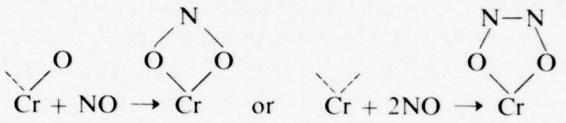

The identification of such infrared-active complexes can be materially reinforced by the use of isotopically labeled ^{15}NO (Figure 2).

The *dispersion D* of a metal catalyst is defined as the fraction of the total number of metal atoms that are at the surface of the metal particles. Figure 3 illustrates this property for model cubooctahedra of Pt.[77] The chemisorptive uptake may be used to calculate a value of the catalyst dispersion by assuming or measuring surface stoichiometries (atoms of adsorbate per surface atom) for the system considered. To obtain the average particle size from chemisorption data,[73] one must make further assumptions regarding particle shape and morphology, and the accessibility of the surface to the chemisorption process. For Pd, the relation $d = 0.9/D$, where d is the average particle diameter (nm), is found to give fair agreement ($\sim 30\%$) with x-ray line broadening values for d.

The absolute measurement of surface stoichiometries of monolayer chemisorption on single crystals would contribute to a better understanding of the chemisorption measurement of surface area and dispersion of high-area catalysts. For instance, as pointed out by Benson *et al.*,[73] there is uncertainty about the stoichiometry of the Pd–CO system since both linear (Pd–CO) and bridged (Pd_2CO) species are detected by infrared spectroscopy on supported Pd

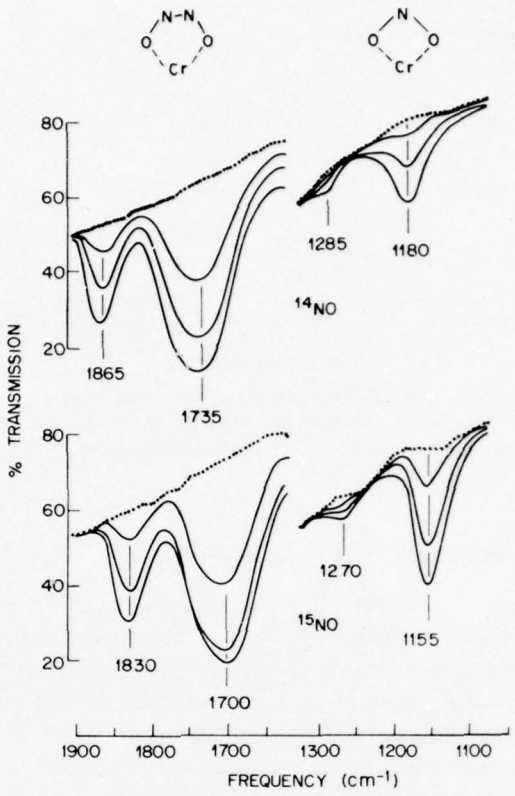

Fig. 2. Adsorption of ^{14}NO and ^{15}NO on self-supported Cr_2O_3. Infrared absorption spectra. Assignments of the two sets of bands as indicated at the top. Curves with decreasing percentage transmission correspond to increasing NO coverage. (After Kugler *et al.*[76])

catalysts.[78] Furthermore, recent low-energy electron diffraction (LEED) studies of the CO + Pd(100) system indicate that at monolayer coverage CO adsorbs out of registry with the underlying Pd(100) lattice.[79]

Measurements of the absolute surface coverage of hydrogen and oxygen monolayers on the (100) face of tungsten have recently been made using calibrated molecular beam techniques.[80] Such measurements are difficult at present and are accurate to about $\pm 15\%$.

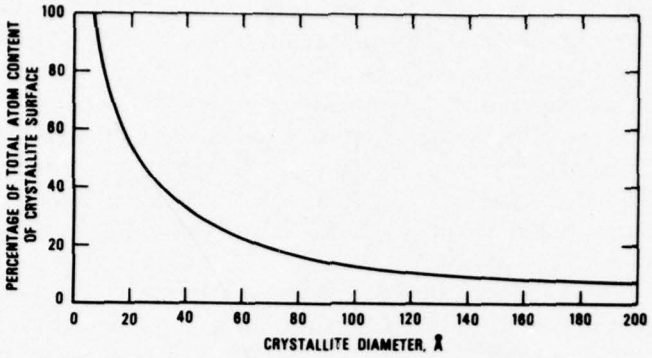

Fig. 3. Variation of the ratio of surface atoms/total atoms for small Pt crystallites as a function of crystallite diameter; the model crystallites are assumed to have face-centered-cubic packing. (From Stonehart and Zucks.[77])

3.3. The Measurement of Catalytic Activity

The "activity" of a catalyst is defined as the rate of conversion of a reactant or the rate of formation of a product under specified conditions of temperature, partial pressures or concentrations of reactants and products, total pressure, and flow rate of the reacting medium through the catalyst mass. The measurement of catalytic activity can be carried out with various objectives. One is to obtain parameters for the design of a catalytic reactor, such as an automotive exhaust reactor with Pt catalyst for the oxidation of CO and hydrocarbons.[81] Another purpose may be to compare the usefulness of catalysts for a given process, e.g., the disproportionation of olefins.[82] Frequently, it is desired to characterize the properties of a surface in terms of the activity for a chosen "test reaction," as in the comparison of *d* metals for ethane hydrogenolysis.[14]

In order to compare the activity of different catalytic surfaces for the same reaction, it is important to make kinetic measurements which can be intercompared, and in the limit, to determine the absolute rates of elementary reaction steps leading to a catalytic product. Absolute rate is defined as the rate per surface site. Since catalytic activity is a surface property, it might appear that reproducible measurements are a hopeless task, since it is well known that the properties of "clean" surfaces are only reproduced by painstaking efforts involving UHV techniques. However, this viewpoint ignores the fact that catalytic surfaces are used and measured under

conditions of a kinetic steady state. Impurities are controlled by the occurrence of both deposition and removal reactions. An example is the use of high hydrogen pressures in hydrogenation reactions to prevent the formation of carbonaceous deposits. The very widespread use of catalysts in the chemical industry and the near-unanimity on the preferred catalyst for a given process attest to the general reproducibility of catalytic surfaces. In detail, rate measurements by different workers on catalysts of the same provenance often agree remarkably well.[83–86]

To determine absolute reaction rates, it is necessary to know the number of active sites and, in general, for multiphase mixtures, the catalytically active phase has to be identified. This identification may be difficult, as illustrated by the several years of effort expended to establish that the active phases in supported and unsupported CO–Mo–S and Ni–W–S catalysts are the intercalated trigonal prismatic layer sulfides MoS_2 and WS_2.[62]

Most catalytic reactions are carried out at high pressures, where conditions of molecular flow are not present, and where the transport properties of the gas phase are involved in determining the rate of impingement of reactant molecules on the catalyst surface. In addition, for dispersed catalysts, one is dealing with nonideal geometric surfaces, where it is important to consider diffusion processes within the pores of the catalyst.[87] In order to make meaningful *comparisons* of catalytic activity of different catalysts under those conditions of high pressure and nonideal substrates, it is common to operate under identical conditions of temperature T and partial pressure of reactants P_i. Often a measurement of the initial rate or the rate at low conversion ratios is made to avoid complexities due to changes in the catalyst or to back reactions. The rate of the catalytic reaction R is expressed per unit area of catalyst surface as

$$R = \left[\frac{\text{moles product}}{\text{catalyst area} \times \text{time}}\right]_{T=\text{const}, P_i=\text{const}}$$

A slight variation on this is to express rates as the turnover number N, defined as

$$N = \left[\frac{\text{molecules product}}{\text{number catalyst sites} \times \text{time}}\right]_{T=\text{const}, P_i=\text{const}}$$

In both cases, chemisorption measurements are often used to estimate surface area or the number of catalytic sites involved, as discussed previously.

By means of detailed studies, it is often possible to separate the rate of chemical conversion per unit area into a concentration- (or partial pressure-) dependent term and a concentration-independent factor,[87]

$$dn/dt = k_s f(c_i)$$

The factor k_s is characteristic of the catalyst and the catalytic reaction and in some cases may be factored into a preexponential factor A and a temperature-dependent term involving the activation energy for the reaction E_{act}:

$$k_s = Ae^{-E_{act}/RT}$$

Thus, assuming that a single activation energy characterizes the reaction, it is possible to intercompare catalytic activities measured at somewhat different temperatures.

Determination of the identity or the rates of the *detailed steps* of a heterogeneous catalytic reaction by the aforementioned kinetic flow technique has rarely been possible. The presence of the surface hampers the use of many spectroscopic techniques successfully used in the elucidation of detailed mechanisms in homogeneous catalysis. In addition, the precise nature of the catalytic surface could rarely be established. Fortunately, the scope of catalytic rate measurements has been extended recently by the introduction by Madix *et al.*[88,89] and Bernasek and Somorjai[90,91] of reactive scattering of molecular beams from surfaces. Some results obtained by these techniques will be discussed in more detail in Section 8. Suffice it to say at this point that rate constants for individual steps can be measured by these techniques.

The coupling of UHV characterization techniques such as low-energy electron diffraction and Auger electron spectroscopy with catalytic rate measurements at conventional pressures has been made by characterizing the single-crystal Pt catalyst in UHV, isolating it in a small part of the UHV apparatus by a bellows mechanism, and introducing the reactants, which after conversion were measured by gas chromatography.[83] These measurements, on the hydrogenation of cyclopropane, were compared with earlier data on supported Pt catalysts of 7–8 orders of magnitude smaller particle size. The turnover numbers for the two systems were equal within a factor of two. These

kinds of comparisons are of great value in defining the meaning of catalytic studies on single crystals, where factors such as crystal orientation and surface composition may be well controlled.

The adsorption and desorption steps in a reaction can also be measured in UHV. Adsorption rates have been measured and expressed as a sticking coefficient S:

$$S = \frac{\text{rate of adsorption}}{\text{rate of impingement}}$$

measurements of S can be made by measuring either the capture rate or the reflection rate at known impingement rate. For active chemisorption, often $S = 1$ at zero coverage[80] and S decreases as coverage increases. These measurements have been made for evaporated films[92] and for single crystals.[80,93] This technique has increased in importance with the introduction of molecular beam kinetics for the study of reactive gas–surface interactions.

3.4. Active Site Character and Measurement

The concept that a catalytic surface possesses a distribution of surface sites having different intrinsic catalytic activities was first enunciated by Taylor[3] in 1925. The opposite concept that a chemisorbed monolayer saturates free and *equivalent* surface valences had been proposed by Langmuir in 1922.[94] Taylor's active site hypothesis was a refinement of Langmuir's concept of a uniform "checkerboard" surface. Taylor conceived the surface as being nonhomogeneous by virtue of the presence of a distribution of substrate atoms having different degrees of coordination with other substrate atoms, i.e., a catalytic surface was not a perfect crystalline surface. In Taylor's model, the sites with the highest catalytic activity were assigned to surface atoms possessing the lowest degree of coordination prior to adsorption, and these were called "active sites." The early experimental evidence for the existence of active sites was obtained from annealing and poisoning experiments, which Taylor summed up as follows: "It has been shown that active catalysts manifest an extraordinary sensitivity to heat treatment and to the action of poisons. Both alter adsorptive capacity and reactivity to different degrees, the reduction in catalytic activity being much more pronounced than the reduction in adsorptive power." The concept of a distribution of active sites was consistent with the "varying capacity of the surface to effect catalysis as revealed by progressive poisoning (experiments). These

indicated that the amount of surface which is catalytically active is determined by the reaction catalyzed."

The basic concept of active sites on catalysts persists today. The challenge to modern surface chemistry is to induce and characterize these sites and to determine their surface density, structure, etc. Many experiments attempted to increase the active site density by means of irradiation,[95] ion bombardment[96] and cold working,[97] stressing,[98] etc. Following such treatment, enhanced catalytic activity has often been measured, and in some cases subsequent treatment to remove the active sites has caused a reduction in catalytic activity. One difficulty with many of the early experiments is that the results may be influenced by impurities introduced or removed during treatment of the catalyst. For example, Farnsworth and Woodcock,[96] working under ultrahigh vacuum conditions, found that the activity of Ni for the hydrogenation of C_2H_4 could be increased 100-fold using Ar^+ bombardment. A tenfold increase in Pt activity was also produced upon Ar^+ bombardment. Annealing caused the activity to return to lower values in both cases. We now know, from Auger electron spectroscopy (AES) studies, that Ni often contains S impurities which diffuse to the surface from the bulk upon annealing, and which may be removed by ion bombardment. Thus, one cannot be certain about the interpretation of these ion bombardment experiments. Later, ion bombardment work was done by Sosnovsky[99] where single crystals were bombarded and then transferred in air to a reaction chamber, where the activity for HCOOH decomposition was found to vary in a complex way with Ar^+ bombardment energy. Again, one would have to question whether the effects measured are related only to the induction of dislocations by ion bombardment, or whether surface impurities introduced by exposure to the atmosphere may somehow be involved.

The identity and properties of active sites are often inferred from the catalytic and chemisorption properties, e.g., in series of oxides with cation or anion vacancies.[38,100,101] Similarly, the so-called B-5 sites on Ni were inferred from N_2 chemisorption and particle size determinations.[102] It is preferable to have independent means to study the structure of the sites and to measure their number.[103] Recently, a number of well-controlled experiments involving spectroscopic methods have been used to help characterize the electronic and structural nature of active sites. In the first examples cited below, correlation of the catalytic activity with the concentration of active sites has been directly observed. More often, the predominant sites for chemisorption (which are not necessarily the sites for catalytic

activity) have been characterized spectroscopically and one example of this is given also.

3.4.1. Active Sites on WS_2- and MoS_2-Based Catalysts

Many electron spin resonance (ESR) studies of catalysts have served to suggest active sites for catalysis.[104] The first observation of a *quantitative* relation between the number of active surface sites identified and characterized by ESR and the rate constant of a heterogeneous catalytic reaction appears to have been made by Voorhoeve[105] for the hydrogenation of benzene on WS_2 and Ni–WS_2 catalysts. These catalysts were prepared in seven different ways, with different nickel and sulfur contents. In all catalysts, an ESR signal with an apparent g value of 2.015 was found, which was assigned to W^{3+} ions at the surface in a sulfur coordination of low symmetry.[106] The linear correlation between the intensity of the ESR signal and the rate constant is given in Figure 4, covering more than three orders of magnitude in activity. The identity of the W^{3+} ion as a surface center was established by the proportionality between surface area and ESR intensity for a series of $Ni_{0.53}WS_2$ catalysts ground to various surface areas and by the response of the signal to exposure of the catalysts to

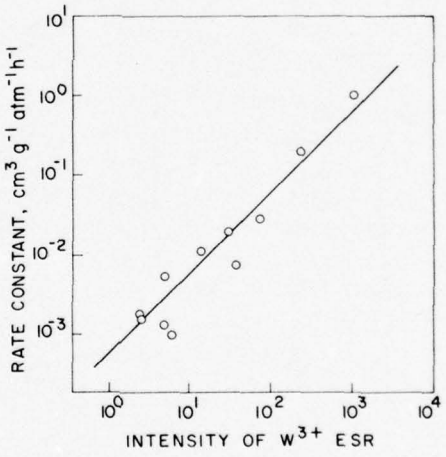

Fig. 4. Identification of W^{3+} as the active site in benzene hydrogenation over WS_2-based catalysts by the linear relation between the ESR intensity and the hydrogenation rate constant. (After Voorhoeve.[105])

benzene and cyclohexene. The dependence on equilibration of the catalyst with H_2S/H_2 mixtures showed that the W^{3+} center was associated with an S^{2-} anion vacancy and the temperature dependence of the signal intensity indicated that tungsten was in a low-spin configuration with spin $S = \frac{1}{2}$. On the basis of this information and stereochemical considerations, the structures of Figure 5 have been suggested for this active center.[107,108] In the WS_2 platelike layer structure, the W^{3+} sites must on energetic grounds occur at the edge of the plates. Benzene is postulated to adsorb as a π-bonded complex.

The active site for hydrogenation of butylmercaptan over MoS_2 has been proposed to be a Mo^{3+} ion on the basis of electrical conductivity measurements[109] and Schuit *et al.*,[62,110,111] on the basis of the analogy with Ni–WS_2 and extensive chemical evidence, have concluded that the active sites in Co–MoS_2 hydrodesulfurization catalysts are Mo^{3+} ions in similar coordination as the W^{3+} sites in Figure 5.

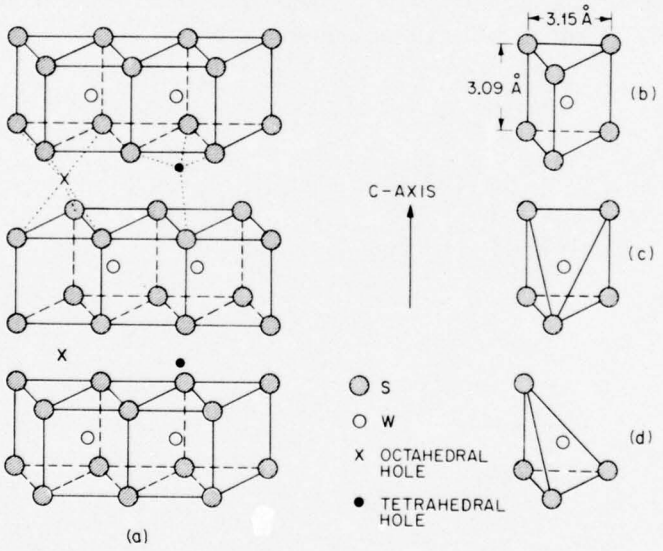

Fig. 5. The structure of tungsten disulfide: (a) The stacking of layers illustrating the position of octahedral holes, which may be partly occupied by nickel; (b) the site symmetry of tungsten ions in the bulk; (c) same for a side face; (d) same for an edge parallel to the *c* axis. (After Voorhoeve and Stuiver.[107])

3.4.2. Active Sites for H_2–D_2 Exchange on MgO

Isotopic exchange between H_2 and D_2 molecules can occur at low temperatures over some transition metal catalysts and over some transition metal oxide catalysts. This process is thought to proceed by dissociative hydrogen chemisorption on the transition metal or its ion.

MgO is also capable of catalyzing H_2–D_2 exchange at 70°K[112] and Harkins *et al.*[113] and Lunsford[114] had suggested that an ESR-active V_I center (a trapped hole) was the active site. Boudart *et al.*[115] have related the rate of exchange to ESR measurements of the concentration of the active site (EPR signal at $g = 2.0030$ and designated V_I) responsible for the catalytic activity. It was found that various MgO powders could be prepared by heating in such a way that their specific activity for exchange varied over a wide range. Heating removes protons, deactivates the catalyst, and causes the ESR signal to decrease. The catalytic activity and the ESR signal

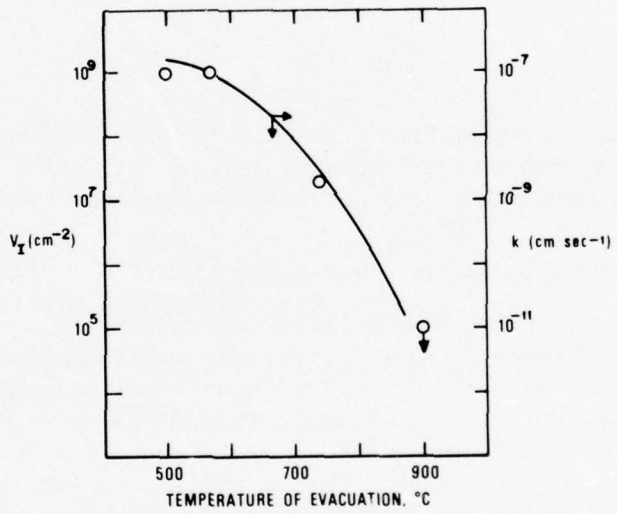

Fig. 6. Correlation of catalytic activity with active site density. The rate constant k for H_2–D_2 exchange at 78°K on MgO following heating in vacuum at various temperatures is shown. The solid line represents the rate constant data and the points represent the measured surface concentration of paramagnetic centers responsible for catalytic exchange. The 900°C point is plotted at the lower limit of sensitivity of the ESR spectrometer. (From Boudart *et al.*[115])

may be restored by treatment of the heated MgO with H_2O. Figure 6 shows that the H_2–D_2 catalytic exchange activity (solid line) varied in parallel to the concentration (circles) of V_I sites over a wide range. No ESR signal was obtained for the catalyst with the lowest activity and the corresponding point at 900°C is plotted at the lower limit of sensitivity of the ESR spectrometer.

The paramagnetic V_I centers are thought to be at the MgO surface because of the rapidity of response of characteristic ESR signals upon exposure to $O_2(g)$ and to $H_2O(g)$, i.e., the sites may be quantitatively titrated. Boudart *et al.*[115] argue that the active site consists of three O^- ions arranged in a triangle on the MgO (111) surface. Adjacent to this site is an OH^- group, which participates in exchange with a D_2 molecule adsorbed between the two closest O^- ions, in an orientation that allows a triangular transition complex to form,

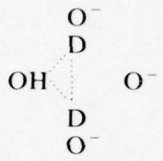

permitting exchange. Such a triangular O^- site should coordinate effectively with lone-pair electrons in H_2O or O_2, with resultant line broadening. The observed spectrum is in agreement with this.

3.4.3. Active Sites for H_2 Chemisorption by ZnO

The adsorption of H_2 by ZnO occurs via two parallel processes, designated Type I and Type II. Type I adsorption is rapid and reversible. Eischens *et al.*[116] found that it yields intense infrared spectra. Type II adsorption is slow and irreversible, and does not yield infrared-detectable species.[116]

Type I chemisorption is accompanied by the development of two infrared bands corresponding to ZnH (1709 cm^{-1}) and OH (3489 cm^{-1}) vibrations.[116] Recently, Kokes *et al.*[117] have probed the nature of the active sites involved in Type I H_2 chemisorption by chemisorption of pure HD. If we envision the active site to be schematically

Zn–O

then HD can chemisorb either as

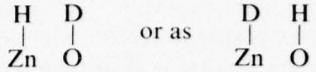

These two structures can be easily distinguished spectroscopically. Upon adsorption at 78°K, the kinetic isotope effect favours the "Zn D" species significantly, while at room temperature the "Zn H" species is favored thermodynamically; at 78°K the Zn D is spectroscopically observed to be favored over the Zn H. Warming to ~250°K causes a rapid and thermally *irreversible* switch as the thermodynamically favored "Zn H" species is formed, as shown in Figure 7. These simple measurements thus indicate that the active site in this case is in fact a Zn–O *pair* site since intensity ratios cannot easily be explained by models involving large separation of the H and D atoms following HD chemisorption at 78°K.

Thus we see from these three examples that in favorable cases it is now possible to correlate spectroscopic measurements with catalytic activity although an underlying physical interpretation may be missing.

3.4.4. Active Sites on Metal Catalysts

If one asks about the status of active site characterization on metal catalysts, it must be said at present that our understanding is not as good as in the specific cases for the oxides described above. As will be discussed later, Boudart[8,103] has divided catalytic reactions

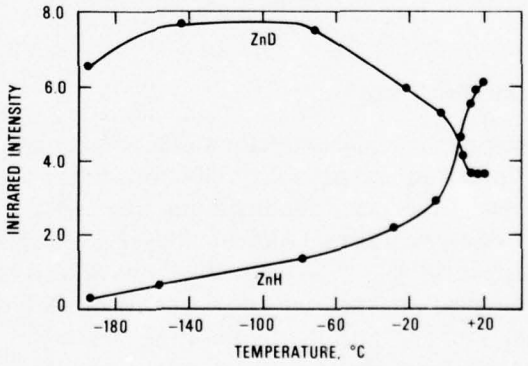

Fig. 7. Infrared measurement of the thermal equilibration of species produced by adsorption of HD on ZnO at −195°C. (From Kokes *et al.*[117])

on metals into two general groups: the *facile* reactions and the *demanding* reactions. Facile reactions are classed as those where specific catalytic activity seems to be kinetically independent of particle size. Demanding reactions occur on surfaces having specific catalytic activity that depends upon catalyst particle size and method of preparation. It is inferred that facile reactions occur generally on most surface sites, whereas demanding reactions may proceed only on specific active sites whose nature can be inferred by indirect means. Several examples of crystallographic effects on surface reactivity of metals are discussed in Section 6.1.

4. The Modern Theory and Spectroscopy of Chemisorption

In recent years, there has been a surge of interest from theorists and experimental physicists in problems associated with surfaces, chemisorption, and catalysis. The theoretical efforts include studies of vibrational surface modes,[118-120] which are important in the understanding of phase transitions at the surface and in phonon-assisted surface chemical processes. Other studies stressing the collective nature of the solid deal with the magnetic properties of surfaces,[121] a subject that is of particular relevance for catalysis on ferromagnetic catalysts. On these catalysts, spin density waves are thought to contribute directly to the kinetics of desorption,[122] and a mean field theory of surface spin fluctuations is being developed.[123,124] The dynamics of dielectric surfaces, a subject that is especially interesting for the effect of ferroelectric phase transitions on the catalytic rate, has been reviewed recently by Kliewer and Fuchs.[125]

4.1. First-Principles Theories

The electronics of semiconductor surfaces, especially Si and Ge, has been studied in detail with self-consistent pseudopotential methods, which have been successful in treating the bulk band structure as well as the intrinsic surface states in good agreement with optical experiments.[126,127] These methods have also been applied to obtain a detailed picture of the covalent adsorption of atomic H on Si and Ge.[128,129]

Chemisorption on transition metals is in a much less clear-cut position. Various theories have been developed, which vary in their approach from an entirely collective picture taking into account the

itinerant electrons of the metal as a first determinant of the chemisorption system, to a free molecule picture in which only one or two metal atoms react with the chemisorbing molecule to form a free compound molecule. Most of these theories are still rather remote from experimental tests and we will not be able to devote much space to them within the scope of this chapter.

The most widespread models for the chemisorption on metals are:

(a) The Anderson model, which was originally given for impurities in dilute magnetic alloys[130] and which uses a virtual level and restricted Coulomb and exchange interactions. It was applied by Newns[131] to chemisorption on refractory metals.

(b) The density functional formalism as used by Smith *et al.*,[132] which treats the substrate as an electron gas.

(c) The induced covalent-bond mechanism introduced by Schrieffer and Gomer,[133] which is based on the surface molecule approach also used by Grimley.[134]

The last approach has been reviewed recently.[135,136] The application of the Anderson model to the adsorption of hydrogen and oxygen on Pd, Ni, etc., leads to difficulties due to the neglect of correlation, while the induced-covalent-bond mechanism overemphasizes correlation. A phenomenological model has been proposed which seeks a middle ground between these models.[137]

Schrieffer *et al.*[133,136,138] have further developed the induced-covalent-bond theory. In analogy with the Heitler–London treatment of H_2, the overlap between the orbital of the adsorbed hydrogen atom and the orbitals of the metal is of crucial importance. Calculation of the local density of states for the atomic *d* orbitals on the surface atom(s) forming the adsorption site provides a chemically appealing way of judging the mode of chemisorption.[136] The methods used are rather approximate, in that matrix elements of the Hamiltonian are taken to be zero on any but nearest-neighbor atoms, while the remaining matrix elements are fitted to the known bulk energy bands.

The concept of a "surface molecule" as an approximation to the description of a chemisorbed species has been considered by Grimley[134] and Thorpe.[139] A surface compound could be constructed by using in chemisorption the atomic orbitals of metal surface atoms that are not involved in bonding to the bulk. But the energies of the orbitals formed must lie outside the energy bands of the metal with

which they interact, or they will be so highly delocalized as to destroy the concept of a surface compound with discrete orbital energies (although a particular geometric configuration may be retained with delocalized bonding electrons). Grimley points out that if the coupling of metal atomic orbitals to the adsorbate is stronger than the metal–metal coupling, then it is still useful to start with the concept of a surface molecule, calculate the orbital energies and wave functions, and then allow for interaction with the itinerant electron states of the rest of the metal. If this latter interaction is weak, the levels will be shifted and broadened even in the vicinity of the conduction band. Grimley has applied these general ideas to the chemisorption of CO on Ni and other metals and he shows that reasonable but arbitrary choices of chemisorption parameters give metal–CO bond strengths which are in qualitative agreement with experimental measurements.

Less approximate calculations are feasible if the size of the adatom–substrate system is limited to a few atoms. Einstein[140] has proceeded this way, taking into account a three-atom chain with adatom Coulomb repulsion, adatom–substrate hopping, and substrate bandwidth as variables. These calculations show that for a weakly bonded adatom, second-order perturbation theory yields a very good approximation of the binding energy. For strong binding, a surface complex (diatomic molecule) perturbatively rebonded to the indented chain gives a solution for the intermediate case which is more accurate than Hartree–Fock approximations. The rebonded surface complex is formed as a single orbital detaches from the chain to form a diatomic covalent molecule with the adatom, in much the same way as the "surface molecule" of Grimley.

A more drastic simplification of the system is provided by the "reaction" of two metal atoms in a dimer with the hydrogen molecule.[141,142] The advantage of this scheme is that it becomes possible to calculate the *energy surface* of the four-center system and to follow the importance of the contribution of various orbitals in the basis set in a generalized valence bond calculation.[141] This was done for the $Ni_2 + H_2 \rightarrow 2NiH$ and $Cu_2 + H_2 \rightarrow 2CuH$ reactions, with the interesting result that the Ni 3*d* orbitals had their main contribution in the lowering of the activation barrier associated with orbital symmetry effects.[141]

The use of molecular orbital theory to describe chemisorption leads naturally to the calculation of the energy levels of a molecular aggregate containing a limited number of substrate atoms in addition to the chemisorbed molecule. Therefore, a computational scheme

developed for large molecules and clusters appears to be of particular use in chemisorption problems. This is the SCF-Xα-SW cluster method developed by Slater and Johnson[50,51] from Johnson's multiple-scattered-wave formalism combined with Slater's self-consistent field method using a statistical α parameter to include exchange correlation. Fundamental to the method is the partition of the cluster into Wigner–Seitz spheres surrounding the atoms. The regions between the spheres are represented by a volume-averaged potential and the whole cluster is enclosed in a sphere, outside of which again a spherically averaged potential is used. Schrödinger's equation is solved in each region and the wave functions and their first derivatives are joined continuously across the boundaries separating the adjacent regions; this matching is achieved using a multiple-scattered-wave approach. The charge density throughout the cluster is then computed, and used (together with Poisson's equation and the Xα exchange-correlation expression) to generate a new molecular potential for which Schrödinger's equation can again be solved. The whole procedure is iterated until self-consistency is reached. The method has been shown[143] to give the correct orbital orderings consistent with Hartree–Fock calculations for the SF_6 molecule and to give orbital energies in very good agreement with ESCA results. It has subsequently been used to calculate energy levels of clusters M_i, where M = Li, Cu, or Ni and $2 \leq i \leq 13$, as well as the levels for NiO_6^{10-}, MnO_4^-, and SiO_2.[51] In chemisorption problems, it has been applied to the adsorption of chalcogens on the (001) "surface" of a Ni_5 cluster[144] and to the chemisorption of CO on the same type of Ni_5[145,146] cluster. A somewhat similar technique, in which no spherical averaging of the potential is used but which is not self-consistent, has been applied to the same adsorption system, CO on (001) Ni_4.[147] The preliminary results by Batra and Bagus are shown in Figure 8 with the early experiments of Eastman and Cashion.[148] The correspondence is reasonably good, but is rather sensitive to the parameters used (cf. Ref. 145 and 146). Interestingly, interaction of CO with the Ni surface perturbed the CO levels to the point where the ordering of the 5σ (lone pair) and 1π levels of adsorbed CO are reversed with respect to their ordering in gas-phase CO. This result is consistent with more extensive calculations using the SCF-Xα-SW procedure on a series of metal carbonyls.[149] The calculations show general support for the idea of "back bonding", i.e., charge transfer from *d* orbitals of the metal into the lowest π^* orbital of CO, but they also show that *s*, *p*, and *d* orbitals on the metal are all involved in the

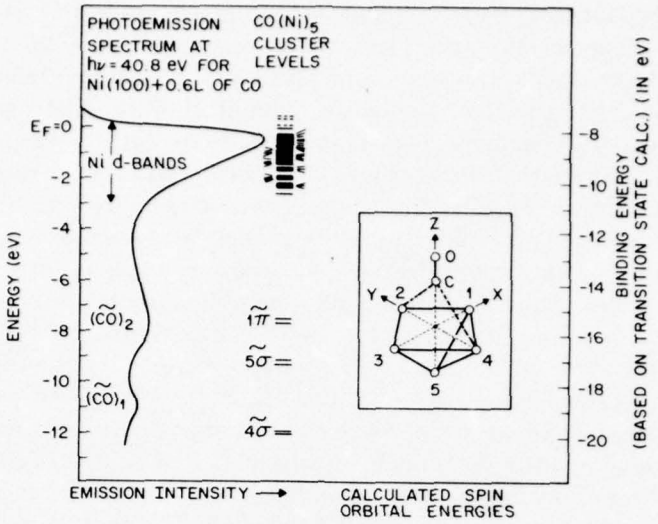

Fig. 8. Comparison of theoretical spin-unrestricted energy levels for the $CO(Ni)_5$ cluster and experimental photoemission spectrum of CO chemisorbed on Ni(100). The insert shows the model cluster. (Experimental data from Eastman and Cashion,[148] calculations and figure from Batra and Bagus.[146])

bonding. The experimental identification of the levels for CO on Ni is discussed in Section 4.3.

4.2. Empirical and Semiempirical Methods

The foregoing methods were quite restricted in the size of the system that could be treated, or in the approximation necessary to obtain a tractable model. Empirical methods, on the other hand, have shown a wide range of application to catalytic problems. The price paid is the danger of "overinterpretation" of the results. We will discuss the CFSO–BEBO model and extended Hückel calculations as applied to chemisorption and catalysis.

4.2.1. The Crystal Field Surface Orbital–Bond Energy Bond Order Model (CFSO–BEBO)

This highly empirical model devised by Weinberg and Merrill[150,151] allows kinetic and thermodynamic predictions

regarding adsorption and reaction of gases at surfaces. The model combines features of the bond energy–bond order relationships found in molecular spectroscopy with the concepts of crystal field theory. The basic assumptions of the CFSO–BEBO approach are as follows:

(1) The surface bond is a localized covalent bond involving primarily *d* electrons of the solid; the electronic structure of the solid is taken from the Engel–Brewer rules.

(2) Adsorption positions on the surface are those sites where strong directional bonding is expected based on predictions of crystal field theory. "Dangling bonds" at the surface are oriented in directions consistent with bonding in the bulk.

(3) The bond energy between two atoms involved in the surface bond is assumed to vary with bond distance and bond order as predicted by spectroscopic measurements of model compounds.

(4) The energy of a single order bond is derived from data on analogous bulk compounds.

To illustrate the model, the CFSO *d* orbitals associated with the Pt(111) surface are indicated in Figure 9.[151] There are no *d* orbitals that emerge from the surface atoms orthogonal to the surface plane; they emerge so that each interstitial position on the surface is a possible center for strong bonding. Half of these positions are out-of-the-plane intersections of three orbitals with e_g symmetry, and half

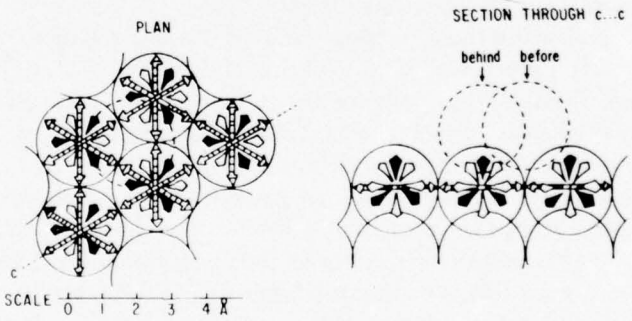

Fig. 9. Crystal field surface orbitals (CFSO) emerging from the Pt(111) surface. Filled arrows: e_g orbitals emerging at an angle of 35°16′ with the (111) plane and intersecting at an angle of 90° in the plane of intersection. Open arrows: t_{2g} orbitals emerging at an angle of 54°44′ with the (111) plane and intersecting at an angle of 60° in the plane of intersection. Cross-hatched arrows: bonding orbitals in the plane of the surface. (From Weinberg *et al.*[151])

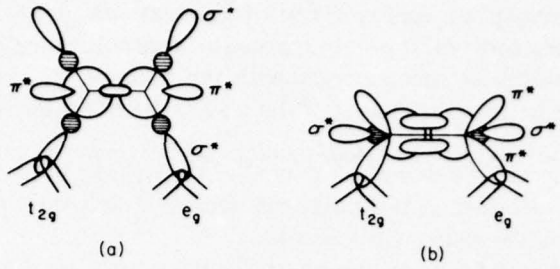

Fig. 10. Orbital models illustrating symmetry-allowed interactions of ethylene on a Pt(111) surface which lead to associative adsorption: (a) formation of Pt–H surface bonds; (b) formation of Pt–C surface bonds. CFSO–BEBO calculations indicate that adsorption into configuration (a) is an endothermic process, whereas configuration (b) is an exothermic interaction. (From Weinberg *et al.*[151])

with t_{2g} symmetry. Based on the model assumptions, predictions of several relevant quantities in gas–surface interactions have been made, namely: (1) binding energies for both atomic and molecular adsorbed species and (2) activation energies for both dissociative and nondissociative chemisorption. The model has been applied to such systems as H_2, CO, H_2O, CO_2, and C_2H_4 on Pt and Ni surfaces with a surprising degree of success.

Predictions of the adsorption and decomposition of ethylene on Pt(111) have agreed well with experimental data.[151] CFSO–BEBO calculations have been made for the two symmetry-allowed interactions of C_2H_4 with Pt(111), which are illustrated in Figure 10. The results indicate that the orientation of Figure 10a, with the initial formation of Pt–H bonds, leads to an endothermic interaction with appreciable activation energy and low sticking probability, clearly an unfavorable situation. In contrast, the formation of Pt–C bonds, as shown in Figure 10b, is exothermic, resulting in dissociation of C_2H_4 to form an acetylenic complex and two adsorbed H atoms. In addition, the calculations predict that the acetylenic surface complex in the first monolayer can adsorb a second ethylene by a type of hydrogen bonding, and that heating the saturated surface leads to further decomposition, resulting in desorption of H_2 and nucleation of a graphite layer. All of these predictions are in good agreement with experiment.

In summary, the CFSO–BEBO treatment is a highly empirical model calculation which provides a useful insight into the energetics and mechanisms of chemisorption and catalysis.

4.2.2. Extended Hückel Methods and Orbital Symmetry

Extended Hückel molecular orbital methods have been extensively applied to organic molecules by Hoffmann[152] and to transition metal complexes by Ballhausen and Gray[153] and Fenske *et al.*[154] Mango and Schachtschneider[40,156] have used a self-consistent charge and configuration (SCCC–EHT) variation of this method in an intercomparison of the effects of various metals on ligand reactions. They point out: "In our opinion the iterative extended Hückel method in any of its variations gives at best a crude description of the ground state of the molecule and hopefully the correct ordering of the highest few filled and lowest few empty molecular orbitals. It should be used only for comparative calculations in a series of related molecules or configurations or to obtain a crude picture of the ground state molecular obitals."[40] The ordering of the highest few filled and lowest few empty orbitals is of importance to apply the concept of "symmetry-allowed" and "symmetry-forbidden" reactions to the catalysis by transition metal surfaces.[40] In view of the prominence of these ideas, based on the Woodward–Hoffmann orbital symmetry conservation rules, in present-day catalytic thought,[157] it is appropriate to give a short outline here, following Mango and Schachtschneider. However, at the outset it should be stressed that the application of the Woodward–Hoffmann rules to catalysis is based on the assumption of *concerted* reactions with high-symmetry transition states, whereas alternative mechanistic schemes are sometimes more likely.[158]

The formation of cyclobutane 1,2 and 3,4 σ bonds by the concerted fusion of two olefin π bonds is a symmetry-forbidden reaction (Figure 11a). This can be understood from the symmetry of the molecular orbitals of cyclobutane and the symmetry of the molecular orbitals formed by the interacting olefinic π systems. The symmetry elements are the ZX and YZ planes in Figure 11a, with Z being the fourfold symmetry axis. The orbitals of the olefinic systems ($\pi_{1,4} \pm \pi_{2,3}$ and $\pi^*_{1,4} \pm \pi^*_{2,3}$) and of the cyclobutane ring (σ and σ^*) are classified as symmetric (S) or antisymmetric (A) about the ZX and YZ planes (Figure 11b). This correlation diagram shows that the highest occupied MO of the reactant system has the same symmetry

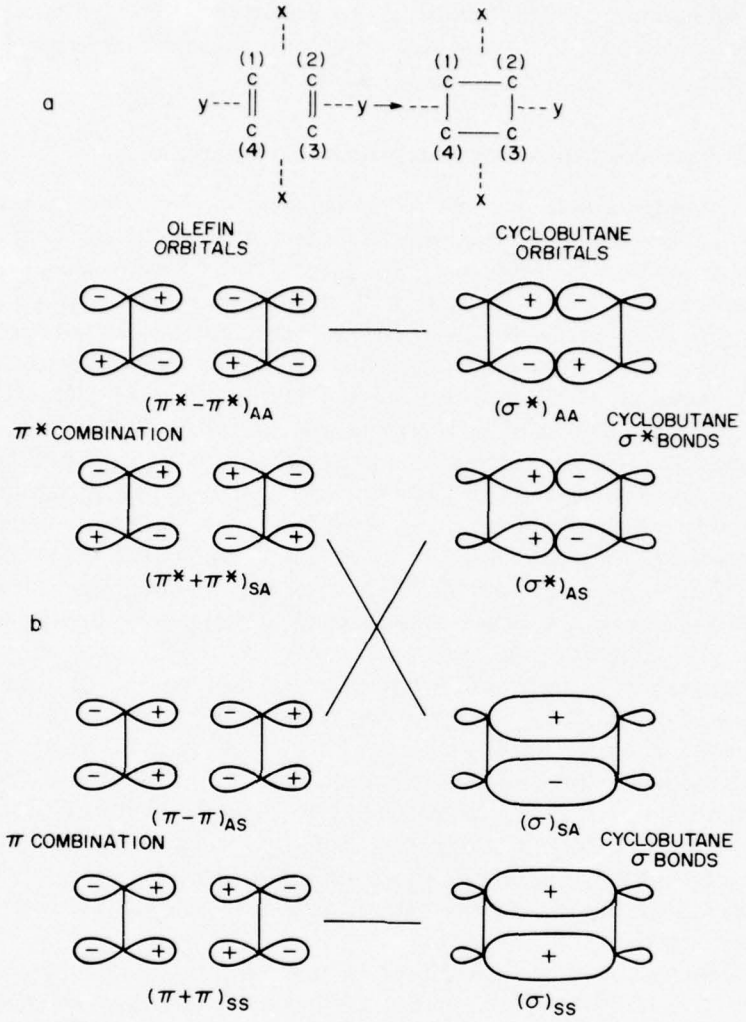

Fig. 11. (a) Transition state symmetry and (b) orbital correlation diagram for the homogeneous cyclobutanation of ethylene. In (a), the hydrogen atoms have been omitted for clarity. (After Mango and Schachtschneider.[40])

as the lowest unoccupied MO of the product, which leads to a high-energy excited state of the cyclobutane. The postulate of conservation of orbital symmetry during concerted reactions[159] makes it impossible to change symmetry during the reaction and hence prevents

transition from the ground state $[(\pi + \pi)^2_{SS}, (\pi - \pi)^2_{AS}]$ to the ground state $[(\sigma)^2_{SS}, (\sigma)^2_{SA}]$. This postulate has been shown by Pearson to stem from the requirements of nonzero overlap between high-energy, occupied MO's of the initial state and low-energy, empty MO's of the final state.[160] It has very general validity.[157,160]

The symmetry restriction can be removed if the olefin molecules are coordinated to an appropriate transition metal atom. This is the basis of the widespread occurrence of catalysis of symmetry-forbidden

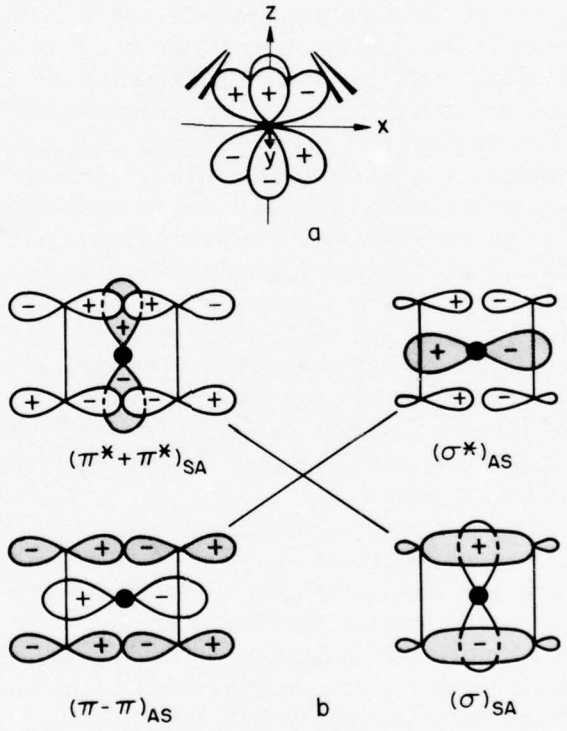

Fig. 12. Catalysis of a symmetry-forbidden reaction by a *d* metal. (a) Two olefin ligands occupying adjacent positions in the metal complex, with d_{yz} and d_{zx} orbitals shown. These have SA and AS symmetry, respectively. (b) The exchange of electron pairs between ligands and metal proceeding through orbitals of SA and AS symmetries. Shaded orbitals are occupied. (After Mango and Schachtschneider.[40])

reactions.[40,156,161] As an illustration, we return to the [2 + 2]-cycloaddition of olefins. In Figure 12a, the olefins are coordinated to the d orbitals of a metal atom on the Z axis under the XY plane. The d orbitals have the proper symmetry to accept electrons from the orbitals that are being raised in energy during the reaction [i.e., $(\pi - \pi)_{AS} \leftrightarrow (\sigma^*)_{AS}$] and to donate electrons to the orbitals that are being lowered in energy during the reaction [i.e., $(\pi^* + \pi^*)_{SA} \leftrightarrow (\sigma)_{SA}$]. This is shown graphically in Figure 12b, where the shading indicates occupied orbitals. To perform this function effectively, the metal can use nearly equivalent nonbonding orbitals of the proper symmetry and a pair of nonbonding electrons. The energy of the d levels used has an optimum position with respect to the π-orbital combinations.[40] The ordering of the d levels of the transition metal atom is of crucial importance in deciding the effect of a given metal complex or metal surface atom on a forbidden reaction. The calculation of the ordering has been done by Mango and Schachtschneider for metal complexes, using the extended Hückel method.[40] The real question is not the positions of the lowest unoccupied and highest occupied levels in a set of MO's. For a chemical reaction to occur with a reasonable activation energy, there must be low-lying excited states for the reacting system of the same symmetry as the ground state.[160] In the exact wave function, we have to mix in the infinite sum of excited states with the ground state, at least in principle, to arrive at the energy of the barrier. In practice, it suffices to take the few lowest-lying states. However, if the density of states in this region is high (many excited states in a small energy increment), then an appreciable number will have to be included.

Orbital symmetry rules define a class of reactions which require a catalyst to proceed. The availability of many atomic orbitals at the surface of a solid generally permits the construction of hybrid orbitals of the proper symmetry for the reaction to proceed.[162]

The extended Hückel method in a non-self-consistent form has been applied to the dissociative chemisorption of diatomic molecules and ethylene on transition metal surfaces, e.g., Ni and W.[163] The lack of self-consistency leads to unrealistic charge distributions for some of the adsorbates. It appears to be too early to decide whether this application of the extended Hückel method gives useful results. The effects of changing the parameters used in the calculation on the results obtained have not yet been examined. In this respect we recall Mango and Schachtschneider's cautionary remarks for the iterative SCCC–EHT quoted above, which must apply a fortiori to the simple EHT.

4.3. Spectroscopy of Surface Molecules and Localized Orbitals at Surfaces

The concept that a chemisorbed species involves localized covalent bonding to atoms in a surface was present in the earliest models of chemisorption. The surface bond(s) formed upon chemisorption have long been thought to be analogous to bonds in chemical compounds.

It is only within the past 20 years or so that spectroscopic methods for probing surfaces have been generally available for detailed characterization of bonding with the chemisorbed layer. The first of these techniques was infrared spectroscopy, followed recently by electron–diffraction, ion scattering, and various electron spectroscopy methods.[164,165] Within the past ten years, theoretical models involving the concept of a local surface molecule have begun to prove useful in calculations relating to chemisorptive bonding, as has been discussed previously.

Infrared spectroscopy was first used to characterize chemisorbed CO species in 1954 by Eischens *et al.*,[166] although the method was used by Terenin[167] in the early 1940's to observe hydroxyl groups present on the surface of oxides. Eischens[166] applied transmission infrared spectroscopy to supported catalysts containing metallic Cu, Ni, Pt, and Pd. The C–O stretching vibration for chemisorbed CO was observed by passing infrared radiation through the supported catalyst samples. Following this pioneering work, the transmission infrared technique has been widely applied to surfaces, and many interesting results have been reviewed in two books.[168,169] Infrared spectroscopy is currently used widely for studies of catalytic materials.

In general, it has been found that the principles useful in interpreting the infrared spectra of chemical compounds are applicable to species on surfaces also. Thus, the concept of group vibrational frequencies, where particular structural groups of atoms are associated with characteristic vibrational frequencies, applies well on surfaces just as it does in molecules. Minor variations in the group vibrational frequency associated with a particular group of atoms may often be attributed to interactions either within the molecule, or between adsorbed molecules, or between the molecule and the surface. Because of the limited spectral range and the low absolute intensities often available in infrared studies on supported surfaces, it is usually not possible to observe a complete infrared spectrum of the chemisorbed species, so that the determination of force constants and molecular

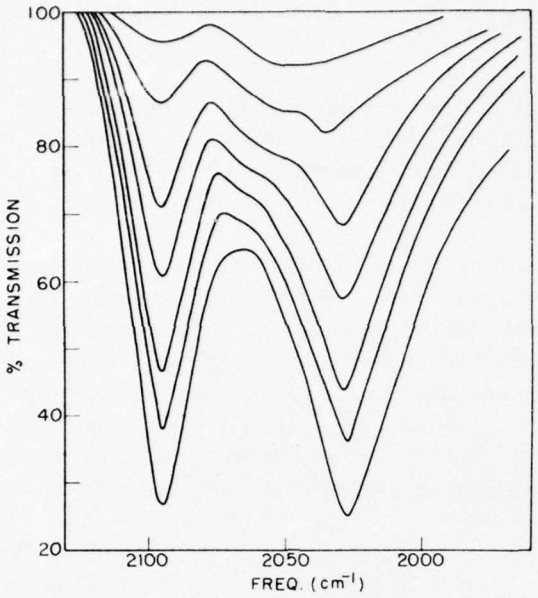

Fig. 13. Infrared spectrum of chemisorbed CO on an unsintered Rh catalyst (2%) supported on Al_2O_3. The development of the carbonyl absorption bands corresponds to increasing the equilibration pressure and surface coverage of CO. Curves are for 1.3×10^{-3} Torr (top curve) to 25.6×10^{-3} Torr (bottom curve) at 300°K. (From Yang and Garland.[170])

geometry of the adsorbed species cannot usually be done as with the more complete spectra of molecules. Thus, arguments about the structure of surface species are often based upon spectral analogies with compounds of known structure. An excellent example of this method, illustrated below, is the comparison of the infrared spectrum of CO chemisorbed on Rh with the spectrum of a Rh carbonyl complex.[170]

In Figure 13, a series of infrared spectra corresponding to the C–O vibrations for increasing CO coverage on highly dispersed Rh is shown. It is seen that two major absorption bands develop together at 2095 and 2027 cm^{-1}. The two major bands are thought to be due to symmetric and antisymmetric C–O stretching vibrations, which could

arise through coupling in an adsorbed species, such as

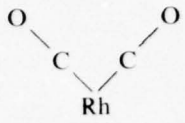

A *single* C–O stretching vibration would be expected to occur at an intermediate frequency for the adsorption of a *single* CO by Rh, and such a species may be responsible for the smaller 2045 cm^{-1} band observed. A comparison with the infrared spectrum (Figure 14) of the $Rh_2(CO)_4Cl_2$ molecule of known structure,[171] namely

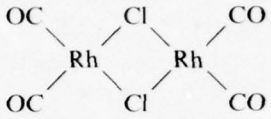

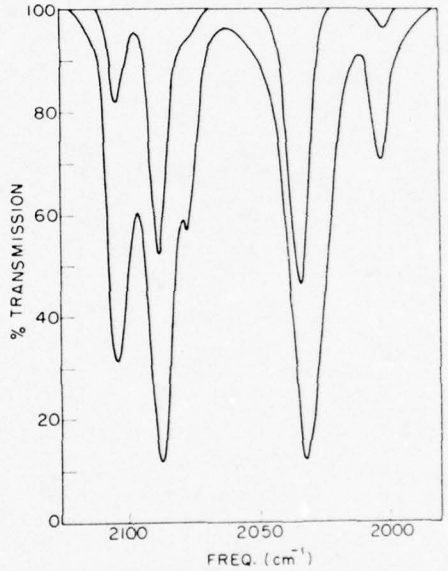

Fig. 14. Infrared spectrum of $Rh_2(CO)_4Cl_2$ in the carbonyl stretch region. Upper curve: CCl_4 solvent. Lower curve: Nujol mull. The strong similarity between these spectra and those of chemisorbed CO in Rh (Figure 13) suggests that two CO molecules chemisorb per Rh atom. (From Yang and Garland.[170])

demonstrates the strong correspondence between the spectra and gives confirmation to the assignment of a double-CO surface species. In the carbonyl spectrum, symmetric and antisymmetric coupling between CO ligands gives two strong bands at 2033 and 2088 cm^{-1}, accompanied by weaker overtones at 2022 and 2104 cm^{-1}. This example shows the usefulness of structural analogies between surface species and chemical compounds. The analogy between chemisorbed CO and metal carbonyls has been extended[172] to include intensity comparisons as well as small spectral shifts due to local electron donation effects in the vicinity of the adsorbed CO species. Recently, infrared spectra of CO adsorbed on atomically clean metal surfaces have been obtained by reflection spectroscopy[173] and compared to spectra on supported metals.[174] In addition to observations of the C–O stretching vibration, it would be useful to observe the lower frequency M–C vibration also, and this has been done by Blyholder,[175] who suspended the metal adsorbent particles in a transparent oil. Measurements in an oil suspension are likely to be influenced by

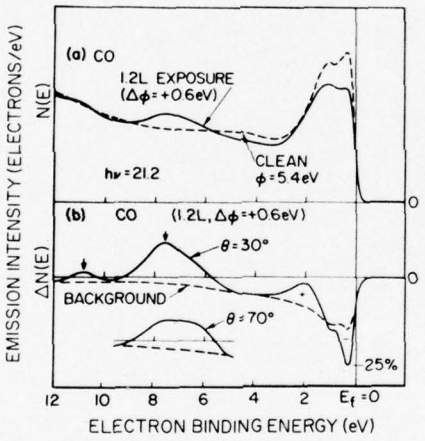

Fig. 15. Ultraviolet photoemission spectra of CO chemisorbed on a Ni(111) crystal. (a) Spectrum of clean surface (dashed curve) compared to spectrum of surface exposed to 1.2 Langmuirs of CO at 300°K. (b) Difference spectra at two angles of incidence of photon beam showing extra features assigned to various molecular orbitals. (From Eastman and Demuth.[176])

contamination effects, although the adsorption of CO may displace some contaminant species.

The character of a surface molecule may be further defined by studies of the distribution of electronic states associated with the chemisorbed species. These measurements are now being made by means of photoelectron spectroscopy using monochromatic ultraviolet excitation. Photoelectrons emitted from the surface containing a chemisorbed layer are energy-analyzed and compared with the photoelectron spectrum from the clean surface. Typical data[176] for the adsorption of CO by Ni(111) are shown in Figure 15, where 21.2-eV ultraviolet radiation has been used for excitation. It is seen that CO adsorption leads to attenuation of emission from the Ni *d* band, 0 to ~ 3.5 eV below the Fermi edge E_F, and to new photoemission features at about -7.5 and -10.7 eV. The new features increase in intensity as CO coverage is increased, and are characteristic of the local surface molecule. There is some controversy about the assignment of the spectral features to particular molecular orbitals.[145,146,164,176,177] The assignments based on the SCF-Xα-SW calculations of Batra and Bagus[146] discussed in Section 4.1 were given in Figure 8. Calculations have also been done by Blyholder,[177] using the CNDO (complete neglect of differential overlap) method. This calculation also suggests that the -7.5-eV feature is caused by the overlap of the 5σ and 1π levels. The -10.7-eV feature is assigned to the 4σ level. A similar assignment has been made by Eastman *et al.*[176,178] and by Fuggle *et al.*[179] In view of the different assignments by the theoreticians and the difficulty in making assignments by analogy with gas-phase spectra, the question is still open as to the order of the 1π and 5σ levels. The experimental data[176,178] and Figure 15 further indicate a lowering of the intensity of the emission from the Ni 3*d* states near the Fermi level and an increase near -1.5 eV (or, equivalently, a shift of the *d* states to higher binding energy). This is indicative of the role of the *d* orbitals in the binding and is a generally observed phenomenon on *d* metals.[164,176,180]

More recently, Demuth and Eastman[49,176] have applied ultraviolet photoelectron spectroscopy to the study of hydrocarbon adsorption and subsequent catalytic decomposition. In their studies of benzene chemisorption by Ni(111) the π level of benzene is preserved by interaction with the surface, but is shifted to higher binding energy. In the case of the chemisorption of ethylene by Ni(111), it was found that at low temperatures (~ 100°K) the chemisorbed ethylene yields a spectrum similar to that of gaseous ethylene

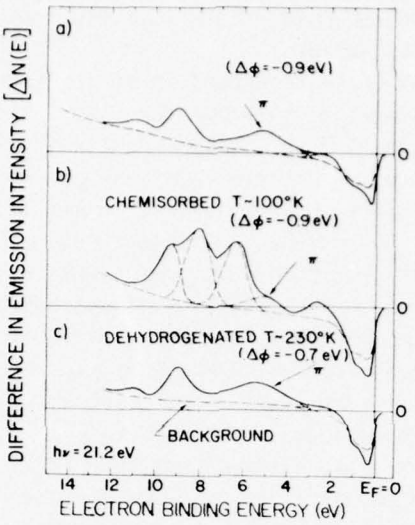

Fig. 16. Ultraviolet photoemission spectra for hydrocarbons adsorbed on Ni(111). (a) Acetylene chemisorption at ~100 or 300°K. (b) Ethylene adsorption at ~100°K. (c) Conversion of chemisorbed ethylene to chemisorbed acetylene achieved by heating (b) to ~230°K. Note the similarity between the spectra of chemisorbed acetylene and ethylene following dehydrogenation by heating. (From Demuth and Eastman.[49])

except for a shift of the π level to higher binding energy, as was seen for chemisorbed benzene. However, upon heating chemisorbed C_2H_4 to about 230°K, dehydrogenation is observed, leaving behind an acetylenic species whose photoemission spectrum is virtually identical to the spectrum found for chemisorbed C_2H_2. This result is shown in Figure 16 and demonstrates the usefulness of photoelectron spectroscopy in understanding catalytic reactions.

4.4. Long-Range Electron Interactions in the Surface Region

The models involving localized surface complexes suggest methods of treating chemical reactions at surfaces in terms of molecular aggregates and therefore do not logically include the possibility of longer range interactions between adsorbed species. One of the major

experimental discoveries about adsorbed layers in the last 15 years is the existence of long-range adsorbate ordering effects on single crystals containing less than a monolayer of adsorbed species.[181] The periodicity of the ordered overlayer is often two, three, or four substrate lattice spacings in a particular direction. These large unit cells may also be due in some cases to short-range interactions, e.g., size mismatch may give rise to coincidence lattices.[181] Coulomb repulsion of charged adsorbates also gives rise to large spacings. For instance, alkali metal adsorbates on Ni or W form, at low coverages, hexagonal arrays with a spacing which varies continuously with increasing coverage.[182] The large unit cells found on clean surfaces of Si and Ge have been explained by a variety of short-range interactions, such as the pairing of neighboring "dangling bonds" or the presence of surface vacancies combined with the formation of buckled "aromatic-like" rings of surface atoms.[183,184]

Long-range effects (such as a charge density wave caused by an instability in the Fermi surface) have been suggested as explanation for the large unit cells of Si and Ge surfaces.[185,186] Prior to the experimental observations of long-range adsorbate ordering, Koutecky[187] and Grimley[188–190] suggested that adsorbate–adsorbate interaction through the substrate might be important in chemisorption. As schematically indicated in Figure 17, the ground-state wave functions for electrons associated with two separated atoms in vacuum decrease quickly toward zero in the space between the nuclei;

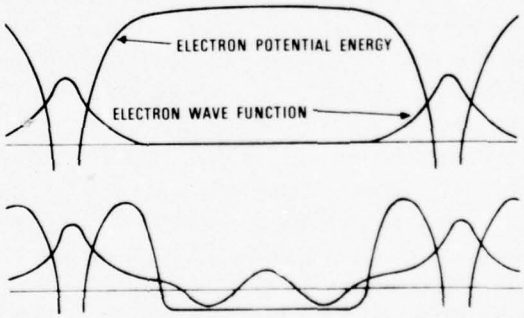

Fig. 17. Schematic illustration of the interaction between atoms. Upper figure: isolated atoms in vacuum, which undergo no interaction. Lower figure: atoms that interact indirectly when placed apart on a metal surface. (From Grimley.[188])

if, however, the nuclei are placed in contact with a metal surface, it is now possible for the electrons to move through the metal between the nuclei because of the lowered potential in the metal. An oscillatory wave function exists along the metal surface, giving rise to an indirect interaction between adsorbate atoms as shown in Figure 17. Grimley[188] first calculated the magnitude of this effect in the asymptotic limit of large spacing between adsorbate atoms on a structureless surface. Representing an adsorbate molecule by a broadened virtual level, he showed that interaction between two molecules will split these levels. Depending on the shape of the resulting double hump in the density of states, the electron occupancy may be either enhanced or decreased, provided that the Fermi level is within the energy range of the hump. For this to be the case, it is generally important that the virtual level is broad compared to its distance from the Fermi level.

Thus, the adsorption of alkali metals would be expected to undergo such indirect interactions because of their low ionization energies, whereas chemisorbed CO, with its highest occupied molecular orbital far below E_F, would not be expected to undergo indirect interaction in this model. However, H(ads) would be expected to undergo such interactions because of an extreme rise of its 1*s* atomic level to the vicinity of E_F due to the large Coulomb integral for this system.

Einstein and Schrieffer,[191] extending the ideas of Grimley, have calculated the indirect interaction for the (100) surface of a simple *s*-band solid. They succeed in explaining the frequently occurring (2×2), (2×4), etc., superstructures. Their model involves four parameters, the Fermi energy, the conduction bandwidth, the atomic energy of the free adatom orbital, and the hopping matrix, which mixes the adatom orbital with the surface orbitals of the substrate atoms. The parameters are adjusted to give an approximate chemisorption energy in agreement with experiments. The indirect adatom–adatom interaction is then calculated as a function of spacing. They conclude that the virtual level approximation of Grimley is not valid in general, since a surface complex will form having new bonding orbitals, which will probably lie in the vicinity of the Fermi level. However, in agreement with Grimley's general conclusions, it is found that the indirect interaction varies from repulsive to attractive as the spacing is changed between adatoms. Reasonable parameter choices [to simulate H(ads) + W(100)] suggest that the $c(2 \times 2)$

lattice structure should be stable and that the disordering temperature observed by LEED for this open surface structure is consistent with the interaction energy calculated. For the pair interaction, it is found that the indirect interaction energy is of the order of 5–10% of the chemisorption binding energy and decreases by a factor of 5–10 per lattice spacing. Furthermore, multibody forces are small compared to pair interactions even at high coverage.

These new concepts related to adsorption are of importance to heterogeneous catalysis in a general way. For instance, the displacement of one adsorbed species by another may be understood more easily if such adsorbate–adsorbate interactions are involved. Such displacement processes could alter the course of a catalytic reaction by changing the nature of the adsorbed layer at steady state. One experimental study using thermal desorption methods has shown that adsorbed CO significantly weakens the strength of adsorption of adsorbed H on the W(100) surface, and that the sign of the surface dipole changes during this interaction.[192] Similar work function results have been obtained on Ni films when H(ads) and CO(ads) interact.[193] It is possible that catalytic poisoning or catalytic activity enhancement by promoters may conceivably involve electronic effects similar to those discussed above. However, Schrieffer and Soven[136] stress that more realistic models must be studied before detailed comparison of the theory of indirect interactions with experiment will be meaningful.

5. Electronic Effects in Catalysis

In this section, we explore the influence of the electronic structure of the catalyst on the various steps in the catalytic process: chemisorption, nature of catalytic intermediate, rate of reaction (catalytic activity). In keeping with common usage, we distinguish between the "electronic factor" in catalysis and other electronic effects more specific to the catalyst surface. As discussed previously, the term "electronic factor" is used by most catalytic chemists to describe attempts to correlate catalytic activity with the bulk electronic properties of the catalyst. Such correlations will be discussed; in addition, present thinking regarding catalytic processes and the molecular orbital character of the catalyst surface will also be examined.

5.1. The "Electronic Factor" in Catalysis by Pure Metals

Atoms at the surface of a metal possess bonding capabilities not exhibited by either free atoms or atoms in the bulk of the solid. There exist at the surface of a solid free orbitals which may be available for bonding to an adsorbate; such orbitals are usually saturated in the bulk and may not be present at all in the free atom. Despite the clear uniqueness and complexity of the electronic character of the surface, it has frequently been assumed that there is some correspondence between the properties of bulk and surface atoms. It has been hoped that this correspondence will be reflected in a correlation between chemisorption behavior and bulk electronic properties, and ultimately, to correlation between catalytic activity and bulk electronic properties.[6]

In support of these ideas, there are distinct trends which have long been known from studies of chemisorption. Whereas oxygen is almost universally adsorbed on clean metal surfaces, certain metals are very specific to hydrogen or nitrogen chemisorption[194] (see Table 1). In general, heats of adsorption for molecules such as H_2 and N_2 are low for the noble metals in group VIII (Rh, Pd, Ir, Pt, etc.), and high for group VA and VIA metals (Ta, Nb, W, Mo, etc.). However, when one attempts to establish a *quantitative* correlation between the heats of adsorption and some electronic property of the solid, problems arise. Thus, the first problem to be faced in seeking such a correlation is: Is there an electronic property of a metal catalyst which *quantitatively* relates to its ability to chemisorb and participate in catalytic reactions? The two theories of the metallic state which have been considered are the band theory of solids and Pauling's valence bond theory.[13] It is clear that recent advances in band theory based on relativistic density-of-states calculations provide a fundamental view of the electronic structure of transition metals and alloys. Pauling's valence bond theory is an empirical formalism which ascribes metallic bonding in transition metals to *dsp*-hybridized orbitals, and assigns the metallic and magnetic properties to electrons in atomic *d* orbitals. The valence bond approach has often been the basis for correlations involving the "electronic factor" in catalysis[6]; the primary reason for this is the fact that a quantitative percentage *d* character can be assigned to the metallic bond in transition metals. Band theory has not yielded a simple quantity which by itself characterizes the bonding of the solid, and has not been as extensively applied to the studies of the electronic factor. There is, of course, a conceptual

correspondence between percentage *d* character and the existence of unfilled *d* bands in the band theory picture.

Attempts at correlations in the past have frequently been confused by inadequate and discordant results as well as the inadequate state of theory.[195] Recent attempts to relate catalytic activity to properties of the bulk solid have been discussed by Sinfelt[14] and by Anderson and Baker.[196] Sinfelt has systematically examined the specific catalytic activity of a series of metals for ethane hydrogenolysis, i.e.,

$$C_2H_6 + H_2 \rightarrow 2CH_4$$

A comparison of supported metals as hydrogenolysis catalysts reveals a dramatic variation in activity, even among similar metals. Figure 18 shows the specific activity of the group VIIA and group VIII metals for this reaction. The figure has three separate parts, representing transition metals of the first, second, and third transition series. The catalysts used in these experiments were silica-supported metals; specific activities were all relative reaction rates per unit surface area of metal at 205°C, and ethane and hydrogen partial pressures were 0.030 and 0.20 atm, respectively. Also shown in Figure 18 are plots of the percentage *d* character of the metallic bond, based on Pauling's valence bond theory.

Among the interesting observations which have been drawn from these data are the following.

(1) The maximum activity for ethane hydrogenolysis in both the second and third transition series is observed for the group $VIII_1$ metals, Ru and Os.

(2) The percentage *d* character correlates moderately well with catalytic activity in the second and third transition series.

(3) There is little correspondence between specific catalytic activity and percentage *d* character when one compares different series of the periodic table, e.g., the percentage *d* character of Ni is slightly less than that of Pt, but Ni is about 10^6 times more active than Pt. Sinfelt[14] has concluded that percentage *d* character is *not* an adequate parameter for characterization of the catalytic activity of transition metals for hydrogenolysis.

Sinfelt's specific observations for this reaction support a conclusion which has long been recognized, namely that a simple unifying theme for catalysis based on the "electronic factor" is probably illusory. Significantly, minute changes in percentage *d* character would have to be responsible for huge changes in catalytic activity. Still, it is anticipated that the observation of trends such as those

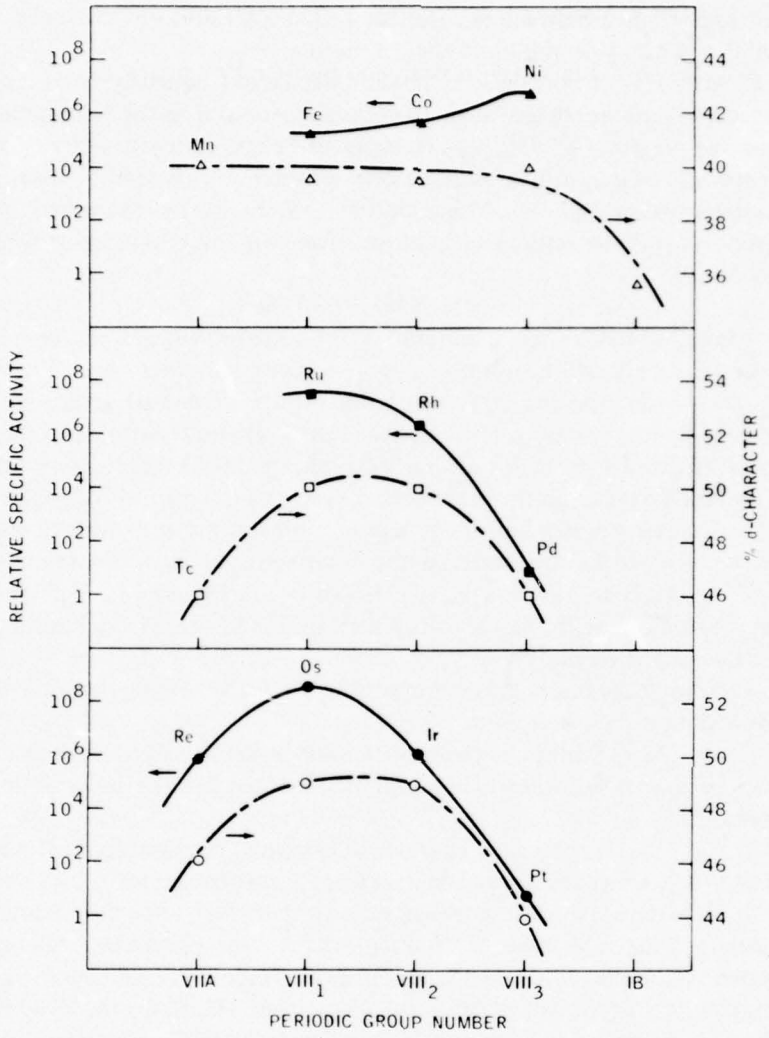

Fig. 18. Relationship between catalytic activity for ethane hydrogenolysis ($H_2 + C_2H_6 \rightarrow 2CH_4$) and the percentage *d* character of the metallic bond of the bulk solid catalyst, based on Pauling's valence bond theory. Three separate panels are shown in the figure to distinguish the metals in the different long rows of the periodic table. (From Sinfelt.[14])

shown in Figure 18 will continue to spur investigators to seek a key relating catalysis to solid-state physics and chemistry.

5.2. The "Electronic Factor" in Catalysis by Alloys

5.2.1. Relationship between Bulk and Surface Properties

Metal alloys have been investigated by a number of workers attempting to study the electronic factor in catalysis.[197,198] The existence of qualitative correlations between catalytic activity and partially filled *d* bands in transition metals has led to the expectation that catalytic activity of alloys would change abruptly once these vacancies were filled by alloying with an appropriate metal. These expectations were based on the rigid band theory of alloys,[199] which predicted that the *s* electrons contributed by the addition of IB metals to the metals of group VIII would fill the unoccupied *d* states on the group VIII metal. Examples of catalytic behavior in line with the rigid band model have been reported in several specific cases for alloy systems such as Pd–Au.[200] However, this close correlation between catalytic data and the rigid band theory proved fortuitous. Photoemission data on the electronic structure of Cu–Ni and Pd–Ag alloys have disproved the validity of the rigid band model[201] and in fact, have shown that the Anderson virtual bound state model is appropriate.[201,202] These data are shown in Figure 19. In addition, many more recent experimental observations have revealed that a simple band-theory picture of catalytic activity is inadequate:

(1) The catalytic activity of alloys depends very much on mode of preparation of the alloy (thin films, powders, wires, and ribbons).
(2) In general, there are major differences between bulk and surface composition of alloys. A further complication is the fact that the surface composition may change during the course of a catalytic reaction.

The activity of alloys formed from the catalytically different group VIII and group IB metals (Ni–Cu, Pd–Ag, Pd–Au) have been studied most extensively. The Pd–Au and Pd–Ag systems form a continuous series of fcc solid solutions over the entire composition range, i.e., they appear to have complete miscibility.[197] In contrast, alloying of Ni with Cu is an endothermic process which results in (a) the formation of single-phase solid solutions at high temperatures, and (b) phase separation due to a miscibility gap at low temperatures.[198] The influence of the expected phase separation on the surface composition of Ni–Cu alloys in the temperature range of

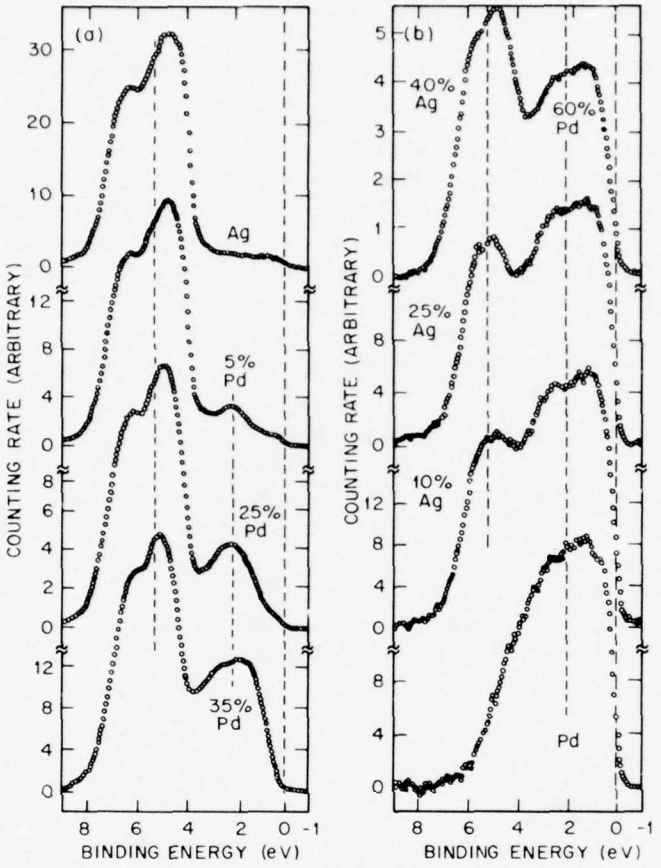

Fig. 19. Valence-band X-ray photoelectron spectra of AgPd alloys obtained with monochromatized X-rays. The alloy compositions refer to atomic fractions. Dashed vertical lines are drawn at the Fermi level and the approximate center of the *d* band for pure Ag and pure Pd. (From Hufner *et al.*[201])

catalytic interest ($\lesssim 400°C$) is an additional complication in the interpretation of catalytic data.

Sachtler and co-workers[203,204] first demontrated the difference between bulk and surface composition of Ni–Cu alloy films prepared by successive evaporation of the component metals under ultrahigh vacuum conditions. They predicted on the basis of a thermodynamic analysis[203] that alloy films sintered at 200°C should consist in two phases at equilibrium; Phase I contains 80% Cu and phase II

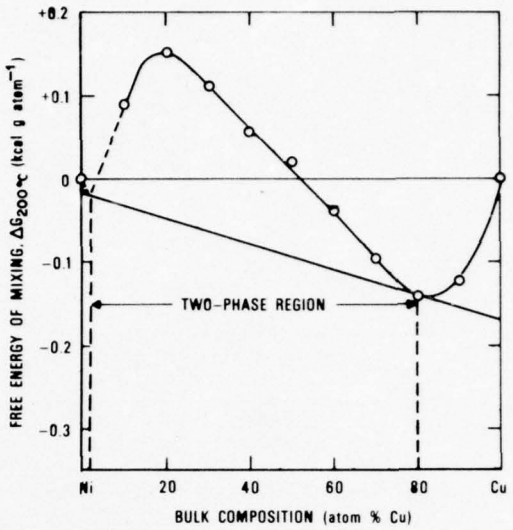

Fig. 20. Calculated values of the free energy of mixing at 200°C as a function of bulk composition for copper–nickel alloys. The minima at bulk Cu concentrations of ~80% and ~2% define the range of a miscibility gap; at equilibrium, all alloys having bulk compositions in this range must consist of two phases. (From Sachtler and Jongepier.[203])

contains 2% Cu. They reasoned that alloys within the miscibility gap (cf. Figure 20) had a constant surface composition (80% Cu–20% Ni), independent of nominal bulk composition. They employed a variety of methods (photoemission work function measurements, chemisorption of hydrogen, catalytic hydrogenation of benzene), which yielded results in support of this point of view. Figure 21 is a plot of the rate of benzene hydrogenation[204] at 150°C over Cu–Ni alloy films as a function of nominal bulk composition. The data indicate a nearly constant hydrogenation rate over a wide range of bulk compositions, as would be expected if the surface composition is invariant over this range. At Cu concentrations of <2% the Cu-rich phase is absent, the surface becomes Ni-rich, and the rate of benzene hydrogenation increases correspondingly.

The surface composition of alloys have been determined more directly using Auger electron spectroscopy (AES). This technique is particularly useful for studies of surfaces because it is sensitive to

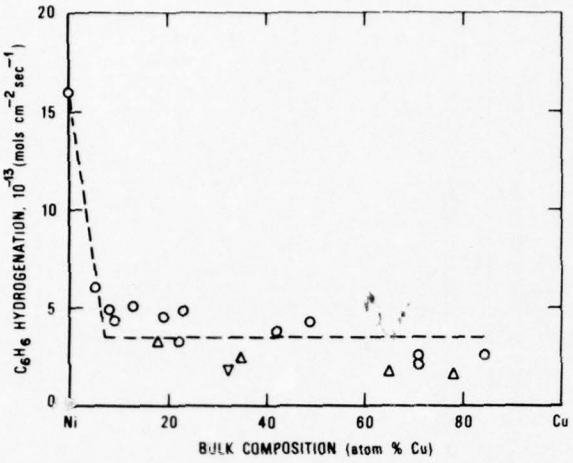

Fig. 21. Rate of benzene hydrogenation to form cyclohexane as a function of the bulk composition of Cu–Ni alloy films. The constancy of reaction rate over a wide range of bulk composition is interpreted as evidence for the near-invariance of the *surface* composition over this range. (From Van der Plank and Sachtler.[204])

the topmost atomic layers of the solid, to a depth of 5–20 Å beneath the surface. Ono and co-workers have applied AES to the study of Cu–Ni alloys,[205,206] and found that the composition of the surface is a sensitive function of the surface treatment. Argon-ion bombardment yielded a Ni-rich surface due to preferential sputtering of Cu; thermal annealing and oxidation–reduction treatments resulted in a Cu-rich surface, in qualitative agreement with the predictions of Sachtler.[203,204] Helms[207] has confirmed these resultes for a 50% Cu–50% Ni alloy by resolving Auger electrons associated with low-energy Ni and Cu transitions (100 and 106 eV, respectively); at these energies, the mean electron escape depth is only ~5 Å, so that the near surface contribution is emphasized. His data are summarized in Figure 22, in which the surface enrichment of Cu in the thermally annealed surface is clearly evident.

Yu *et al.*[208] have examined the surfaces of Cu–Ni alloys using ultraviolet photoemission techniques, and found that the surface electronic structure changes significantly from the bulk electronic structure on the annealed alloy surface, and correlates with the surface composition as measured by AES.

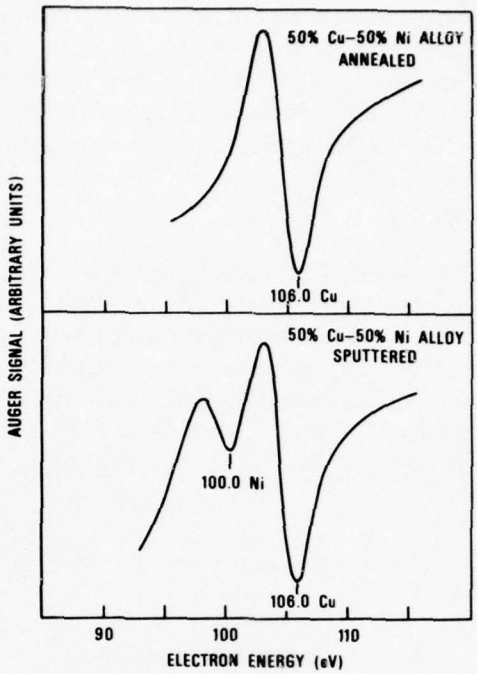

Fig. 22. Auger electron spectra of the surface of a 50% Cu–50% Ni alloy sample. The feature at 100.0 eV indicates that Ni is present along with Cu on the surface after sputtering (ion bombardment) with 300-eV argon ions. The Ni feature disappears after annealing in vacuum at 600°C, demonstrating that copper segregates to the surface under these conditions. (From Helms.[207])

A theory which allows predictions of the surface composition of binary alloys based on bulk thermodynamic data has been developed by Williams and Nason.[209] The model is developed using a pairwise bonding approach, with a broken bond surface. The alloy free energy is minimized by allowing exchange of atoms between surface layers and the bulk. The surface atom fraction is different from the bulk atom fraction for all compositions. In general, it is found that the alloy element with the lower heat of vaporization is enriched with respect to its bulk atom fraction. This conclusion is in agreement with the recent calculations of Van Santen and Sachtler.[210] The model of Williams and Nason[209] also predicts the effect of chemisorption of a

foreign component. The atomic fraction in the surface of the alloy element that bonds more strongly to the adsorbing species should increase after chemisorption and surface equilibration. The model qualitatively explains the behavior of clean, thermally annealed Ni–Cu alloy surfaces, as well as the influence of chemisorption.

5.2.2. Catalysis by Alloys

A remarkable aspect of catalysis by alloy surfaces is the strong element of specificity exhibited for certain hydrocarbon reactions. Sinfelt's recent data[14] on the hydrogenolysis of ethane to methane and dehydrogenation of cyclohexane to benzene demonstrate this clearly, and his data are shown in Figure 23. The data are plotted as specific activity (reaction rates at 316°C) as a function of *bulk* alloy composition. The catalysts were in the form of finely divided metal

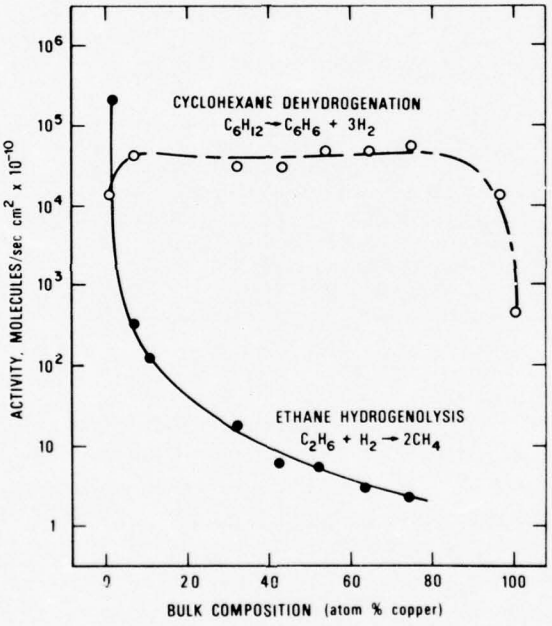

Fig. 23. Variation in the activity of copper–nickel alloy catalysts for different hydrocarbon reactions. Activities for cyclohexane dehydrogenation and ethane hydrogenolysis are plotted as a function of the bulk alloy composition. (From Sinfelt.[14])

granules having surface areas of 1–2 m^2/g. The catalytic activity of Ni for ethane *hydrogenolysis decreases by orders of magnitude with the addition of a small fraction of Cu, but the rate of cyclohexane dehydrogenation is constant over a wide range of bulk composition.* Sinfelt observes that intermediates in hydrogenolysis reactions are generally assumed to be unsaturated hydrocarbon residues multiply bonded surface metal atoms, so that one would expect such reactions to be sensitive to surface structure and composition (geometric effect). In addition, the presence of Cu may affect the strength of bonding of the intermediates to the Ni surface atoms (electronic effect). In contrast, cyclohexane dehydrogenation is relatively insensitive to these same factors. It may also be argued that the nature of the reaction itself affects the surface composition (Cu/Ni ratio), as predicted by Williams and Nason[209] for chemisorption.

According to Soma–Noto and Sachtler,[211,212] one of the most spectacular discoveries in heterogeneous catalysis in the last decade is the marked effect of alloying on the catalytic *selectivity* of metal catalysts (i.e., the relative rates of parallel reaction paths for formation of different products from the same reactants). Even for a binary alloy AB where A is inactive for the reaction considered, selectivity can differ from that of the pure metal B. They ascribe this phenomenon to two possible causes:

(a) A geometric "ensemble effect." An adsorbing molecule can form bonds with one or with two or more surface atoms; during the course of further reaction, each of these different chemisorption complexes will result in a different product. Selectivities will change as the surface atoms are diluted by inert atoms simply because the relative concentrations of ensembles having a small number of atoms will increase upon alloying with an inactive metal.

(b) An electronic "ligand effect." The strength of the chemisorption bond between even a single metal atom and an adsorbed atom will depend upon the chemical nature of the neighbors of the metal atom. Changing the chemisorption bond by alloying will result in a change in selectivity.

To examine the relative contributions of the "ensemble effect" and "ligand effect" in alloy catalysis, Soma-Noto and Sachtler[211] investigated infrared spectra of carbon monoxide adsorbed on supported Pd–Ag alloys. CO is strongly chemisorbed only on the Pd atoms. The CO spectra yielded information regarding the relative concentrations of monoadsorbed (linearly bonded) CO and diadsorbed (bridge-bonded) CO; they also indicated the manner in which

the infrared stretching frequency depends on the chemical nature of the metal atoms adjacent to the adsorbing Pd atom. The results indicated that the relative concentrations of linear to bridge-bonded CO changed with alloy composition, but the infrared frequencies remained almost constant. They concluded that for this system, the geometric "ensemble effect" is much more pronounced than the electronic "ligand effect." Further evidence for the dominance of the "ensemble effect" in adsorption of CO on Ni–Cu alloys was reported in another infrared study by Soma-Noto and Sachtler.[212] On the other hand, Williams and Boudart[213] have reported that oxygen does not adsorb on a Ni–Au alloy if the surface contains less than 30% Ni, suggesting that an electronic or "ligand effect" may be operative in this case.

5.2.3. "Bimetallic Cluster" Catalysts

Sinfelt[214] has examined the catalytic activity of highly dispersed bimetallic catalysts containing copper and ruthenium or osmium; the total metal concentration on the silica support was of the order of 1–2% by weight. Despite the low metal concentration and high dispersion, and despite the fact that copper is almost totally immiscible with Ru or Os in the bulk, the addition of the Cu drastically affected the specificity of Os and Ru for hydrogenolysis and dehydrogenation of cyclohexane. In view of the strong interaction between the metallic components (as demonstrated by the catalytic data), it was concluded that "bimetallic clusters" were formed on the support. The term "bimetallic clusters" rather than alloys was used because the metallic combinations employed do not form bulk alloys. The nature of these bimetallic clusters[215] has yet to be resolved completely (are the metals miscible in small particle form, or does one metal form a coating on the surface of the second?), but these investigations have opened up a new area of interest in catalysis by bimetallic systems.

5.3. Electronic Effects in Carbides

Levy and Boudart[216] have recently observed that tungsten carbide exhibits catalytic behavior which is typical of platinum but which is not characteristic of W. Specifically, WC catalyzes the formation of water from H_2 and O_2 at 300°K and the isomerization of 2,2-dimethylpropane to 2-methylbutane. They conclude that the surface electronic properties of W are modified by carbon in such a

way that they resemble those of Pt. Bennett *et al.*[217] have recently studied the band structure of W, Pt, and WC using ESCA (X-ray photoelectron spectroscopy) and conclude that the valence band density of states at the Fermi level of WC is more like Pt than W. Houston *et al.*[218] have presented evidence to the contrary, so the matter is far from settled. Nonetheless, this situation illustrates nicely the trend of present-day thought in catalysis: Progress in understanding the role of electronic factors in catalytic processes will very likely come from a combination of the careful kinetic measurements of the catalytic chemists and the surface spectroscopic measurements of the surface chemists and physicists.

5.4. Electronic Effects in Catalysis by Semiconductors

As in other areas of catalysis, the views on the electronic factor in catalysis by semiconductors have gradually shifted from an emphasis on collective effects to an emphasis on localized electronic effects and point defects. However, the complexity of catalytic phenomena is such that the hope for a unified theory of catalysis on solid surfaces appears utopian. The application of modern electron spectroscopies to oxide surfaces is expected to provide a wealth of solid-state information with which catalytic properties may be correlated.[219]

5.4.1. The Collective Properties of the Semiconductor as a Factor in Catalysis

On the heels of spectacular developments in the theory and understanding of the nonmetallic solid state, attempts were made during the late 1940's and the 1950's to relate the catalytic activity of these solids to their collective electronic properties, namely ferromagnetism, ferroelectricity, conductivity type, the position of the Fermi level, and the band gap. Suggestive relations between chemisorption and conductivity had already been found by Wagner and Hauffe[24] and for some perovskite-type oxides, catalytic excursions near the ferroelectric[220] and ferromagnetic[221] Curie temperatures were found by Parravano.

The electronic theory of catalysis on semiconductors as developed by Hauffe,[21,22] Wolkenstein,[19,20,222] and others and subsequently elaborated by Garrett,[31] Lee,[223,224] and Krylov[225] starts from the simple idea of a chemisorption event coupled with

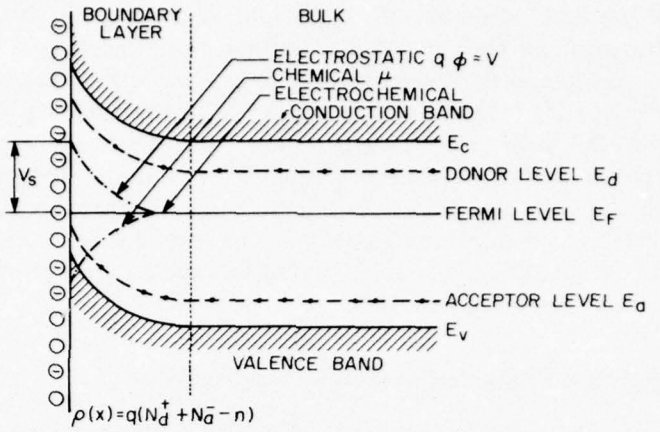

Fig. 24. Simple band picture for anionic chemisorption. (⊖) Charged adparticles; (○) uncharged adparticles; (●) an electron occupying an impurity state. For electrons (negative charge) the electrostatic potential energy has opposite sign to the electrostatic potential. Band bending is due to electrostatic charge on the surface. Note partial ionizaton of adsorbed particles and impurities. (From Garcia-Moliner.[32])

transfer of an electron from an adsorbate to the solid or *vice versa*. If charge transfer leads to a change in the concentration of mobile carriers in the bulk, i.e., the adsorbed particle acts as a donor or acceptor, then the electrochemical potential of the carriers in the bulk will in turn have an effect on the equilibrium concentration of chemisorbed species. The same potential will then also affect the rate of a catalytic reaction in which these chemisorbed species might participate. The concentration of active species at the surface will be determined by the position of the electrochemical potential at the surface (in the absence of an external field, this is the Fermi level E_F) with respect to the positions of the donor or acceptor levels (induced surface states) associated with chemisorbed particles (Figure 24). The calculation of the concentration and degree of ionization of the chemisorbed species may be done in a self-consistent scheme similar to that used for bulk impurities using the Poisson equation.[32,222,226] Wolkenstein and Garcia-Moliner find that a Fermi-statistical treatment of the concentrations of ionized and neutral species adsorbed at the surface leads to a dependence on the Fermi level as shown in

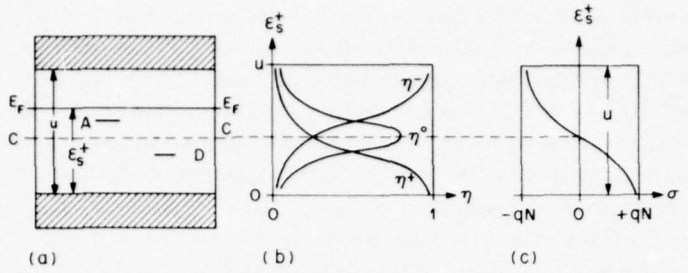

Fig. 25. The charge state of the adsorbate as a function of the position of the Fermi level: (a) The adsorbed molecule is characterized by one donor level *D* and one acceptor level *A*. (b) Relative abundance of adanions (η^-), adcations (η^+), and neutral adparticles (η°). (c) Average charge state. In (b) and (c) the vertical axis is the position of E_F. *C* is band center. (From Vol'kenshtein.[222])

Figure 25. This stage of the theory, which is an equilibrium theory in that it relates the catalytic activity to the equilibrium concentrations of electrons and holes, can be tested by the relation it predicts between changes in the Fermi level and changes in the catalytic activity, *provided the mechanism of the reaction has been established first*. The changes in catalytic activity are then expected to follow the concentration profiles sketched in Figure 25. Due to changes in the character of the rate-limiting step (e.g., from electron transfer to the surface to electron transfer to the adsorbate) as the Fermi level is changed, the correlation between E_F and the rate constant k may not be monotonic.[222]

The tests of this theory have involved the measurement of the rate of some test reaction as a function of the bulk doping of the catalyst, or as a function of the band gap of the catalyst. The latter method, which is described in detail by Krylov,[225] has been criticized, particularly on the basis that the induced surface states for a particular reaction on the various catalysts bear no simple relation to the band gap. Effects of the E_F on the rate may, in principle, be studied by changing E_F in one catalyst by illumination, by an external field, or by straining the catalyst sample. Unfortunately, side effects such as the creation of defects, trap centers, or dislocations and the polarization of adsorbed species in the external field make the interpretation of such experiments hazardous unless several of these techniques are employed concurrently. Apparently, this has not been done. Common are attempts to relate the reaction rate to the doping level of the bulk. This approach was used most extensively for the two

best-studied semiconducting-catalyst systems, NiO and ZnO. For example, Parravano[28] and Schwab and Block[29] used doping with monovalent and trivalent ions in these catalysts. The relations found between doping and activation energy for the oxidation of CO and the decomposition of N_2O were suggestive of a correlation between these parameters. However, as Garrett[31] pointed out, there should be, on fundamental grounds, no simple relation between activation energy and the temperature dependence of the semiconductor parameters. Moreover, in Parravano's and Schwab and Block's measurements, the relation between the rate constant (as opposed to the activation energy) and the doping level is not at all clear-cut. In fact, the effects of doping level are most pronounced at high temperatures (200–400°C) where the simple electronic picture of the catalytic process is probably invalid for two reasons: The semiconductor is in the intrinsic range, with the Fermi level close to the middle of the gap, and the mechanism of the reaction is intrafacial, with participation of lattice oxygen. Gravelle *et al.*[227,228] have additionally argued that the oxidation of CO over doped and pure NiO follows two different mechanisms, through a CO_3^-(ads) species on NiO(Li) and through O(ads) on NiO and NiO(Ga). Deren *et al.*,[229] working with single-crystal NiO(Li) catalysts, have shown only minor effects of doping on the rate of CO oxidation at 250°C, and changes of less than a factor ten at 400°C, while, moreover, the changes were not monotonic with increasing Li content. In view of the complexities of the transport properties of NiO discussed by Adler,[230] including the partial compensation of Li doping with oxygen vacancies, it is not surprising that the large amount of work on NiO catalysis has not materially advanced the status of the electronic theory of catalysis.

Changing the scene to the catalytic properties of ZnO, for which catalyst a large body of data is also available, does not provide any more encouragement. The effects of doping are inconclusive for similar reasons as for NiO: variable mechanisms of the test reactions and small effects on the rate constant, while the only clear effects are on the activation energy. Parenthetically, it may be remarked here that two effects are likely to interfere in this type of measurement: the phase segregation of low-melting compounds at the surface and the variation of the oxidation state of the catalyst with temperature. The first effect may yield anomalously low rates,[231,85] while the second effect may yield apparent activation energies which are very dependent on the history of the sample and the experimental details.[85,232]

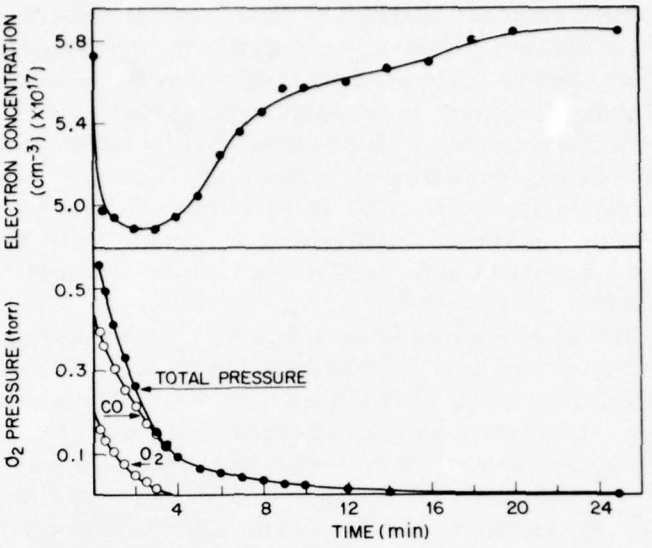

Fig. 26. Electron concentration as measured by the Hall effect and ambient gas composition change observed during carbon monoxide oxidation over an indium-doped ZnO sample at 350°C. (From Chon and Prater.[33])

The foregoing has stressed the difficulties which have arisen in experimental tests of the relation between semiconductor properties of catalysts and catalytic properties. Nevertheless, strong evidence of a semiquantitative nature is provided by the many measurements of the conductivity of catalyst samples during the catalytic process, and particularly by some remarkable experiments by Chon and Prater on ZnO during CO oxidation.[33] These authors measured the Hall voltage on a bulk polycrystalline sample during catalysis and thereby established the concurrent changes in the number of carriers and the changes in the reaction rate (Figure 26). This type of measurement eliminates the difficulties associated with interpretation of conductivity measurements, namely intergranular resistance and mobility changes, and establishes the correlation (if not the causal relation) between carrier density and activity.

Further progress in the electronic approach to the catalysis on semiconductors is likely to arise from a more complete picture of the transport properties of the semiconducting catalyst, preferably using

single-crystal samples. The theory of the catalysis on semiconductors as outlined above is grossly oversimplified in the following respects:

(a) It is based on the band model, which may be less than appropriate for the relevant states of catalysts such as NiO.[230,233]

(b) It ignores pinning of the Fermi level by surface states. As pointed out by Wolkenstein,[20] following Bardeen,[234] a high density of surface states resulting from surface defects, intrinsic surface states, or surface states created by adsorption of reactants results in a Fermi level at the surface which is independent of the bulk Fermi level.

(c) It ignores trapping levels, which intervene in the transfer of carriers between the adsorbed species and the bulk bands.

Detailed studies of ZnO and TiO_2 by Gray[235] have shown a very large variety of trapping levels extended over a large fraction of the gap. Modern thinking is very much concerned with the effect of trap states on the catalytic properties and with the complexities introduced by changes in carrier lifetime, changes in ionization of donors, and interaction of surface and bulk trap states with the bulk bands.[235–238] The variation of the photoinduced catalytic activity

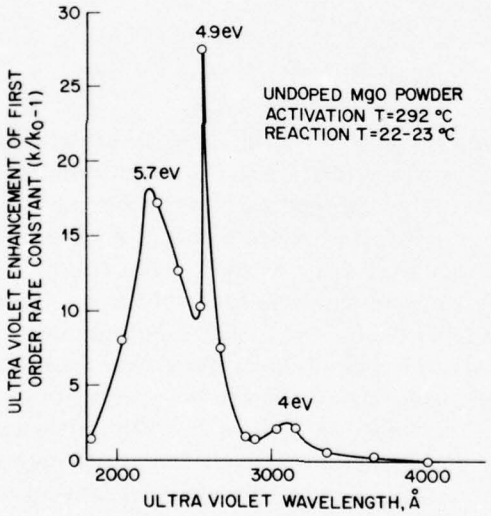

Fig. 27. Reaction rate spectrum for the H_2–D_2 exchange on irradiated MgO powder. Enhancement factor as a function of wavelength, showing the activity of various traps in the bandgap. k_0 is the rate constant in the absence of irradiation. (From Harkins *et al.*[113])

with photon energy is an example of the way these problems may be experimentally elucidated.[113] The results for MgO are shown in Figure 27. The emphasis on defects forms a natural bridge with the work of Kokes *et al.*,[239] which is almost exclusively focused on the defect structure of the surface (of ZnO catalysts) rather than on the semiconducting properties.

In the above discussion of the electronic theory of catalysis on semiconductors, the chemisorption of gas molecules was taken to involve mobile carriers, which were released again (or taken up again) during the further course of the surface reaction or during desorption of the product. In contrast to this equilibrium approach, there have been attempts to correlate catalytic reactivity with the nonequilibrium electronic processes. Wolkenstein[222] has discussed the possibility that excitons diffusing to the surface might provide the energy to surmount the activation barrier for a reaction. In the case of electron–hole pairs (Mott excitons), the measured activation energy would then be diminished by the energy of the band gap. A more specific discussion limited to the annihilation of electron–hole pairs during the surface reaction has been given by Lee.[223] Consider the reactions

$$A + n \leftrightarrows A^-$$

$$D + p \leftrightarrows D^+$$

$$A^- + D^+ \rightarrow AD$$

in which A and D are the reaction partners and n and p are the carriers. The energy required to create a pair of carriers, i.e., $(E_c - E_v)$, will contribute to the measured activation energy if the rate-determining step is the creation of these pairs. For an intrinsic semiconductor, a correlation of linearly increasing activation energy with increasing band gap is then expected. Although a correlation has indeed been observed (between the activity and the band gap) for an important number of catalysts (Figure 28), such relations must have a somewhat more complicated cause, since in general the pre-exponential factor also changes appreciably.[225] Finally, it has to be stressed that in the presence of large numbers of donor and acceptor impurities, no relation with the band gap is expected.

Collective properties are of course not limited to transport properties. There is no room at this point to discuss collective properties arising from spin or dipole ordering,[122,220,221,240,241] but some attention is warranted for the relation between catalytic

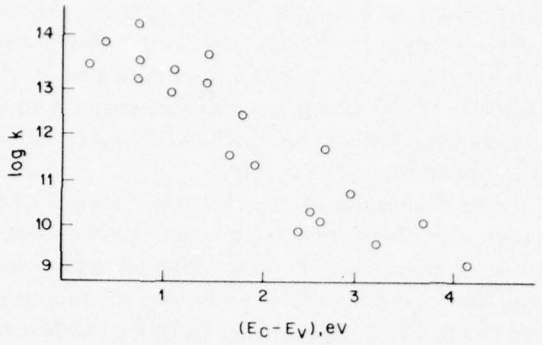

Fig. 28. The dependence of the rate constant k for dehydrogenation of isopropanol at 200°C on the width of the bandgap of III–V, IV–IV, II–VI, and I–VII semiconductors. (After Krylov.[225])

activity and thermodynamic functions of the catalyst. This relation was established for the decomposition of formic acid on metals by the work of Fahrenfort *et al.* discussed in Section 8.3. Following this, correlations have been sought and found between the averaged heat of oxide catalysts and their activity for oxidation reactions. The important parameter is expected to be the metal–oxygen bond strength in the adsorption complex, taken to include the atoms making up the environment of the active site. Instead, however, the average bond energy is used, since this is more easily available from tabulated data. The correlations found for the oxidation of propylene over a series of metal oxides[242,243] are quite satisfactory (see Figure 29) and can be understood on the basis of the intrafacial mechanism of the reaction at high temperatures, with lattice oxygen participating in the process. Refining this concept to include the selectivity in addition to the activity, Sachtler *et al.*[244] have correlated these catalytic parameters with the differential enthalpy and free energy of lattice oxygen in the oxidation of benzaldehyde to benzoic acid over MnO_2, V_2O_5, and V_2O_5–SnO_2 catalysts. However, a localized bond model requires correlation with the metal–oxygen bond in the active complex and such a correlation was recently established for the selective reduction of NO to dinitrogen products over perovskite-like oxide catalysts[245] (Table 2).

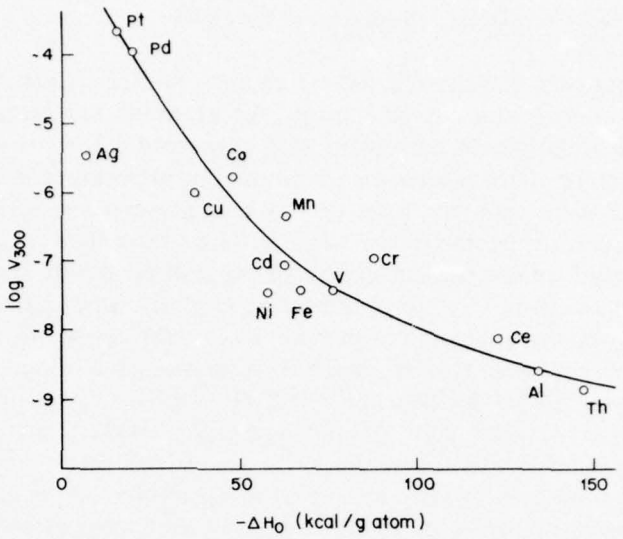

Fig. 29. The dependence of the rate of the oxidation of propylene at 300°C (V_{300}) in an excess of oxygen on the enthalpy of formation per oxygen atom (ΔH_0) of the oxide catalyst. Data for BaO, MgO, and ZnO omitted because of immeasurably low V_{300} values. (From Morooka and Ozaki.[242])

TABLE 2
Correlation between Binding Energy of Surface Oxygen and $N_2 + N_2O$ Yield

Ranking in order of decreasing $N_2 + N_2O$ yield	Δ(A–O) + Δ(A′–O),* kcal/mole
Bi, K	−25
La, □	−34
La, Rb	−41
La, K	−42
La, Na	−42
La, Pb	−47
La, Sr	−54

* Calculation of Δ(A–O) from Δ(A–O) = $(\Delta H_f - m\,\Delta H_s - \frac{1}{2}nD_0)/12m$, where ΔH_f, ΔH_s, and D_0 are, respectively, the enthalpy of formation of one A_mO_n, the enthalpy of sublimation of A, and the dissociation energy of O_2.

5.4.2. Local and Defect Properties of the Solid

It has been emphasized above that the influence of defects on the semiconductive and catalytic properties of solids has received increasing attention. In agreement with this trend, efforts to identify the structure of active sites are of paramount importance in modern catalysis. Some examples have already been presented in Section 3.4. In Section 6, the geometric aspects of surface sites will be discussed in some detail. In the present discussion we will be mostly concerned with the electronic nature of the active complex, when the latter is taken to be the aggregate of the site, its nearest neighbors, and the adsorbed particles. This approach to catalysis has in modern times been spearheaded by Dowden.[34,35] His work provides a logical connection between coordination complex chemistry and heterogeneous catalysis. In recent times, the role which cation and anion vacancies and their coordination play in the mechanism of oxidation reactions has received particular attention, and some examples will be included in this section.

The crystal field theory of catalysis takes as its starting point the change of coordination of the surface ion in the act of adsorption. For instance, on the (001) surface of NiO, a Ni^{2+} ion has a square pyramidal coordination, which upon adsorption of a ligand becomes more symmetric, approaching more nearly the octahedral coordination in the bulk. Calculations[35,246] of the crystal field stabilization energy contribution to the heat of chemisorption found that a minimum resulted for d^0, d^5, and d^{10} (as expected) and pronounced maxima at d^3 and d^8. In correlating these results with patterns of catalytic activity for oxides of the transition series (Ti^{4+} to Zn^{2+}), two caveats have to be heeded.[35] The first is that comparison should properly be made only for oxides of the same stoichiometry and lattice structure, e.g., in the series MgO–MnO–NiO or Al_2O_3–Cr_2O_3–Fe_2O_3. The second is that during chemisorption and catalysis the valence of the ions should not change, since the energy differences accompanying valence change are large compared with the crystal field stabilization effects. The "twin-peaked" pattern suggested by the crystal field stabilization terms was found experimentally for H_2–D_2 exchange at temperatures of -195 to 20°C.[34] Similar patterns have also been found for the disproportionation of cyclohexene, the dehydrogenation of propane, and the hydrogenation of ethylene, as reviewed by Cimino.[247] These correlations suffer from the fact that the oxides compared are not isostructural. Cimino and co-workers have made

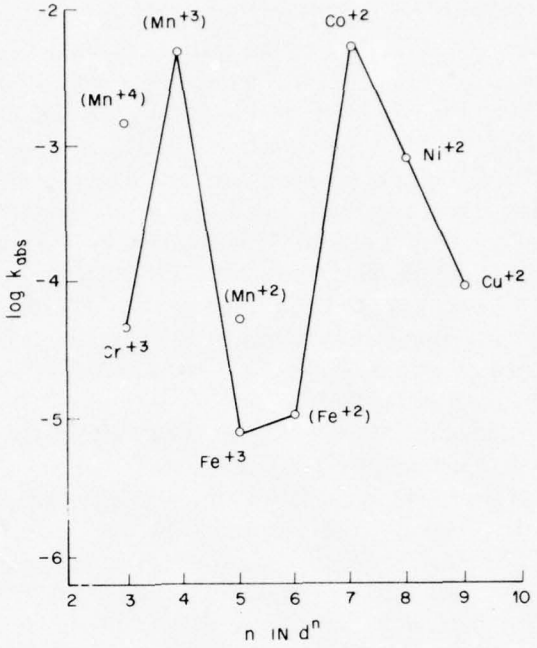

Fig. 30. Correlation of the absolute rate constant per transition metal atom for N_2O decomposition at 315°C with number of *d* electrons. Solid solutions of 1 at % in MgO. Valence states in parentheses may be slightly impure; i.e., Mn^{4+} containing a slight amount of Mn^{3+}, etc. (From Cimino.[247])

extensive studies of MgO catalysts with transition metal ions atomically dispersed on Mg sites, thus ensuring an isostructural series, and have used these in the decomposition of N_2O. They have again found a marked "twin-peaked" pattern (Figure 30) with maxima at Mn^{3+} and Mn^{4+} (d^3 and d^4) and Co^{2+} (d^7) and a minimum at Fe^{3+} and Fe^{2+} (d^5 and d^6). The fact that N_2O decomposition involves the charged adsorbed species N_2O^- and O^- indicates that the metal ions must change valence during the reaction. It is surprising that this does not destroy the "twin-peaked" pattern, since the crystal field stabilization effects are likely to be small compared to the valence change energies.

A study[38] which heeds both caveats discussed above, and avoids valence changes while working with an isostructural series of semiconducting ternary oxides, employed the cubic perovskite-like oxides

$\{La_{1-x}^{+3}M_x^{+3\pm1}\}[TM_{1-x}^{+3}TM_x^{+3\mp1}]O_3$, where $M = Ce^{4+}, Pb^{2+}, Ca^{2+}, Sr^{2+}$ and TM = Cr, Mn, Fe, Co. The test reaction was the oxidation of CO. The activity pattern showed a maximum with the Fermi level near the bottom of the d_{z^2} level. This is the position which is optimal for the bonding of CO to the transition metal ion, since the nearly empty d_{z^2} level is capable of accepting the carbon lone pair, while the lower lying and occupied d_{yz} and d_{zx} levels can effectively donate electrons into the π^* CO orbital. This study showed how useful the principles of the crystal field theory are in understanding activity patterns, even though in the neutral adsorption of CO the "crystal field stabilization" invoked by Dowden for ionic adsorbates is not applicable and a twin-peaked pattern is not found.

Isolated ions and similarities with coordination chemistry are particularly important in the catalytic chemistry of the transition metal ion-exchanged zeolites (aluminosilicates, which, due to their cagelike structure, have been called "molecular sieves"). The diamagnetic matrix makes it advantageous to use optical and ESR spectroscopy. The detailed information obtained in these studies is well illustrated by the work of Chao and Lunsford on the adsorption of NO on Ag in Y-type zeolite[248] and that of Klier *et al.*[249] on the π-adsorption complexes of olefins and acetylene on Co(II) ions in zeolite A.

In the oxidation of olefins over bismuth molybdate catalysts and in the redox reaction of NO with CO and H_2 over perovskite-like oxides of manganese, the catalytic activity has been directly linked with defects in the lattice. These studies are of special relevance in the present context since they demonstrated the importance of defects in contradistinction to the transport properties of the catalysts.

The system Bi_2O_3–MoO_3 has been studied in detail by Batist, Schuit, Matsuura, and co-workers[250,251,100] to establish the relation between the solid-state chemistry and catalytic action of this commercially important selective oxidation catalyst. Using the oxidative dehydrogenation of 1-butene to butadiene as their test reaction in a kinetic, crystallographic, and chemisorption study, they concluded that the most active compound in the Bi–Mo–O phase diagram was koechlinite, Bi_2MoO_6. The process was found to be an example of intrafacial catalysis, involving lattice oxygen. Two types of adsorption centers were distinguished by the chemisorption measurements on reduced $Bi_2MoO_{5.5}$ and oxidized Bi_2MoO_6. The first is called the *A* center, which is a single site which slowly but strongly adsorbs butadiene. The second, so-called B center, consisting of several

surface oxygen atoms, adsorbs 1-butene, *cis*-2-butene, butadiene, and *trans*-2-butene in a fast process leading to relatively weak binding. The conversion of butene to butadiene involves the *A* and *B* centers simultaneously. At temperatures below 400°C, only the *A* center is involved in the incorporation of O_2 in the lattice, with rapid diffusion of O^{2-} providing the oxygen necessary for the oxidation reaction. These results are explained by a model of the structure of koechlinite. The structure consists of plates of $(Bi_2O_2)^{2+}$ and $(MoO_2)^{2-}$ in alternate stacking, with a layer of bridging O^{2-} between (Figure 31). One-fourth of the oxygen at the edge of the Bi_2O_2 layer is removable and is replenished at low temperature by O^{2-} from the same layer, whereas at $T > 400$°C, O^{2-} can diffuse from one layer to the next. The olefin dissociatively adsorbs on a *B* site (Figure 31) as an allyl radical, transfers to a bismuth vacancy, and loses a second H atom to a second *B* site while the Mo^{IV}/Mo^{VI} redox reaction provides balancing of the charge states.[251]

The role of Bi vacancies postulated in the above-discussed work on Bi_2MoO_6 has a dramatic parallel in the work of Sleight, Aykan, and co-workers.[252 254,101] They have approached the study of the selective oxidation catalysts by adopting catalysts based on the

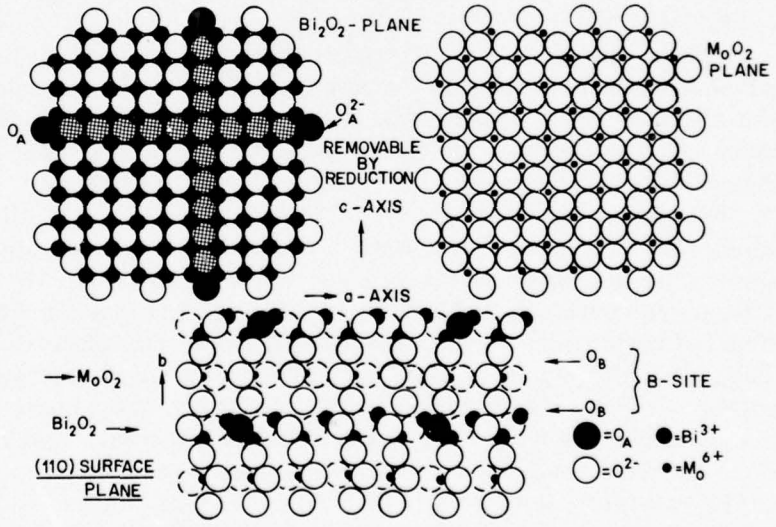

Fig. 31. The surface boundary (110) plane of Bi_2MoO_6 showing the Bi_2O_2 and MoO_2 layers (top) and the alternate stacking with bridging oxygen (bottom). (From Matsuura and Schuit.[100])

scheelite ($CaWO_4$) structure. In this structure, extensive substitution for Ca and W is possible and point defects are easily introduced, notably vacancies on the Ca site. For the AMO_4 structure, A is coordinated to eight different MO_4 tetrahedra. The structure type is very flexible, allowing A to be from monovalent to tetravalent and M to be from monovalent to octavalent. A-site vacancies may be introduced by proper choice of A, M, and the stoichiometry to obtain $A_{1-x}\phi_xMO_4$, where ϕ represents the vacant A site. Scheelites with M = V, Mo, and W have been made and studied as catalysts.[253,254] In a very large series of these catalysts, it was observed that the simultaneous presence of A vacancies and of Bi was necessary to obtain high activity and selectivity for the ammoxidation of propylene:

$$H_2C{=}CH{-}CH_3 + NH_3 + \tfrac{3}{2}O_2 \rightarrow H_2C{=}CH{-}C{\equiv}N + 3H_2O$$

or the oxidative dehydrogenation of butene to butadiene. The role of bismuth apparently is to rapidly replenish the active site with oxygen, similar to the Batist–Schuit–Matsuura mechanism above. The role of the defect is to attract a proton from the olefin by Coulombic forces. The activity of $Pb_{1-3x}Bi_{2x}\phi_xMoO_4$ for the 1-butene oxidation accordingly increases linearly with x in the range of $0 < x < 0.06$.[252]

The role of cation vacancies has also been demonstrated for the reduction of NO to dinitrogen products ($N_2 + N_2O$) over perovskite-like catalysts.[38,255] The perovskite structure, of the formal stoichiometry ABO_3, contains A ions in a dodecahedral hole formed by eight BO_6 octahedra sharing corners. Even more than the scheelite structure, the perovskite structure is extremely flexible with respect to substitutions in the A and B sites. Many hundreds of compounds with this structure are known. For the reduction of NO with CO and H_2, a series of manganites $A_{1-x}\phi_xMnO_3$ was studied. The reaction was shown to be intrafacial, involving lattice oxygen. In the comparison of $La_{0.91}\phi_{0.09}MnO_3$ and $LaMnO_3$, it was found that the former was a much more active catalyst for the reduction of NO. By comparison of a series of compounds with approximately equal proportions of Mn^{3+} and Mn^{4+} prepared by substitution of La^{3+} in $LaMnO_3$ with appropriate proportions of K^+, $Bi^{3+} + K^+$, Sr^{2+}, or vacancies, it was shown that the activity for NO reduction was directly related to the contribution of the occupants of the A sites to the binding of surface oxygen (Table 2). This contribution was calculated for the

process

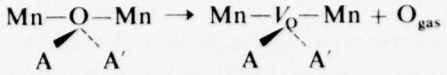

where Mn–O–Mn stands for the surface of the oxide and V_O for an oxygen vacancy. The latter was proposed to be the active site for the dissociative chemisorption of NO.

The above examples show how in modern catalytic work the solid-state chemistry, and particularly the defect chemistry, of the catalyst plays a major role. Even though the proposed mechanisms may prove inaccurate in detail, they appear to be sufficiently well-founded to prove the essential importance of localized and defect influences on catalytic activity. This is especially significant since the same catalysts, bismuth molybdates and manganite perovskites, have featured prominently in collective solid-state physics approaches to catalytic activity.

6. Geometrical Effects in Catalysis

In the introduction, it was already noted that the separation between geometric and electronic effects is an artificial one. It will have surprised no one that as the discussion in the last section progressed from collective properties to localized and defect properties, the geometry of the active site was explicitly considered together with the electronic effects. In the present section, oxides will therefore not be discussed, except to note that a general rule has been found stating that transition metal ions in tetrahedral coordination are much less active in redox reactions than those in octahedral coordination.[247] Ion scattering studies of Co^{3+} in octahedral and tetrahedral coordination have provided an explanation for this rule.[256] At the surface, tetrahedrally coordinated Co ions were found to be largely shielded from the gas phase, in accordance with observations that CO chemisorbs on CoO with the NaCl structure, but not on CoO with the ZnS structure.

6.1. Correlations between Kinetics and Surface Structure of Metallic Catalysts

High-area metal catalysts are often prepared by dispersion of the metal on the surface of a support. This dispersion process leads to more efficient use of the active metal component, reaching a limit

where each metal atom is exposed to reactants (dispersion = 1). The widespread use of highly dispersed catalytic metals has led to an important theme in catalytic research which asks whether the catalytic activity per exposed atom of active material varies as the degree of dispersion changes. As pointed out by Poltorak and summarized in an excellent review by Boudart,[8] one should expect major changes in the physical nature of metal crystallites as their sizes decrease below about 50 Å. This is because the fraction of atoms in the surface of a crystallite increases markedly in this range as well as because an appreciable fraction of abnormal surface atom coordination situations begin to occur at ~ 50 Å particle size (see Figure 3). Thus, on this basis, one might expect electronic as well as geometric differences to occur as crystal size is decreased below 50 Å.

Within the last several years, careful kinetics experiments designed to answer the question of the relation of specific catalytic activity to dispersion have been carried out. It has been found in certain catalytic systems that little change in *specific activity* occurs over many orders of magnitude variation in dispersion, and these catalytic systems have been designated "structure-insensitive" or "facile" by Boudart.[257] Other reactions whose specific rate depends on catalyst structure are termed "structure-sensitive" or "demanding" reactions. Boudart[8] points out that, in view of the general historical irreproducibility of kinetic measurements on catalysts, some of these results "may be viewed as opening a new era in our confidence in catalytic data." In addition, since the comparison of catalytic activity for certain facile reactions has been extended all the way to bulk metal foils[257] and to single crystals,[258] the way is now opened for meaningful catalytic experiments to be done on single crystals where modern techniques of surface characterization can be applied[1] and where important parameters can be well controlled. A corollary assertion about "structure-sensitive" catalytic reactions has been advanced by Boudart,[103] namely, that reactions proceed *on all sites available*, although not necessarily with exactly equal rates. This observation is supported by controlled poisoning experiments by Kral,[259] who demonstrated that the fraction of active sites on a catalyst varied over a range from about one to about 10^{-3} for various hydrogenation reactions. This fraction is termed the Taylor ratio. With a ratio near unity, one is dealing with a "structure-insensitive" reaction.[8] It should be pointed out that in some cases[257] where "structure-insensitive" reactions are being studied, when the weight percent of metal is made very low (~0.1–0.05%) the specific activity

is also found to be low. This may be due to uncontrolled poisoning effects, specific support effects which are only detected at low metal concentrations, or to reduced precision in the kinetic measurements. A number of structure-insensitive reactions are listed in Table 3.

Since many factors may be responsible for changes in catalytic activity for supported catalysts having different degrees of dispersion, it is important to carefully study changes in specific activity before concluding that a reaction is "structure insensitive" or "structure sensitive." One way to do this is to examine parallel reactions starting from the same reactants but proceeding through different intermediates to yield different products. If one of these reaction paths is "structure insensitive," then it may be used as an internal control in experiments involving different catalyst preparations. The ratio of the rate of the second reaction to the control reaction may then be used to judge whether the second reaction is structure insensitive or not. Changes in relative rates for various catalyst dispersions are termed selectivity changes and control of catalyst selectivity is of great importance in practical catalysis. Examples of reactions proceeding in parallel are found in studies of neopentane isomerization (to isopentane) compared with neopentane cracking (to isobutane and methane) on Pt.[8] Another example is the comparison of benzene hydrogenation (to cyclohexane) with benzene isotopic exchange with deuterium on Ni.[16] In both of these cases, the first reaction was found to be "structure insensitive."

When one comes to speculate about the factors which are responsible for a reaction being either sensitive or insensitive to catalyst structure, details of the reaction mechanism must be invoked. Thus, a structure-insensitive reaction might involve the formation of intermediates in the rate-controlling step which do not demand very specific geometric arrangements of the atoms of the catalyst.

A second possibility advanced for the meaning of structural insensitivity has to do with the possibility that these reactions are associated with the structural properties of the intermediates themselves, and therefore are little influenced by the surface structure of the catalyst itself. This explanation has been advanced by Yates *et al.*[260] to explain the similarity in the kinetics of liberation of CH_4 from W(111) and W(100) single crystals covered with a layer produced by adsorption of formaldehyde. In these studies, it appears that CH_4 is produced in two distinct thermal processes on *both* crystal faces with maximum liberation rates at about 270 and 500°K as shown in Figure 32. In addition, work function changes for the adsorbed layer on the

TABLE 3
Structure Insensitive Catalytic Reactions

Reaction	Catalyst	Dispersion range	Specific activity range	Ref.
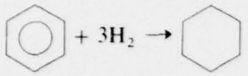	Pt/SiO_2	70×	1.7×	306
	Ni/SiO_2 $Ni/SiO_2 \cdot MgO$ $Ni/SiO_2 \cdot Al_2O_3$	20×	~2×	307
	Pd/SiO_2 Pd/Al_2O_3 Pd black	30×	~1.6×	307
	Pt/SiO_2 Pt/Al_2O_3	6×	1.1×	307
	Ni/MgO	30×	2.7×	308
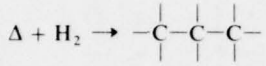	Pt/Al_2O_3 Pt/SiO_2 Pt foil Pt single crystal	2×10^4×	2.5×	257, 258
	Pt/Al_2O_3	3×	~1.3×	309

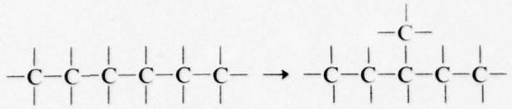	Pt/Al_2O_3	3 ×	~1.3 ×	309
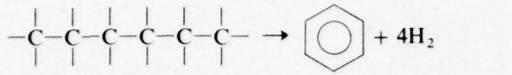	Pt/Al_2O_3	3 ×	~1.3 ×	309
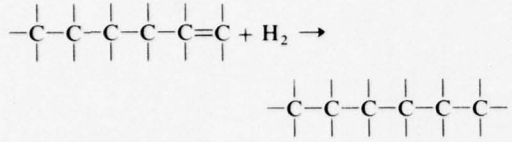	Pt/SiO_2	4 ×	~2 ×	310
$H_2 + D_2 \rightarrow 2HD$	Pt/SiO_2	4 ×	~2 ×	310
$2SO_2 + O_2 \rightarrow 2SO_3$	Pt/SiO_2 Pt	—	—	311
$2H_2 + O_2 \rightarrow 2H_2O$ (in excess O_2)	Pt/SiO_2 Pt	7 ×	2.1 ×	262, 313
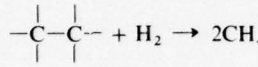	Ni/SiO_2	3 ×	1.5 ×	312
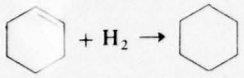	Pt/SiO_2 Pt/Al_2O_3	7 ×	1.09	262
$2CO + O_2 \rightarrow 2CO_2$	Pd(100) Pd(110) Pd(111) Pd(polycrystalline)	— — — —	— — — —	299
$2H_2CO \rightarrow CH_4 + CO_2$	W(100) W(111)	— —	— —	261

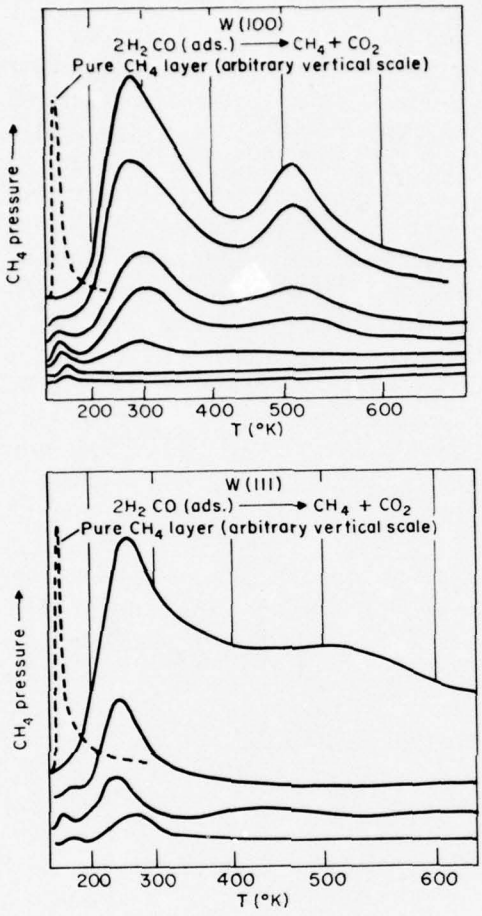

Fig. 32. Structure insensitivity of the catalytic production of CH_4 from adsorbed H_2CO on two single-crystal planes of tungsten. Following adsorption of varying amounts of H_2CO on the crystals at $\sim 100°K$, heating causes liberation of CH_4 in two stages in both cases. The kinetics of CH_4 evolution differ significantly from that observed for CH_4 desorption from pure physically adsorbed CH_4 layers, and is thought to reflect the catalytic decomposition of intermediates at elevated temperatures. Upper figure: Desorption traces from W(100) surface. Lower figure: Desorption traces from W(111) surface. (From Yates *et al.*[260])

two crystal faces are very similar, indicating that the experiments are probably detecting intrinsic properties of surface complexes which are not strongly dependent on underlying crystallography. Recently, Boudart[261] has made a similar suggestion regarding the $H_2 + O_2$ reaction on Pt, which is structure sensitive in excess H_2, but structure insensitive in excess O_2. The oxygen is postulated to chemisorb in such a way as to erase surface anisotropies and reaction occurs on the "platinum oxide molecule" surface layer. This means that in the latter case, we deal with an intrafacial catalytic process.

Recently, Somorjai and his co-workers have carried out several pioneering experiments designed to test whether specific surface geometric factors such as step density can affect the rate of catalytic reaction. In the first work of this type, the isotopic H_2–D_2 exchange reaction was examined using a chopped molecular beam.[262,263] From a planar Pt(111) surface, no HD production could be measured, whereas above a stepped surface containing nine-atom-wide Pt(111) terraces separated by one-atom-high steps, about 5–10% of HD product is detected. In both cases, the Pt surface temperature was 1000°K while the beam temperature was 300°K. As shown in Figure 33, the spatial distribution of unreacted H_2 or D_2 is peaked at the specular angle (45°) while HD product is desorbed with a cosine distribution, indicative of thermal equilibration of the product HD. These results suggest that a stepped Pt surface provides sites capable of catalyzing an efficient exchange mechanism, possibly H(ads, at step) + D_2(ads) $\longrightarrow$ *HD*(ads) + *D*(ads).

At $T < 500$°K, Bernasek and Somorjai[90] suggest that the rate-limiting step is the diffusion of D_2 across the (111) terraces to H atoms chemisorbed at the step. The activation energy for this process is 4.5 ± 0.5 kcal/mole. At $T > 600$°K, an Eley–Rideal process involving the collision of an incident D_2(g) molecule with an adsorbed H atom at the step begins to become important.

It should be pointed out that these experiments using a chopped molecular beam plus phase-sensitive detection of product are designed to detect surface events which occur on a time scale of the order of milliseconds for this system; processes which occur more slowly are not measured. Recently, Rye and Lu[264] have used a steady-state method to compare the rate of HD production on various single-crystal faces of Pt. This method samples surface events occurring on a much longer time scale than the molecular beam method. They too find that the Pt(111) surface is less reactive than a stepped Pt(111) surface, but the factor difference in rates is only about two

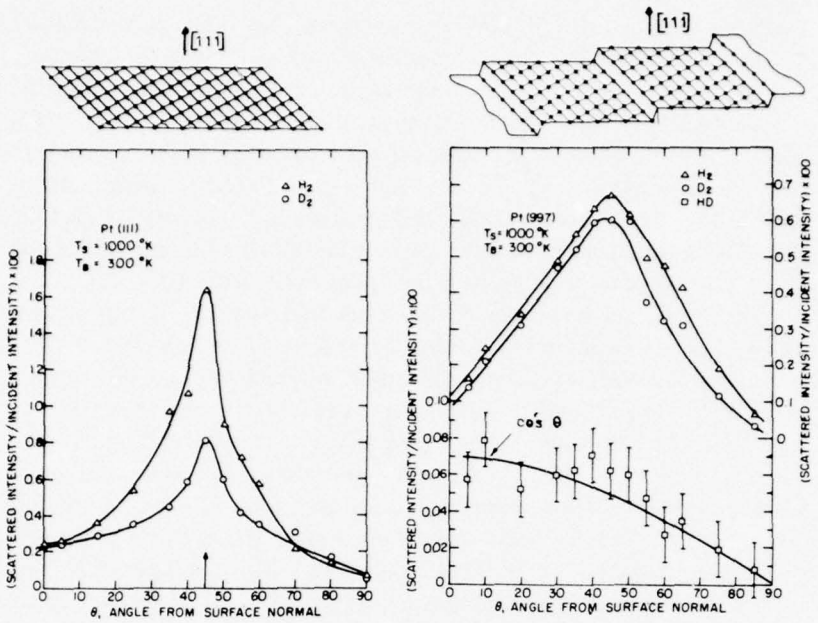

Fig. 33. Angular distribution of isotopic hydrogen molecules from Pt(111) and a stepped Pt surface containing (111) steps. Left figure: H_2 and D_2 scattered from D + Pt(111). No HD production is observed. The H_2 and D_2 reflected beams have maximum intensities at the specular angle (45°). Right figure: H_2, D_2, and HD scattering from stepped surface. The HD scattering appears to be cosine-like, indicating that HD product has come to thermal equilibrium with the surface prior to desorption. (From Bernasek and Somorjai.[90])

at 700°K. This smaller difference in observed ratios of rates is understandable if the Pt(111) surface is more active for exchange when exchange events occurring over a longer time scale are counted.

Somorjai and co-workers have attempted to extend these comparisons of planar and stepped Pt(111) surfaces to surface-catalyzed hydrocarbon reactions of importance in petroleum chemistry. In particular, the reactions of *n*-heptane on platinum have been studied, and various reactions have been observed as shown below:

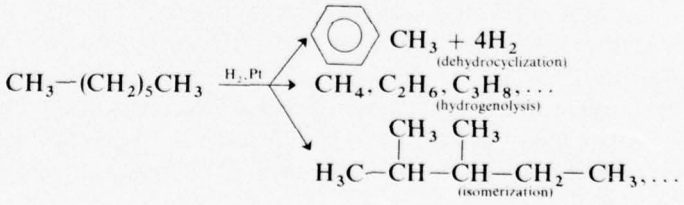

Both the hydrogenolysis and isomerization processes seem to exhibit little sensitivity to step density; in addition, a disordered carbonaceous layer forms when these reactions take place at low pressures, and this layer does not hinder the reactions in any way. In contrast, the dehydrocyclization reaction to form toluene occurs only when an *ordered carbonaceous layer* is formed on a *stepped* platinum surface, and terraces of six atom width seem to exhibit the highest catalytic activity for this reaction.[9,265] Recently, irreproducible factors in these experiments have been discovered; the unique activity of six-atom stepped surfaces is presently being reinvestigated.[266]

The relation between studies of catalytic processes on dispersed catalysts and on single-crystal substrates is evident from the above examples. Unfortunately, at this time, few examples are available demonstrating the use of single-crystal substrates as catalysts at high pressures. Recently, Somorjai and co-workers have utilized a Pt single crystal as a catalyst for the hydrogenolysis of cyclopropane.[258] Initial specific rates were identical to within a factor of *two* when compared with dispersed Pt catalysts. This work was carried out in an auxiliary high-pressure reaction chamber. Figure 34 shows the

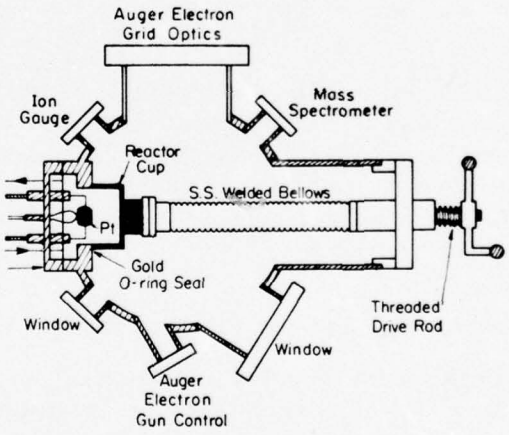

Fig. 34. Schematic view of an ultrahigh vacuum system containing a high-pressure reactor cup for measuring the catalytic activity of a single crystal of Pt. The reactor cup may be isolated from the vacuum chamber and catalytic reaction rates may be measured using gas chromatography in a recirculating flow system. (From Khan *et al.*[83])

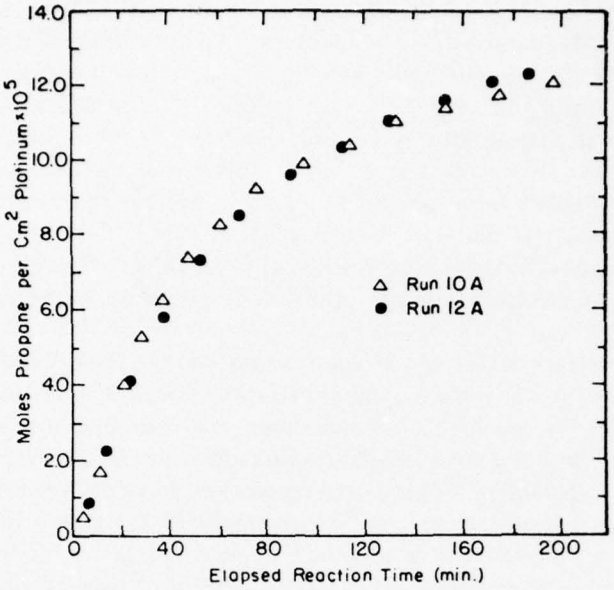

Fig. 35. Reproducibility of the rate of cyclopropane hydrogenolysis ($C_3H_6 + H_2 \rightarrow C_3H_8$) on a stepped Pt single crystal surface [Pt(s)-6(111) × (100)]. $P_{C_3H_6} = 135$ Torr, $P_{H_2} = 675$ Torr, $T_{crystal} = 74°C$. (From Khan *et al.*[8.31])

high-pressure chamber within an ultrahigh vacuum apparatus and Figure 35 indicates the reproducible rate of cyclopropane formation observed in duplicate measurements on a Pt single crystal. It is anticipated that measurements of this type will eventually lead us to a more complete understanding of the structural factors which are significant in catalytic processes.

6.2. Recent Investigations of Small Catalyst Particles

As has already been discussed in Section 3.1, practical metal catalysts are frequently used in powder form, or in supported form (finely dispersed metal particles supported on a high-area insulating substrate). An understanding of the physical and chemical properties of such small particles has a clear relevance to an understanding of catalytic processes. The existence of "demanding" reactions, in which catalytic activity and selectivity are known to vary greatly as a function of particle size,[8] has served as a spur to studies of small particles.

In particular, there has been a great deal of theoretical interest demonstrated recently in the geometric and electronic properties of small metallic "clusters" of particles.

6.2.1. Pairwise Interaction Models

For many years, it has generally been assumed that microcrystals of a material have the same crystal structure and symmetry as the bulk macrocrystals. This assumption is the basis for particle size determinations using electron diffraction techniques, for example.[267] More recently, however, it has been recognized that microcrystals frequently exhibit fivefold rotational symmetry—a symmetry which is forbidden in long-range crystalline lattices by the requirement of periodicity. Figure 36 is an electron micrograph showing several pentagonal gold crystals which were observed following deposition of thin gold films on a mica substrate.[268] Bagley[269] has shown that it is possible to produce a space-filling, hard sphere structure which has fivefold symmetry; this structure, shown in Figure 37, is simply not a periodic structure. It can be regarded as a fivefold twin of close-packed material surrounding a small seed of fivefold rotational symmetry.

The origin of the seed of fivefold symmetry has been discussed by Hoare and Pal[270] and by Burton.[271] If one examines the growth sequence of a crystal in which the atoms interact by simple Lennard-Jones type of pairwise interactions, the structures will deviate from the normal fcc structure. A surprising result was the observation that

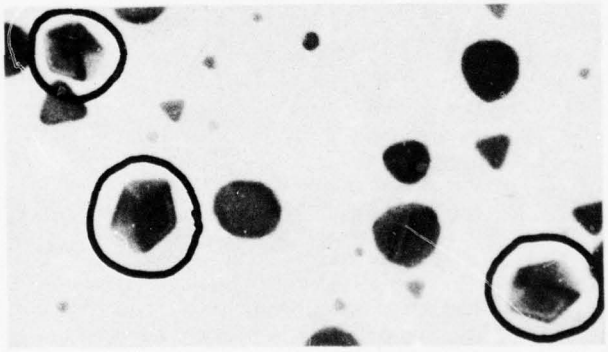

Fig. 36. Electron micrograph of several pentagonal gold crystals grown by evaporation of gold onto a heated mica substrate. (From Allpress and Sanders.[268])

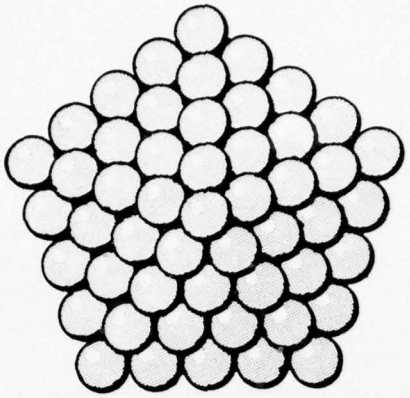

Fig. 37. Model of a fivefold symmetric crystal obtained by the continued packing of hard spheres on a seed of fivefold symmetry. Note that the exposed surfaces have close-packed (111) orientations. (From Bagley.[269])

the most stable geometry for a 13-atom cluster is not the fcc structure of Figure 38a, but is the fivefold symmetric icosahedral structure of Figure 38b. The 13-atom fcc structure is unstable, and would shear into the icosahedron if the fcc structure were somehow constructed. The

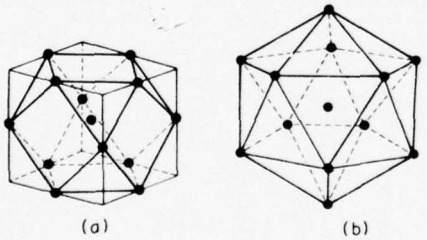

Fig. 38. (a) Thirteen-atom cubooctahedral cluster showing the nearest-neighbor environment corresponding to atoms packed in a face-centered cubic lattice. Note that the surface arrangement of atoms contains elements of both (100) and (111) surfaces. (b) Thirteen-atom icosahedral cluster. Note the axes of fivefold symmetry, as well as the fact that all of the exposed surfaces have (111) symmetry. (From Johnson and Messmer.[50])

next largest perfect icosahedron is a 55-atom cluster, which Burton reasons is the seed on which crystals exhibiting fivefold symmetry (Figure 36) have grown. It is also of interest to note that the surface planes of the 55-atom icosahedral clusters all have the structure of close packed (111) planes, whereas many planes in a 55-atom fcc structure are square (100) planes. Atoms in (111) planes have higher coordination numbers (more nearest neighbors) than those in (100) planes, so that elimination of (100) planes in rearrangement from the fcc to the icosahedral structure increases the number of nearest-neighbor bonds and lowers the energy of the system.

6.2.2. Quantum Chemistry of Small Particles

There have been a number of applications of molecular orbital theory to chemisorption and catalysis in the last few years. Reviews by Johnson and Messmer[50] and by Slater and Johnson[51] contain excellent overviews of the state of various molecular orbital approaches to catalysis problems. As discussed in Section 4, these authors have developed a technique called the "self-consistent-field X-alpha scattered wave" cluster method (SCF-Xα-SW). This approach has been applied to small Cu_8 and Ni_8 clusters having simple cubic geometry, the simplest structure which has been used to characterize small catalytic particles.[51] The SCF-Xα energy levels computed for Cu_8 and Ni_8 particles are shown in Figure 39. There is remarkable similarity between the electronic structure of the eight-atom clusters and the bulk solids, e.g., the complete set of Cu_8 energies can be characterized as a dense band of *d* levels bounded above and below by levels which are predominantly *s*- and *p*-like in character, but with some *d* admixture. The electronic structure of the Ni_8 cluster is similar to the spin-polarized band structure for ferromagnetic crystalline Ni, particularly with respect to the high density of *d* states around the Fermi level. However, the spin magneton number per atom (0.25) in paramagnetic Ni_8 is considerably less than the value for ferromagnetic crystalline Ni (0.54). This decrease is consistent with the paramagnetic susceptibility measurements of Carter and Sinfelt[272] for highly dispersed, silica-supported Ni. Carter and Sinfelt had concluded that the decrease in susceptibility was large when the metal particles become sufficiently small and significant fractions of the atoms are present on the surface.

SCF-Xα-SW calculations for 13-atom Li clusters[51] suggest that the icosahedral geometry is more stable than the cubooctahedral

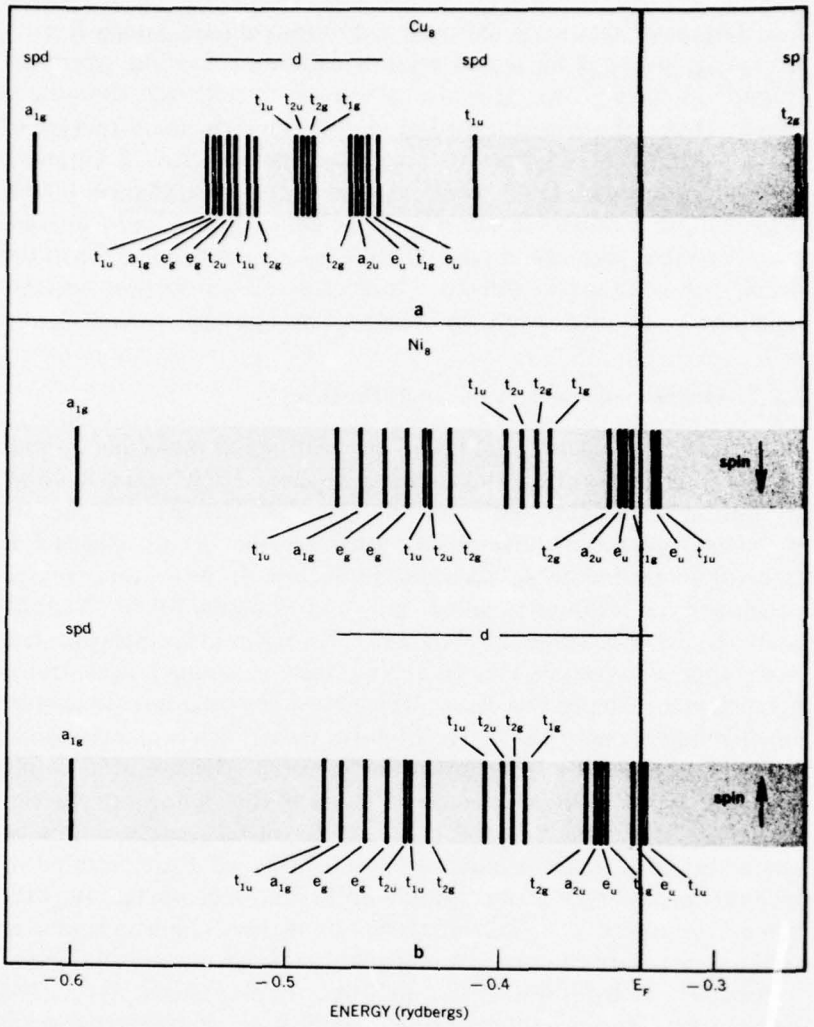

Fig. 39. Theoretical energy levels for copper and nickel clusters computed using the SCF-Xα method. Part (a) shows the SCF-Xα electronic energy levels for a simple cubic Cu_8 cluster; part (b) shows the spin–polarized SCF-Xα electronic energy levels of a simple cubic Ni_8 cluster. For each cluster, the results are shown for a nearest-neighbor internuclear distance equal to that in the corresponding bulk crystal. The levels are labeled according to the irreducible representations of the cubic (O_h) symmetry group. The "Fermi level" E_F separates the occupied levels from the unoccupied ones. (From Slater and Johnson.[511])

geometry, a result in good agreement with the pairwise interaction calculations (Section 6.2.1).

6.3. Stereochemical Methods as an Aid to the Determination of Catalytic Mechanisms

The determination of the structures of intermediate species in heterogeneous catalysis is an important driving force in catalytic research. Ideally, this objective also includes a specification of the structure of the catalytic site, which, as we have seen, is at present often an elusive goal. While studies of the kinetics of catalytic processes are an important aspect of the determination of catalytic mechanisms, kinetic arguments are, by themselves, usually not a completely definitive factor in selecting a model to describe the reaction. Often many dissimilar mechanisms give the same overall kinetics.[2] For this reason, in the case of complex molecules, stereochemical methods are often used to aid in the definition of the mechanism of a catalytic reaction, or in the definition of the geometry of adsorbed species involved in the reaction. A few examples of the usefulness of stereochemical arguments will be given below. Burwell[273] and Siegel[274] have discussed in detail the stereochemical evidence for various bonding modes in hydrocarbon adsorption and reaction. We will consider as a first example the catalytic reaction of a disubstituted acetylene (2-butyne) with hydrogen on a Pd catalyst. 2-Butyne is a linear molecule. It is well known that, in general, the *cis*-addition of two hydrogen atoms to the triple bond occurs, i.e., that both hydrogens add to the same side of the triple bond. In this case, *cis*-addition would therefore give an olefin in which the two methyl groups are on the side of the double bond opposite the H atoms. There is additional experimental evidence showing that deuterium addition yields the *cis*-dideutero species as a product. This further confirms that the two methyl groups do not interact with the surface. Thus, a proposed mechanism is

$$D_2 + 2Pd \rightarrow 2D\text{-}Pd$$

$$H_3CC{\equiv}CCH_3 + 2Pd \rightarrow \begin{matrix} H_3C & & CH_3 \\ & C{=}C & \\ Pd & & Pd \end{matrix}$$

$$D{-}Pd + \begin{matrix} CH_3 & & CH_3 \\ & C{=}C & \\ Pd & & Pd \end{matrix} \rightarrow \begin{matrix} CH_3 & & CH_3 \\ & C{=}C & \\ D & & Pd \end{matrix} \rightarrow \begin{matrix} CH_3 & & CH_3 \\ & C{=}C & \\ D & & D \end{matrix}$$

An alternative mechanism is that the 2-butyne reactant molecule collides with two sites containing adsorbed deuterium and that reaction occurs to yield the *cis*-dideutero species. Kinetic studies indicate that this alternative mechanism is not applicable since the process is roughly zeroth order in 2-butyne (i.e., almost pressure independent) and first-order in deuterium.[273]

As a second example of the utility of stereochemical reasoning, we consider, following Burwell,[273] the hydrogenation of molecules (olefins) containing a carbon–carbon double bond. Again, there is ample evidence that *cis*-addition of two hydrogens generally occurs, but the question arises as to whether this addition occurs from the gas phase to the topside of the adsorbed species, or from adsorbed hydrogen underneath the surface complex. Two general configurations for an olefin adsorbed on substrate atoms M are possible,

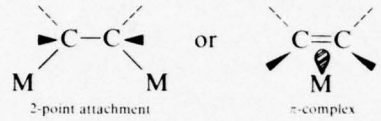

The two-point attachment would involve sp^3 hybridization of each C atom, whereas the π-complex could form with preservation of the planar geometry of the olefin. The discrimination between these two structures is, at present, difficult using chemical methods alone.[275]

In order to determine whether topside addition of hydrogen to an olefin is possible, Burwell[276] cited the work of others[277] dealing with the catalytic hydrogenation of large cyclic olefins. This work concerned the hydrogenation of *trans*-cyclononene, which contains a carbon–carbon double bond with one side protected by a chain of seven CH_2 groups connected *trans* across the double bond as shown schematically below:

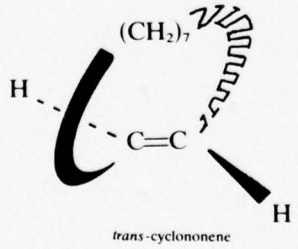

trans-cyclononene

This molecule is effectively hydrogenated catalytically, suggesting that H attack occurs *under* the molecule, involving electrons that were used to produce the chemisorption bond initially.

Fig. 40. Three stereochemical views of a chemisorbed olefin. Left figure: Carbon–carbon single bond with two-point attachment to surface atoms. Staggered conformation of sp^3 carbon orbitals. Central figure: Same as above, except eclipsed conformation of sp^3 carbon orbitals. Right figure: π-complex single-point attachment. Carbon is hybridized in sp^2 state. (From Burwell.[273])

We can ask even more detailed questions regarding the stereochemical nature of surface species involved in catalytic reactions. Burwell[273] has considered three possible stereochemical conformations for an adsorbed olefin as shown in Figure 40. The left-hand diagram represents a staggered form of a two-point attachment species; the central diagram represents an eclipsed form of a two-point attachment species; the right-hand diagram represents a π-complex. By freezing in either of the first two configurations using ring structures to orient C–H bond directions, it has been possible to show that the

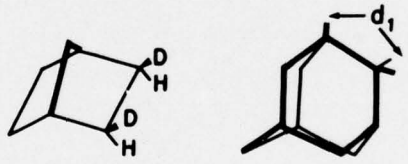

exo-norbornane-d_2 adamantane-d_1

Fig. 41. Stereochemical views of two cyclic hydrocarbon molecules in which the rigidity of the ring structure produces eclipsed or staggered C–H bonds. Left: exo-norbornane; eclipsed C–H bonds undergo double site deuterium exchange in one period of adsorption. Right: adamantane; staggered C–H bonds undergo single-site deuterium exchange in one period of adsorption. (From McMahon and Clarke[278] and Schrage and Burwell.[279])

eclipsed form is necessary for deuterium exchange to occur on the two C atoms together. Thus, as summarized in Figure 41, two deuterium atoms initially exchange with hydrogens in adsorbed norbornane[278]; the original C–H bonds here are held in the eclipsed conformation by the ring structure in the norbornane. In particular, the readily exchangeable hydrogens are in the equatorial position pointing outward, roughly in the plane of the ring. The interpretation was made using NMR analysis of exchanged products, and suggests that the molecule adsorbs on edge by means of two-point attachment. By contrast, adamantane (Figure 41) contains only staggered C–H bonds and exchanges only a single deuterium initially over Pd,[279] as deduced by mass spectrometry of the products.

As a final example of the influence of stereochemical factors on catalytic processes, we turn to a brief discussion of the stereoregular polymerization of propylene, as discovered by Ziegler and Natta, leading to the award of a Nobel Prize in Chemistry in 1963.[280] The basic discovery was that certain catalysts containing transition metals caused propylene to polymerize in such a way that the asymmetric carbon atoms in the polymer are all either right-handed (*d*-configuration) or left-handed (*l*-configuration). An asymmetric carbon atom is tetrahedrally bonded to four *different* substituents. This configuration of substituents implies the possibility of two conformations of the carbon atom and its substituents, which are mirror images. Such a polymer is termed isotactic and is schematically shown below, where the asterisk indicates an asymmetric C atom:

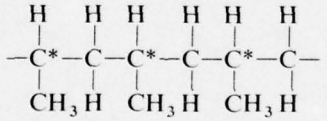

In a monumental series of three papers,[281] Cossee and Arlman have described the electronic and crystallographic factors responsible for olefin stereospecific polymerization on the surface of transition metal halides, specifically $TiCl_3$. The specific adsorption and polymerization of the parent olefin is envisioned to occur in the vicinity of a Ti^{+3} ion which is incompletely coordinated with Cl^- ions near the surface of an α-$TiCl_3$ crystal. The olefin is postulated to be bound to Ti^{3+} via a π-bond as shown in Figure 42, where ethylene is depicted as the adsorbed olefin. The Ti^{3+} ion, designated M, is octahedrally coordinated along the *x*, *y*, and *z* axes with either a Cl^- (designated X) or an alkyl group designated R as shown in Figure 43. It is seen that

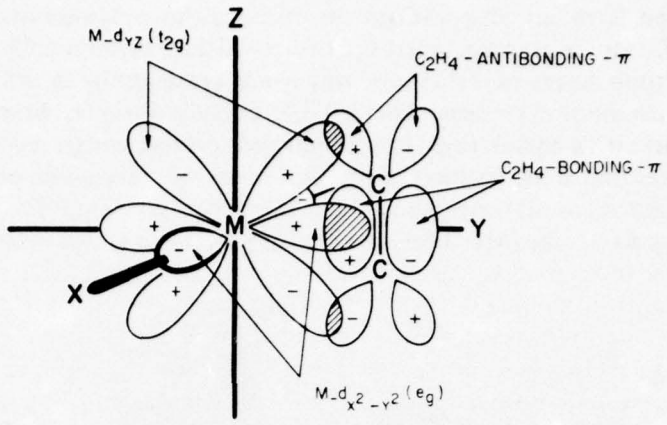

Fig. 42. Schematic view of π-bonded ethylene on a transition metal atom M. This complex is proposed as the initial species in the stereoregular polymerization of olefins by Ziegler–Natta catalysts. (From Cossee and Arlman.[281])

the olefin coordinates with the metal M via an octahedral site which is initially unfilled. The polymerization step, involving the linkage of R to one end of the olefin, is depicted in the third step of Figure 43. The final result is to generate an R–CH_2–CH_2– group linked to M, plus a new vacant octahedral position at the point where R originally existed. The model of Cossee and Arlman now requires R–CH_2–CH_2– to migrate back to the original site which contained R, so that adsorption of another olefin molecule can occur at the same site as before, since the model for production of isotactic polymer requires that the active polymerization site have identical stereochemical conformation for each polymerization step.

The basic idea formulated above has been woven by Cossee and Arlman[281] into a crystallographic model which seems appropriate

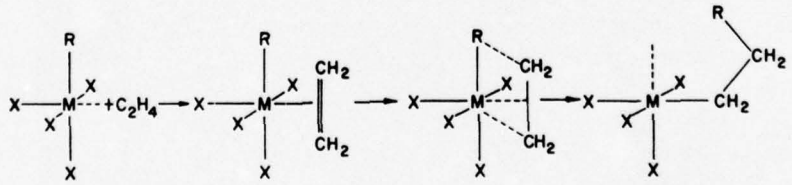

Fig. 43. Schematic view of polymerization step in Ziegler–Natta catalysis. R is an alkyl group which adds to the adsorbed olefin. In this model, R–CH_2–CH_2– migrates back to the original R site ready for another polymerization step. M = Ti^{3+}; X = Cl^-. (From Cossee and Arlman.[281])

to explain recent observations regarding olefin polymerization on α-$TiCl_3$ single crystals. α-$TiCl_3$ consists of hcp layers of Cl^- ions separating layers of Ti^{3+} ions, which are octahedrally coordinated with neighbor Cl^- ions. The α-$TiCl_3$ crystals form as hexagonal platelets with (0001) faces. For a finite size crystal, charge neutrality requires that some fraction of the Ti^{3+} ions will have an incomplete octahedron of Cl^- neighbors, i.e., there will be some Ti^{3+} sites having a Cl^- vacancy. These are the sites that are active centers for

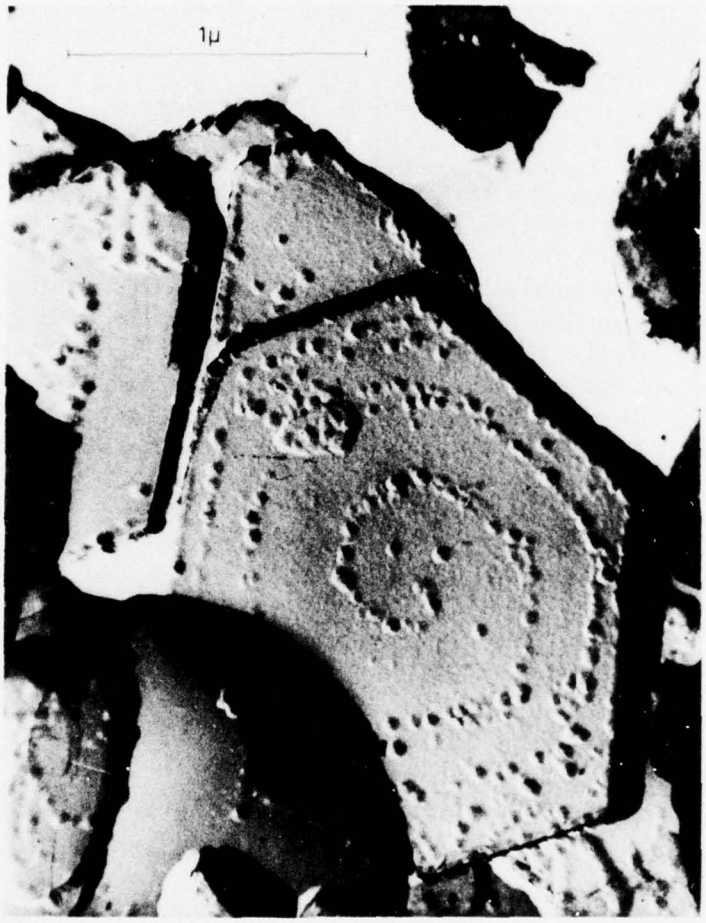

Fig. 44. Electron micrograph of α-$TiCl_3$ crystals containing polypropylene molecules at crystal edges and along spiral dislocation. (From work of Rodriguez and van Looy,[282] courtesy of Boudart.[110,3])

olefin adsorption and polymerization. Independent of the shape and size of the α-$TiCl_3$ crystal, the number of these vacancies is approximately equal to the number of Ti^{3+} ions located on the *edge* of the hexagonal platelets. Furthermore, electrostatic calculations indicate that Cl^- ions are more likely to be absent from the crystal edge than from the (0001) faces. Thus, polymerization should occur specifically at edge sites. These basic conclusions, arrived at theoretically in 1963, have been confirmed by dramatic electron micrographs of α-$TiCl_3$ crystals following their use in propylene polymerization. As shown in Figure 44, Rodgriguez and Van Looy[282] have observed that polypropylene is selectively formed at the platelet edges (black), as well as along spiral dislocations (white) within the (0001) plane. Both of these regions would be expected to be Cl^- deficient. Boudart[103] has pointed out that not every site in the spiral dislocation is active, perhaps because of the requirement of very specific geometry for a Cl^--deficient center to be active for polymerization. Burwell[273] suggests that while the mechanism proposed above may be inaccurate in detail, it represents a historical landmark in heterogeneous catalysis because of the detailed understanding which has been made possible through consideration of stereochemical data.

7. Reduction and Enhancement of Catalytic Activity: Poisons and Promoters

Two factors of immense practical importance in industrial catalysis are (a) the degradation of catalyst activity as a function of time in use and (b) the enhancement of catalytic activity by the addition of promoter materials to the "pure" catalyst. Connecting catalyst deactivation and catalyst promotion is the fact that both of these processes proceed via alteration of the structural and/or electronic properties of the initially pure catalyst. Details of these electronic and structural modifications are explored in the following paragraphs.

7.1. Catalyst Deactivation

The decay in activity of a catalyst as a function of time in use may be due to a number of factors.[283] (a) Certain catalysts are poisoned by impurities in the feed gas, (b) others sinter and lose surface area under reaction conditions. (c) Under some conditions, catalysts may be self-poisoned via the deposition of by-products on the surface from

decomposition of the reactants or products. In this case, the poisons can frequently be removed in a regeneration step in which the catalyst can be brought back to its original activity. (d) The surfaces of certain catalysts recrystallize under reaction conditions to expose facets having a symmetry different from the as-prepared catalyst. (e) During the catalytic process, the oxidation state of the catalyst may change. In the present discussion, the emphasis will be on poisoning by impurities, self-poisoning, and surface recrystallization. Sintering will be discussed in Section 7.2, since an important use of promoters is for prevention of sintering.

Catalyst poisoning by impurities in the reactants is a serious problem in a number of applications. One such problem of current concern for energy production is the catalytic methanation reaction[284] (the hydrogenation of carbon monoxide to methane), the crucial reaction in the manufacture of methane gas from coal. With the nickel catalysts presently employed in methanation reactors, it is usual to limit sulfur compounds in the $H_2 + CO$ feed gas to less than 1 ppm in order to avoid deactivation by sulfur poisoning. Despite the realization that sulfur adversely affects catalyst performance, there is little understanding of the mechanisms by which catalyst poisons act. As an example of the complexities involved in the understanding of poisoning processes, the most active methanation catalysts, Ni and Ru, are both highly susceptible to sulfur poisoning where the less active metals Mo and W are resistant to sulfur poisoning, and are frequently sulfided before use as methanation catalysts! In another example, the use of catalysts for the removal of CO, hydrocarbons, and NO from automotive exhaust, it was found that not only sulfur, lead, and halides from gasoline and gasoline additives but also phosphorus from motor oil additives poisoned the catalysts.

In spite of complexities of catalyst poisoning, answers are just starting to appear to such questions as: Does the poison inhibit the reaction by blocking active sites on a one-to-one basis, or does the poison operate via a long-range electronic interaction through the substrate (see Section 4.4)? Alternatively, does the presence of sulfur compounds result in a restructuring or recrystallization of the catalyst surface?

Because such small traces of impurities are able to poison catalysts, experimental studies are frequently limited by the sensitivity of chemical analytical methods. Several recent studies[285,286] of catalyst poisoning using Auger electron spectroscopy (AES) have demonstrated the utility of a specifically surface-sensitive technique

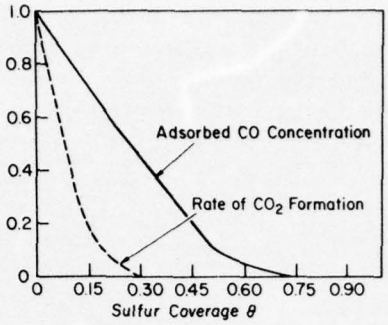

Fig. 45. Effect of sulfur as a poison in the oxidation of CO to form CO_2 on a (110) Pt surface. Composite plot of the normalized adsorbed CO concentration (expressed as a fraction of a monolayer) and normalized rate of CO_2 formation, both shown as a function of calibrated sulfur coverage (θ is the fraction of a monolayer of sulfur). (From Bonzel and Ku.[286])

for such investigations (as indicated in Section 5.2.1, AES is sensitive to the top few atomic layers of a solid). Bhasin[285] has shown that a surface concentration of 13 atoms of Pb per 100 surface atoms of Cu is sufficient to cause a dramatic reduction in the ability of powdered copper catalysts to catalyze the reaction of methyl chloride with silicon. Bonzel and Ku[286] used low-energy electron diffraction (LEED) and AES in a comprehensive study of the effect of sulfur on the catalytic oxidation of CO ($2CO + O_2 \rightarrow 2CO_2$) on a Pt(110) surface. They demonstrated that a very low sulfur coverage on Pt is needed to poison this reaction; as shown in Figure 45, the steady-state rate of CO_2 production decreases to less than 10% of its initial value at a sulfur coverage of $\sim$0.20 monolayer. Figure 45 also shows that the concentration of adsorbed CO on the S-covered surface does not decrease as rapidly as the CO_2 production. This observation, when coupled with other kinetic evidence, led to the conclusion that the sulfur poisoning of CO oxidation on Pt(110) is correlated solely with the adsorption of oxygen on the partially S-covered surface. That is, the presence of sulfur limits the dissociative adsorption of oxygen. They reason that this is largely a site-blocking effect, but cannot eliminate the possibility of a longer range electronic effect.

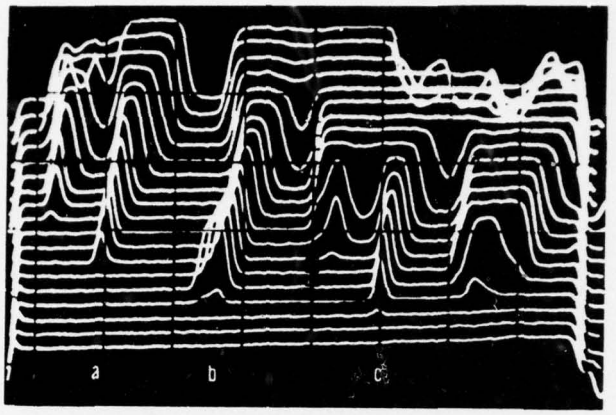

Fig. 46. Illustration of the non-uniform distribution of S left on an initially uniformly S-covered Pt(110) surface following reaction with O_2 at 2×10^{-7} Torr, $T_{(Pt)} = 350°C$. The curves are oscilloscope traces of the maximum in the sulfur Auger peak as a function of position on the Pt surface, and indicate that isolated patches of S are formed during the reaction. Note the ridges a, b, and c. (From Bonzel and Ku.[286])

Bonzel and Ku[286] also examined the interaction between adsorbed sulfur and oxygen on the Pt(110) surface, and found that SO_2 was the reaction product. For low sulfur coverage, $\theta < 0.28$, the reaction was quite fast, whereas for higher sulfur concentrations, $0.28 < \theta_s < 0.75$, the reaction became very slow. In this latter range, the reaction proceeded inhomogeneously, and resulted in a nonuniform distribution of adsorbed sulfur. Figure 46 shows several oscilloscope traces resulting from a two-dimensional scan of the sample surface using AES. These traces clearly indicate that the sulfur remains on the surface in discrete "patches" following the oxidation reaction and that under these conditions, the poisoned surface consists of a mixture of clean regions and sulfur-covered regions.

In addition to poisoning by impurities, catalysts are also susceptible to self-poisoning by the reactants, products, or both. In a careful study of self-poisoning, Hegedus and Petersen[287] have applied a method known as the single pellet diffusion reactor technique to the problem of poisoning of a supported Pt catalyst during the hydrogenation of cyclopropane to propane ($H_2 + C_3H_6 \rightarrow C_3H_8$). The technique allows one to discriminate among impurity poisoning, parallel self-poisoning, series self-poisoning, and triangular self-poisoning, whose poison precursors are, respectively, an impurity in

the feed gas, the reactant itself, the product itself, or both the reactant and the product. By careful experimentation so as to eliminate impurities, and by comparison of data with the theoretical models, they concluded that the catalyst was poisoned by both the reactant cyclopropane (A) and product propane (B) (triangular self-poisoning) at temperatures between 50 and 75°C according to the mechanism

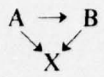

where X is the poison structure on the catalyst surface. The exact nature of X is not well-defined, but it is clearly a carbonaceous residue due to decomposition of A and B.

Another example of self-poisoning is the fouling of a methanation catalyst due to carbon deposition. Mills and Steffgen[284] have tabulated the effects of temperature, pressure, and H_2/CO ratios on the degree of carbon deposition. In this case, equilibrium thermodynamics was used to define the boundaries above and below which extensive carbon deposition occurs.

As indicated previously, the effects of self-poisoning are often reversible, and such poisoned catalysts may frequently be returned to their original activity by regeneration steps such as changing feed stock ratios, catalyst temperature, etc.

Somorjai[9] has pointed out that deposition of a carbonaceous overlayer on the surface of a catalytically active metal does not always result in self-poisoning. An *ordered* carbonaceous overlayer on a stepped Pt single-crystal surface is necessary for high activity in the catalytic dehydrocyclization of *n*-heptane to toluene. In contrast, however, a *disordered* carbon-containing layer will inhibit the same reaction. Thus, the real catalyst in this reaction is not the clean Pt metal, but rather the metal surface covered in a special way with a well-defined carbonaceous layer.

Another possible mechanism of catalyst poisoning involves faceting, i.e., changes in surface structure, in the presence of impurities adsorbed on the surface. There is good evidence that in some cases, Pt and Pt alloy surfaces develop crystal planes having (100) orientation in the presence of sulfur.[288] As Somorjai[289] has pointed out, adsorbed impurities change the free energy of a surface. If the foreign atoms alter the surface free energy of various crystal planes by different amounts, they can induce the rearrangement of the surface structure to form crystal planes that have lower surface free energy in the presence of the adsorbed impurity than in the absence of the impurity.

If this model of poisoning is correct, then "structure-sensitive" reactions should be affected by impurities that induce recrystallization, whereas "structure-insensitive" reactions should be relatively unaffected. To date, there does not appear to be enough evidence to draw a firm conclusion concerning the role of surface recrystallization in catalyst poisoning, but it is a promising area of investigation.

7.2. Enhancement of Catalytic Activity: Promoters

It has long been recognized that the activity of catalysts for certain reactions may be enhanced by the incorporation of small quantities of specific additives (promoters) during the preparation of the catalyst. Two well-studied examples of catalyst promotion involve the use of oxide promoters in iron catalysts for ammonia synthesis, and the role of Ca promotion in the Ag-catalyzed oxidation of ethylene.

In a pioneering series of experiments, Emmett and Brunauer[290] showed that the addition of promoter oxides such as Al_2O_3, K_2O, and Na_2O increases considerably the total surface area per gram of a reduced iron synthetic ammonia catalyst. By using gas adsorption techniques to determine surface areas, they found that iron synthetic ammonia catalysts promoted with small amounts of oxides ($\sim 1\%$) have $\sim 60\%$ of their surface covered with promoter. More recently, Solbakken *et al.*[291] have verified this earlier result using an isotope exchange method, and further showed that the promoter molecules (in this case, Al_2O_3 in Fe) are present at the surface in a single atomic layer.

Alumina incorporated in iron catalysts is known to be a textural promoter which prevents sintering; sintering of unpromoted iron particles occurs quite easily, whereas singly promoted (one promoter oxide) catalysts have a much better resistivity toward sintering. Thus, at least part of the mechanism for the promotion of catalytic activity is the fact that the surface area of the catalyst is not reduced by sintering during the course of reaction.

Topsoe *et al.*[292] have challenged the traditional view that textural promotion of Fe by Al_2O_3 is purely a surface effect. They recognized, as have others, that a major fraction of the promoter must remain inside the iron crystallites, even though the surface has a high coverage of promoter. Using Mössbauer spectroscopy, they found that the Al_2O_3 is present in the iron in the form of ~ 30-Å inclusions of $FeAl_2O_4$ in the incompletely reduced catalyst and of

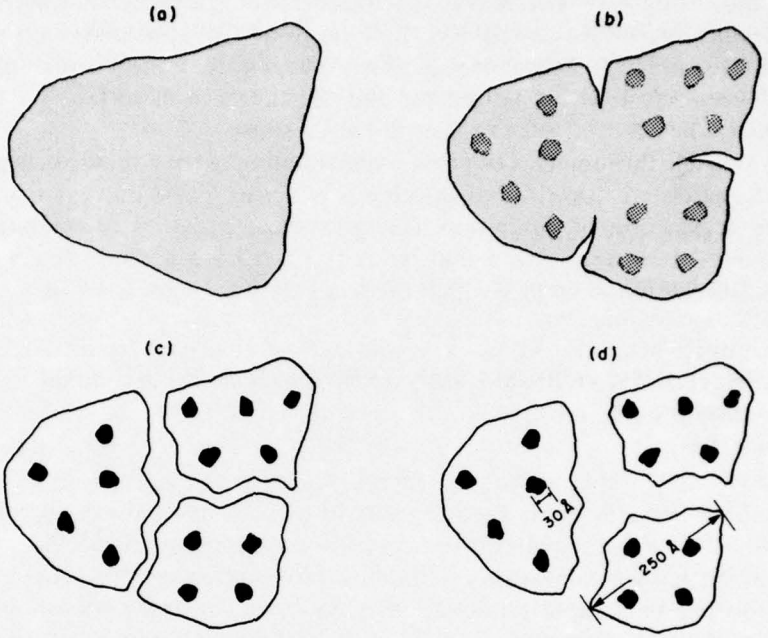

Fig. 47. Model of the effect of a textural promotor (Al_2O_3) on the reduction of an iron synthetic ammonia catalyst. (a) Unreduced large catalyst particle with the promotor distributed homogeneously. (b) Catalyst after a short reduction; aluminum-rich regions appear. (c) Catalyst after further reduction consists of pure α-Fe and $FeAl_2O_4$ inclusions. (d) Fully reduced catalyst. Consists of small α-Fe particles with Al_2O_3 inclusions. (From Topsoe *et al.*[292])

Al_2O_3 itself after thorough reduction. They suggest that the existence of strain in the iron particles created by the occluded Al_2O_3 phase will shift the equilibrium particle size to smaller particles. Thus, small catalyst particles are stabilized against sintering by the occluded promoter. Their model of the effect of Al_2O_3 on the reduction process of an iron catalyst is shown in Figure 47.

The remarkable selectivity of silver catalysts in the oxidation of ethylene to ethylene oxide has also been a subject of intense investigation. Kilty and Sachtler[293] have reviewed the literature concerning this reaction, and conclude that the formation of diatomic adsorbed oxygen (O_2^-) on the catalyst surface is the key to the selective oxidation reaction. Furthermore, the selectivity is enhanced by a CaO promoter in technical Ag catalysts. Forsalti *et al.*[294] found an increase in selectivity upon irradiating a supported Ag catalyst by γ-rays, and

found, using ESCA (electron spectroscopy for chemical analysis, a specifically surface-sensitive technique), that Ca appeared on the surface under these conditions. They suggest that the correlation between selectivity enhancement and the presence of surface Ca is due to the adsorption of O_2^- on these Ca sites.

In conclusion, it is clear that understanding of the complexities of catalyst deactivation and promotion is receiving a new impetus from the application of modern surface-sensitive techniques to catalytic systems. It is anticipated that we may soon have a more detailed understanding of factors which cause a catalyst's activity to vary.

8. Recent Examples of Catalytic Research on Well-Defined Surfaces

In the preceding pages, several examples of catalysis on well-defined surfaces have already been discussed. In many cases, the insensitivity of the catalyst to the method of preparation provides a surface that is operationally well-defined. In some cases, this behavior appears due to rapid solid-state diffusion under reaction conditions. Sometimes, a degree of confidence as to the nature of the catalytic surface may be gained by crushing crystals to obtain fresh surface area of the same composition as the bulk. This method is particularly suitable for the oxide catalysts discussed in Section 5. Where applicable, the use of the UHV techniques of surface physics is of much advantage, and a degree of characterization can then be obtained by LEED, AES, and other spectroscopies. The presence of steps and of some point defects is often still difficult to detect by these methods. Even so, high-index faces of Pt have been well-characterized by these methods, as discussed in Section 6. In the present section, some additional examples are discussed to illustrate the use of UHV methods in catalytic research.

8.1. Catalytic Decomposition of Ammonia on Tungsten Single Crystals

An interesting experiment to accurately compare the catalytic activity of different single-crystal surfaces is the recent work of McAllister and Hansen.[295] These workers used standard ultrahigh procedures to prepare clean tungsten crystals; the catalyst crystals were then exposed to NH_3 at pressures up to 10^{-1} Torr. The crystals were heated with a focused beam of light to temperatures in the range

800–970°K and the kinetics of catalytic decomposition was studied. It was shown that NH_3 decomposes stoichiometrically on all three crystal faces into N_2 and H_2 following the rate expression

$$\text{rate} = A + BP_{NH_3}^{2/3}$$

No influence of N_2 or H_2 on the decomposition kinetics was detected over a wide partial pressure range in accordance with the above expression. A significant retardation of the decomposition rate on W(111) was observed when ND_3 was substituted for NH_3 ($B_{NH_3} = 1.47B_{ND_3}$), indicating that the breaking of an N–H bond is involved in the rate-limiting step at higher NH_3 pressures, where the B term becomes dominant. It is proposed that the "B" process occurs on a substantially complete nitrogen adlayer of stoichiometry W–N, with complex intermediates being formed which eventually liberate N_2 and H_2, leaving behind W–N.

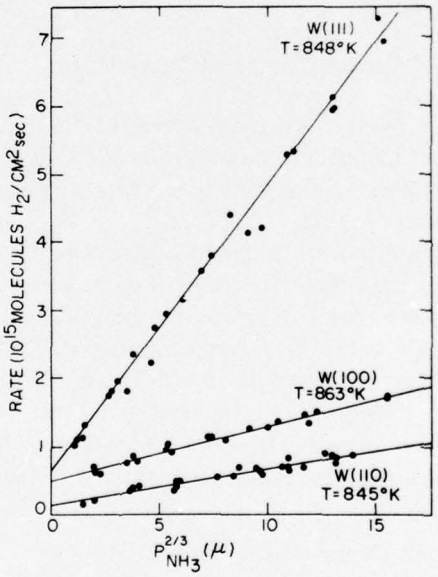

Fig. 48. Comparison of NH_3 decomposition rates on three tungsten single crystals at similar temperatures. The tungsten (111) crystal is the most effective catalyst of the three. The pressure is in units of 10^{-3} Torr. (From McAllister and Hansen.[295])

At low NH_3 pressures, the "*A*" process contributes significantly to the overall rate, and the model devised suggests that a surface process

$$2W\text{–}N \rightarrow W_2N + \tfrac{1}{2}N_2(g)$$

is rate limiting. The rate of N_2 liberation observed at low NH_3 pressures (i.e., the value of *A*) is of the same order of magnitude as that observed in thermal desorption experiments from pure nitrogen adlayers on polycrystalline surfaces, thereby giving support to the model proposed.

In Figure 48, a comparison is given of the rates of decomposition of NH_3 on the three tungsten crystals. Although the crystal temperatures differ slightly in the figure, it can be seen that the W(111) plane is significantly more active than either W(100) or W(110). No explanation is offered for the enhanced activity of the W(111) plane. This impressive measurement thus forms a sound basis for future theoretical considerations of the effect of surface structure and perhaps electronic factors on the rate of catalytic decomposition of NH_3.

8.2. Oxidation of Carbon Monoxide by Platinum

One of the most thoroughly investigated catalytic reactions through the years has been the oxidation of CO by Pt. This reaction has been both intriguing and vexing, starting with the classic work of Langmuir[296] and ranging to the recent studies on single crystals of Pt using modulated molecular beam techniques.[297] The same basic questions are as important today as they were over 50 years ago, namely, is the basic mechanism of the reaction unique, or does it depend on experimental boundary conditions? Two points of view concerning mechanism have been advanced.[298] In the so-called "Langmuir–Hinshelwood" (LH) mechanism, both reactants have to be adsorbed on the surface of the catalyst in order to form the reaction product. For example, the LH mechanism in CO oxidation is

$$CO(a) + O(a) \rightarrow CO_2(g) + 2M$$

where M represents a bare site on the surface. In the "Rideal–Eley" (RE) mechanism, only one reactant has to be firmly adsorbed on the catalyst while the other has to strike the adsorbate from the gas phase in order to form a bond between them. For example, a possible RE

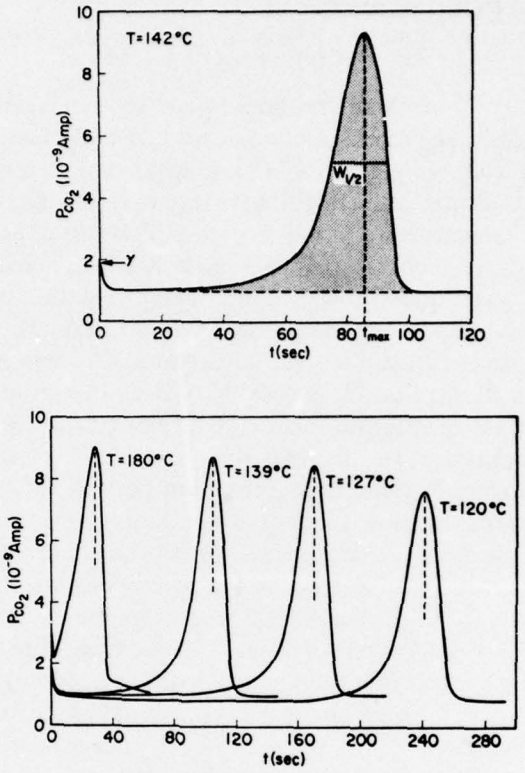

Fig. 49. *Upper figure*: Langmuir–Hinshelwood (LH) mechanism in CO oxidation. Plot of the partial pressure of CO_2 as a function of time, with the Pt(110) crystal at 142°C in an O_2 atmosphere. At time $t < 0$, the gas phase contains $CO + O_2$ as well as product CO_2; at $t = 0$, the partial pressure of CO is suddenly decreased. Since CO_2 formation increases and goes through a maximum at t_{max}, it follows that *only the CO present on the surface can contribute to the CO_2 formation.* Also, the strong temperature dependence of t_{max} suggests that oxygen must replace CO adsorbed on the surface in order for the reaction to proceed. This means that CO_2 is formed by a reaction between adsorbed CO and adsorbed oxygen (LH). *Lower figure*: Theoretical plots of CO_2 evolution curves based on the LH mechanism for CO_2 formation. Both the time at which the maximum occurs and the width of the peak are functions of the sample temperature. Note the correspondence between the upper experimental plot and these curves. (From Bonzel and Ku.[298])

mechanism in CO oxidation is

$$O(a) + CO(g) \rightarrow CO_2(g) + M$$

Langmuir[296] originally proposed that "oxygen is removed from the surface not by the reaction of adjacent CO molecules, but by the action of CO from the gas phase" (RE mechanism). In a recent series of experiments, Bonzel and Ku[298] have reported that the two different reaction mechanisms were found to prevail depending on the experimental conditions chosen. Bonzel and Ku employed a kinetic perturbation technique in their studies of CO oxidation on a Pt(110) surface. In the temperature range $100 < T < 220°C$, where CO was preadsorbed on the Pt surface, the subsequent adsorption of O_2 was dependent on desorption of part of the CO as shown in Figure 49, and the resultant reaction to form CO_2 exhibited the characteristics of an LH mechanism. In this case, the onset of CO_2 formation was delayed by a characteristic time (induction period) which depended strongly on temperature. On the other hand, when oxygen was preadsorbed on the Pt surface at $T > 90°C$, the subsequent reaction with CO occurred immediately, and was temperature independent, consistent with an RE mechanism. These experiments are illustrated in Figure 50. The conclusions of Bonzel and Ku regarding the reaction mechanisms are in excellent agreement with the conclusions of Ertl and co-workers[299] based on studies of CO oxidation on Pd single crystals, as well as with the data of White and co-workers[300] for polycrystalline Pd. Unanimity regarding the mechanism of CO oxidation on Pt has not yet been reached, however; in a recent molecular beam study, Palmer and Smith[297] have concluded that *all* of their CO oxidation results are consistent with an LH mechanism.

8.3. Decomposition of Formic Acid by Metals

Studies of the catalytic decomposition of formic acid (HCOOH) have long fascinated research workers for a variety of reasons, including the simplicity of the major products (H_2, CO, H_2O, CO_2) and the existence of different reaction paths.[301,302] Formic acid can decompose along three different pathways:

$$\text{HCOOH} \begin{cases} \rightarrow H_2 + CO_2 & (1) \\ \rightarrow H_2O + CO & (2) \\ \rightarrow H_2O + CO_2 + H_2CO & (3) \end{cases}$$

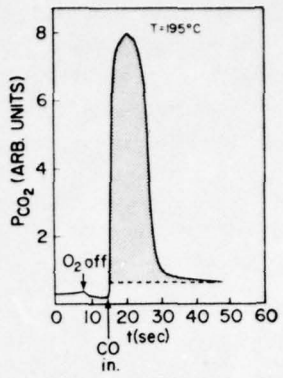

Fig. 50. Rideal–Eley (RE) mechanism in CO oxidation. Plot of partial pressure of CO_2 as function of time with the sample in a CO atmosphere. At $t < 0$, the sample is exposed to O_2, and the oxygen flow is stopped at 8 sec. At $t = 15$ sec, CO is admitted to the sample and, immediately, CO_2 is evolved. The CO_2 evolution rate is dependent on CO pressure but independent of temperature at $T > 90°C$, indicating a RE mechanism involving reaction of O(*a*) and CO(g) to make CO_2. (From Bonzel and Ku.[298])

Reaction (3) is not observed on metals; the dehydrogenation reaction (1) is considered to be the major reaction on metal catalysts, and the dehydration reaction (2) seems to be specific to certain oxide catalysts. In the following paragraphs, we will attempt to summarize what is known about this reaction based on two types of experiments:

(a) Studies of decomposition of HCOOH on finely dispersed metals, powders, films, and wires using kinetic methods combined with infrared absorption spectroscopy; HCOOH pressures were in the range greater than a few millitorr in these studies.

(b) Studies of decomposition of HCOOH on single crystals of Ni under ultrahigh vacuum conditions, using LEED, AES, and flash desorption mass spectrometry.

One of the primary objectives of the studies of decomposition of HCOOH has been to identify the catalytic intermediate and to correlate the nature of the intermediate with the specificity of the reaction. Kinetic methods, coupled with isotope substitution techniques, provided the first information concerning the mechanism of decomposition. It was speculated rather early (1918) that the formation of metal formates might play a role, but the application of infrared spectroscopy (1959–1960) to the study of HCOOH on metal catalysts greatly clarified the picture; the background of the kinetic and infrared studies is reviewed by Mars *et al.*[301] In a combination kinetic and infrared study of the decomposition of HCOOH on a Ni-on-silica catalyst, Fahrenfort and Sachtler[17] found that (a) formate ions ($HCOO^-$) exist on the surface during the decomposition reaction, and (b) decomposition of the formate is the rate-controlling step in the

formation of reaction products. Further evidence that the decomposition proceeds via a formate reaction intermediate is based on the observation of similarities between the stability and decomposition of bulk formates and the catalytic activity of the relevant metal or oxide. Thus, the apparent mechanism is

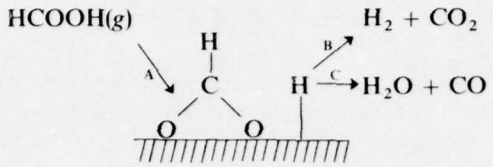

where the structure of the intermediate is only schematically illustrated. Dependent on experimental conditions of temperature and pressure, the rate-controlling step shifts from step A to step B or C on different metal catalysts. Fahrenfort and Sachtler[17] have plotted a "volcano curve" in which a relationship between the catalytic activity of heavy metals and the heats of formation of their formates is

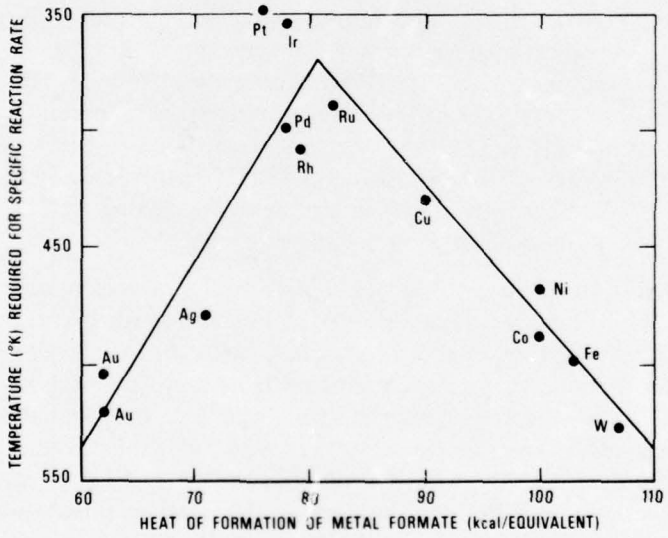

Fig. 51. Correlation between catalysis and thermochemistry: relationship between the catalytic activity of different metals for the decomposition of formic acid (HCOOH) and the corresponding heat of formation for the bulk metal formate. The temperature required for a specific rate of decomposition on a metal is plotted vs. the heat of formate formation. A low value of temperature implies a low activation energy for the catalytic decomposition. (From Sachtler and Fahrenfort.[17])

observed (Figure 51). They concluded that the noble metals like Au and Ag exhibit a high activation energy for step A and a relatively unstable formate, whereas on other metals (Ni, Co, Fe, W) the stability of the formate is so high that step B or C governs the overall reaction rate. The best catalysts are those metals (Pt, Ir, etc.) whose formate stabilities are between the two extremes, so that neither the formation nor the decomposition of the formate intermediate will severely limit the reaction rate.

It should be cautioned that the present treatment of this complex problem is necessarily superficial, and that a closer look at the details of formation, structure, and decomposition of the intermediate reveals a host of difficulties. This has also been demonstrated recently in an elegant series of experiments in which Madix and his colleagues[303-305] have examined the decomposition of HCOOH on both clean and carbon-covered Ni(110) single-crystal surfaces using LEED, AES, and thermal desorption mass spectrometry.

One of the first surprises to come from this work was the observation that desorption of adsorbed HCOOH on Ni(110) yielded four

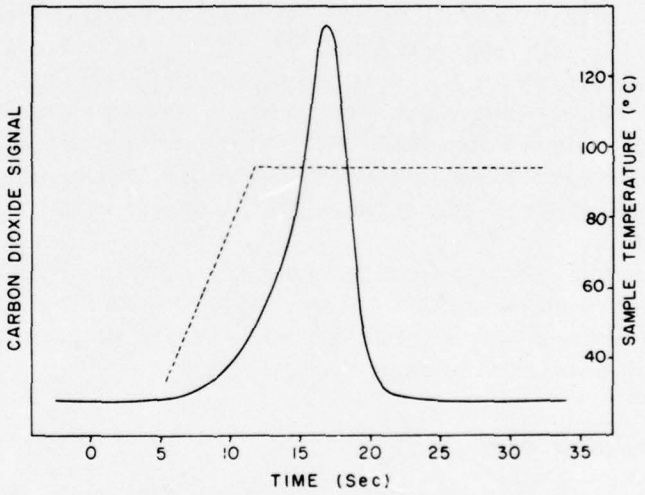

Fig. 52. Autocatalytic decomposition of HCOOH on a Ni(100) surface. The HCOOH-covered surface was heated in vacuum (dashed curve indicates sample temperature vs. time) and decomposition was monitored by observing the evolution of CO_2 from the surface. At constant temperature, the reaction rate *increased* as surface coverage *decreased*, evidence of explosive decomposition. (From Falconer *et al.*[304])

decomposition products (H_2, CO_2, H_2O, and CO) whose concentration is a function of the initial coverage.[303] At a coverage of one monolayer, the ratio CO_2:CO was found to be 1:1. The previously reported selectivity of Ni for the dehydrogenation reaction is not seen when the Ni substrate is atomically clean prior to adsorption.

Second, the kinetics of decomposition of the adsorbed species cannot be ascribed to simple desorption kinetics; the desorption peaks of H_2, CO_2, and CO are much too narrow for desorption to be the rate-controlling process in their liberation (Figure 52). Falconer *et al.*[304] have shown that the narrow thermal desorption peaks were the result of a self-accelerating surface reaction; i.e., a surface explosion. To verify this, they observed the decomposition of adsorbed HCOOH at constant temperature by following the desorption of CO_2 from the surface. As shown in Figure 41, the HCOOH-covered sample was heated in vacuum to a temperature below the thermal desorption temperature and held constant. At constant T, the rate of reaction *increased* as surface coverage *decreased*, clear evidence for an "explosive" autocatalytic reaction. The details of this process are currently under study.

Finally, these workers[305] observed that contamination of the Ni(110) surface with a carbide layer resulted in an increased specificity for the dehydrogenation reaction (CO_2:CO $\sim$ 10:1), but a much decreased activity for HCOOH decomposition ($\sim$100 times slower than on the clean surface at certain temperatures). They also concluded that the decomposition of DCOOH on the carbide surface clearly indicated that the reaction intermediate was DCOO (dominant desorption products were H_2 at $\sim$290°K, followed by D_2 and CO_2 at $\sim$450°K).

One can conclude from this type of experiment that even an idealized system, like HCOOH decomposition on a well-characterized single crystal, is very complicated, and that the simplicity of the mechanism suggested by earlier work is illusory.

9. Concluding Remarks

This review has attempted to bring together the major streams of thought in the field of heterogeneous catalysis. One is derived from our experience with practical catalysts of high surface area; another is from the recent injection of modern methods of surface characterization into this field. In addition, we have shown how increasingly sophisticated methods of solid-state chemistry and theoretical

chemistry are being brought into the field, which has thereby become one of the outstanding examples of interdisciplinary science. Since heterogeneous catalysis is essentially concerned with the enhancement of the rate of desirable reactions, we have chosen, where possible, to use kinetic measurements as a bridge between these two broad areas of research activity. In addition, it is apparent that linkages exist via other routes, such as the various spectroscopies, coordination chemistry, and stereochemistry. All of these ways of thinking about surface processes play a central role in recent developments within the field.

It seems clear that we are entering a period of intense experimental activity where much will be learned about the fundamental nature of surface processes. The problem of understanding heterogeneous catalysis is particularly difficult since even with the new surface measurement techniques, it is often necessary to reason indirectly about mechanisms and intermediates which are of catalytic importance. These difficulties have, so far, prevented the formulation of predictive theories of catalytic activity, although a number of semi-empirical correlations are now evident. It is anticipated that as we learn more of the atomic nature of surfaces and surface processes, we will stimulate theoretical activity directed to an understanding of the factors influencing the rate of catalytic reactions. This is the frontier of an exciting field of intellectual endeavor of immense importance to mankind.

Acknowledgment

The portion of this work completed at the National Bureau of Standards was supported in part by the Office of Naval Research.

References

1. J. T. Yates, Jr., Catalysis, *Chem. Eng. News*, **52**, 19–29 (1974).
2. R. L. Burwell, Jr., Heterogeneous catalysis, in *Catalysis—Progress in Research* (F. Basolo and R. L. Burwell, Jr., eds.), Plenum Press, London and New York (1973), pp. 51–74.
3. H. S. Taylor, A theory of the catalytic surface, *Proc. Roy. Soc. A* **108**, 105–111 (1925).
4. J. M. Thomas, Enhanced reactivity at dislocations in solids, *Advan. Catal.* **19**, 293–400 (1969).
5. J. M. Thomas and W. J. Thomas, *Introduction to the Principles of Heterogeneous Catalysis*, Academic Press, London and New York (1967).

6. G. C. Bond, *Catalysis by Metals*, Academic Press, London and New York (1962).
7. A. A. Balandin, Modern state of the multiplet theory of heterogeneous catalysis, *Advan. Catal.* **19**, 1–210 (1969).
8. M. Boudart, Catalysis by supported metals, *Advan. Catal.* **20**, 153–166 (1969).
9. G. A. Somorjai, The surface structure of and catalysis by platinum single crystal surfaces, *Catal. Rev.* **7**, 87–120 (1972).
10. D. W. Griffiths and M. L. Bender, Cycloamyloses as catalysts, *Advan. Catal.* **23**, 209–261 (1973).
11. M. Boudart, Pauling's theory of metals in catalysis, *J. Am. Chem. Soc.* **72**, 1040 (1950).
12. O. Beeck, Hydrogenation catalysts, *Disc. Faraday Soc.* **8**, 118–128 (1950).
13. L. Pauling, A resonating-valence-bond theory of metals and intermetallic compounds, *Proc. Roy. Soc. A* **196**, 343–362 (1949).
14. J. H. Sinfelt, Catalysis by metals, *Catal. Rev.* **9**, 147–168 (1974).
15. A. T. Gwathmey and R. E. Cunningham, The influence of crystal face in catalysis, *Advan Catal.* **10**, 57–95 (1958).
16. R. Van Hardeveld and F. Hartog, Influence of metal particle size on nickel-on-aerosil catalysts on surface site distribution, catalysis activity and selectivity, *Advan. Catal.* **22**, 75–114 (1972).
17. W. M. H. Sachtler and J. Fahrenfort, The catalytic decomposition of formic acid vapour on metals, in *Actes du Deuxième Congrès International de Catalyse*, Editions Technip, Paris (1960), pp. 831–852.
18. A. A. Holscher, Adsorption studies with the field-emission and field-ion microscope, Thesis, Leiden (1967).
19. Th. Wolkenstein, Effect of small quantities of impurities on the catalytic activity of ionic catalysts, *J. Phys. Chem. USSR* **24**, 1068–82 (1950).
20. Th. Wolkenstein, The electron theory of catalysis, *Advan. Catal.* **12**, 189–264 (1960).
21. K. Hauffe and H. J. Engell, The mechanism of chemical sorption from the standpoint of the disorder theory, *Z. Elektrochem.* **56**, 366–73 (1952).
22. K. Hauffe, in *Semiconductor Surface Physics* (R. H. Kingston, ed.), pp. 259–282, Univ. Pennsylvania Press, Philadelphia (1957).
23. P. B. Weisz, Electronic barrier layer phenomena in chemisorption and catalysis, *J. Chem. Phys.* **20**, 1483–84 (1952).
24. C. Wagner and K. Hauffe, The stationary state of catalysts in heterogeneous reactions, I., *Z. Electrochem.* **44**, 172–8 (1938).
25. F. S. Stone, in *Chemistry of the Solid State* (W. E. Garner, ed.), pp. 367–404, Academic Press, New York (1955).
26. C. Wagner, The mechanism of the decomposition of nitrous oxide on zinc oxide as catalyst, *J. Chem. Phys.* **18**, 69–71 (1950).
27. W. E. Garner, T. J. Gray, and F. S. Stone, The oxidation of copper and the reactions of hydrogen and carbon monoxide with copper oxide, *Proc. Roy. Soc. A* **197**, 294–314 (1949).
28. G. Parravano, The catalytic oxidation of carbon monoxide on nickel oxide I. Pure nickel oxide, II. Nickel oxide containing foreign ions, *J. Amer. Chem. Soc.* **75**, 1448–1454 (1953).
29. G. M. Schwab and J. Block, Über die Oxydation von Kohlenmonoxyd und den Zerfall von Distickstoffoxyd an definiert halbleitenden Oxygen, *Z. Physik Chem. N.F. (Frankfurt)* **1**, 42–62 (1954).

30. G. Parravano and M. Boudart, Chemisorption and catalysis on oxide semiconductors, *Advan. Catal.* **7**, 50–74 (1955).
31. C. G. B. Garrett, Quantitative considerations concerning catalysis at a semiconductor surface, *J. Chem. Phys.* **33**, 966–979 (1960).
32. F. Garcia-Moliner, The band picture in the electronic theories of chemisorption on semiconductors, *Catal. Rev.* **2**, 1–66 (1969).
33. H. Chon and C. D. Prater, Hall effect studies of carbon monoxide oxidation over doped zinc oxide catalysts, *Disc. Faraday Soc.* **41**, 380–393 (1966).
34. D. A. Dowden, N. Mackenzie, and B. M. W. Trapnell, The catalysis of H_2–D_2 exchange by oxides, *Proc. Roy. Soc. London* **237A**, 245–254 (1956).
35. D. A. Dowden, Crystal and ligand field models of solid catalysts, *Catal. Rev.* **5**, 1–31 (1972).
36. R. J. H. Voorhoeve and L. E. Trimble, Reduction of nitric oxide with carbon monoxide and hydrogen over ruthenium catalysts, *J. Catal.* **38**, 80–91 (1975).
37. R. W. Joyner, B. Lang, and G. A. Somorjai, Low pressure studies of dehydrocyclization of *n*-heptane on platinum crystal surfaces using mass spectrometry, Auger electron spectroscopy, and low energy electron diffraction, *J. Catal.* **27**, 405–415 (1972).
38. R. J. H. Voorhoeve, J. P. Remeika, and L. E. Trimble, Defect chemistry and catalysis in oxidation and reduction over perovskite-type oxides, *Ann. N.Y. Acad. Sci.* (1976).
39. R. L. Banks and G. C. Bailey, Olefin disproportionation, *I&EC Product Res. Develop.* **3**, 170–173 (1963).
40. F. D. Mango and J. H. Schachtschneider, in *Transition Metals in Homogeneous Catalysis* (G. N. Schrauzer, ed.), pp. 223–296, Marcel Dekker, New York (1971).
41. F. D. Mango, Molecular orbital symmetry conservation in transition metal catalysis, *Advan. Catal.* **20**, 291–326 (1969).
42. P. Mars and D. W. Van Krevelen, Oxidations carried out by means of vanadium oxide catalysts, *Chem. Eng. Sci. Suppl.* **3**, 41–59 (1954).
43. G. W. Keulks, The mechanism of oxygen atom incorporation into the products of propylene oxidation over bismuth molybdate, *J. Catal.* **19**, 232–235 (1970).
44. D. J. Hucknall, *Selective Oxidation of Hydrocarbons*, Academic Press, London (1974).
45. Y. Morooka and A. Ozaki, Regularities in catalytic properties of metal oxides in propylene oxidation, *J. Catal.* **5**, 116–124 (1966).
46. Y. Morooka, Y. Morikawa, and A. Ozaki, Regularity in the catalytic properties of metal oxides in hydrocarbon oxidation, *J. Catal.* **7**, 23–32 (1967).
47. O. A. Hougen and K. M. Watson, *Chemical Process Principles*, Part III, *Kinetics and Catalysis*, Wiley, New York (1947).
48. M. Boudart and R. L. Burwell, Jr., Mechanism in heterogeneous catalysis, in *Techniques of Chemistry*, Vol. 6, Pt. 1 (E. S. Lewis, ed.), John Wiley and Sons (1974), pp. 693–740.
49. J. E. Demuth and D. E. Eastman, Photoemission observations of π–d bonding and surface reactions of adsorbed hydrocarbons on Ni(111), *Phys. Rev. Letters* **32**, 1123–1127 (1974).
50. K. H. Johnson and R. P. Messmer, Clusters, chemisorption and catalysis, *J. Vac. Sci. Technol.* **11**, 236–242 (1974).
51. J. C. Slater and K. H. Johnson, Quantum chemistry and catalysis, *Physics Today* **1974** (October), 34–41.

52. C. L. Thomas, *Catalytic Processes and Proven Catalysts*. Academic Press, New York (1970), Ch. 1.
53. P. B. Weisz and C. D. Prater, Interpretation of measurements in experimental catalysis, *Advan. Catal.* **6**, 143–196 (1954).
54. P. H. Emmett (ed.), *Catalysis*. Vols. III–V, Reinhold, New York (1955, 1956, 1957).
55. F. G. Dwyer, Catalysis for control of automotive emissions, *Catal. Rev.* **6**, 261–292 (1972).
56. E. G. Rochow, *An Introduction to the Chemistry of the Silicones*. 2nd ed., Wiley, New York (1951).
57. R. J. H. Voorhoeve, *Organohalosilanes. Precursors to Silicones*. Elsevier, Amsterdam (1967).
58. F. G. Ciapetta and C. J. Plank, Catalysis preparation, in *Catalysis*. Vol. I, *Fundamental Principles* (P. H. Emmett, ed.), Reinhold, New York (1954), pp. 315–352.
59. H. Adkins and H. R. Billica, Preparation of Raney nickel catalysts and their use under conditions comparable with those for platinum and palladium catalysts, *J. Amer. Chem. Soc.* **70**, 695 (1948).
60. V. Haensel and R. Burwell, Catalysis, *Sci. Am.* **225**(6), 46–58 (1971).
61. V. Haensel, Catalytic cracking of pure hydrocarbons, *Advan. Catal.* **3**, 179–198 (1951).
62. G. C. A. Schuit and B. C. Gates, Chemistry and engineering of catalytic hydrodesulfurization, *AIChE J.* **19**, 417–438 (1973).
63. M. N. Berger, G. Boocock, and R. N. Hawarr, The polymerization of olefins by Ziegler catalysts, *Advan. Catal.* **19**, 211–241 (1969).
64. W. R. Kleckner and R. C. Sutter, in *Encyclopedia of Chemical Technology* Vol. II, 2nd ed., pp. 307–337, Interscience, New York (1966).
65. M. Leva, *Fluidization*. McGraw-Hill, New York (1959).
66. O. T. Zimmerman and I. Lavine, *Chemical Engineering Laboratory Equipment Design. Construction. Operation*. Industrial Research Service, Dover, N.H. (1955).
67. R. E. Kirk and D. F. Othmer (eds.), *Encyclopedia of Chemical Technology*. Interscience, New York (1963–70).
68. P. H. Emmett, Measurement of surface area, in *Catalysis*. Vol. I, Reinhold, New York (1965), pp. 63–67.
69. S. Brunauer, P. H. Emmett, and E. Teller, Adsorption of gases in multimolecular layers, *J. Amer. Chem. Soc.* **60**, 309–19 (1938).
70. J. E. Benson and M. Boudart, Hydrogen–oxygen titration method for the measurement of supported platinum surface areas, *J. Catal.* **4**, 704–710 (1965).
71. D. M. Young and A. D. Crowell, *Physical Adsorption of Gases*. Butterworths, London (1962).
72. J. H. Sinfelt, Catalytic hydrogenolysis over supported metals, *Catal. Rev.* **3**, 175–203 (1970).
73. J. E. Benson, H. S. Hwang, and M. Boudart, Hydrogen–oxygen titration method for the measurement of supported palladium surface areas, *J. Catal.* **30**, 146–153 (1973).
74. T. E. Whyte, Jr., Metal particle size determination of supported metal catalysts, *Catal. Rev.* **8**, 117–134 (1974).
75. H. Chon, R. A. Fisher, E. Tomeszko, and J. G. Aston, Chemisorption of hydrogen and oxygen on platinum black at low temperatures, in *Actes Congr. Intern. Catalyse 2e, Paris* 1960, Vol. 1, pp. 217–224.

76. E. L. Kugler, A. B. Kadet, and J. W. Gryder, The nature of NO adsorption on chromia, *J. Catal.* (to be published).
77. P. Stonehart and P. H. Zucks, Sintering and recrystallization of small metal particles. Loss of surface area by platinum-black fuel cell electro-catalysts, *Electrochim. Acta* **17**, 2333–2351 (1972).
78. R. P. Eischens, S. H. Francis, and W. A. Pliskin, The effect of surface coverage on the spectra of chemisorbed CO, *J. Phys. Chem.* **60**, 194–201 (1956).
79. J. C. Tracy and P. W. Palmberg, Structural influences on adsorbate binding energy. I. CO on (100) palladium, *J. Chem. Phys.* **51**, 4852–4862 (1969).
80. T. E. Madey, Adsorption of oxygen on tungsten (100): Adsorption kinetics and electron stimulated desorption, *Surface Sci.* **33**, 355–376 (1972); Chemisorption of H_2 on W(100), *Surface Sci.* **36**, 281–294 (1973).
81. S. E. Voltz, C. R. Morgan, D. Liederman, and S. M. Jacob, Kinetic study of carbon monoxide and propylene oxidation on platinum catalysts, *Ind. Eng. Chem. Prod. Res. Develop.* **12**, 294–301 (1973).
82. C. P. C. Bradshaw, E. J. Howman, and L. Turner, Olefin dismutation: reactions of olefins on cobalt oxide–molybdenum oxide–alumina, *J. Catal.* **7**, 269–276 (1967).
83. D. R. Kahn, E. E. Petersen, and G. A. Somorjai, The hydrogenolysis of cyclopropane on a platinum stepped single crystal at atmospheric pressure, *J. Catal.* **34**, 294–306 (1974).
84. Y. F. Yu Yao, The oxidation of hydrocarbons and CO over metal oxides IV. Perovskite-type oxides, *J. Catal.* **36**, 266–275 (1975).
85. P. K. Gallagher, D. W. Johnson, Jr., J. P. Remeika, F. Schrey, L. E. Trimble, E. M. Vogel and R. J. H. Voorhoeve, The activity of $La_{0.7}Sr_{0.3}MnO_3$ without Pt and $La_{0.7}Pb_{0.3}MnO_3$ with varying Pt contents for the catalytic oxidation of CO, *Mater. Res. Bull.* **10**, 529–538 (1975).
86. V. A. Dris'ko, Specific activity of metallic catalysts, *Russ. Chem. Rev.* **43**, 435–451 (1974).
87. P. B. Weisz and C. D. Prater, Interpretation of measurements in experimental catalysis, *Advan. Catal.* **6**, 143–196 (1954).
88. R. J. Madix and M. Boudart, Sticking probabilities by an effusive beam technique, the germanium–oxygen system, *J. Catal.* **7**, 240–251 (1967).
89. R. J. Madix and A. Susu, Reactive scattering of halogen molecules from ⟨111⟩ surfaces of silicon and germanium: Comparison with oxygenic species, *J. Catal.* **28**, 316–321 (1973).
90. S. L. Bernasek and G. A. Somorjai, Molecular beam study of the mechanism of catalyzed hydrogen–deuterium exchange on platinum single crystal surfaces, *J. Chem. Phys.* **62**, 3149–3161 (1975).
91. S. L. Bernasek and G. A. Somorjai, Small molecule reactions on stepped single crystal platinum surfaces, *Surface Sci.* **48**, 204–213 (1975).
92. D. O. Hayward, D. A. King, and F. C. Tompkins, Sticking probabilities, heats of adsorption and redistribution processes of nitrogen on tungsten films at 195 and 290°K, *Proc. Roy. Soc.* **297A**, 305–320 (1967).
93. A. A. Bell and R. Gomer, Adsorption of carbon monoxide on tungsten. Abundances, dipole moments, and sticking coefficients, *J. Chem. Phys.* **44**, 1065–1080 (1966).
94. I. Langmuir, Chemical reactions on surfaces, *Trans. Faraday Soc.* **17**, 607–675 (1922).

95. E. H. Taylor, The effects of ionizing radiation on catalysts, *Advan. Catal.* **18**, 111–258 (1968).
96. H. E. Farnsworth and R. F. Woodcock, Effects of radiation quenching, ion bombardment and annealing on catalytic activity of pure Ni and platinum surfaces, *Advan. Catal.* **9**, 123–130 (1957).
97. I. Yasumori, T. Kabe, and Y. Inoue, Radiochemical study of active sites on palladium *J. Phys. Chem.* **78**, 583–588 (1974).
98. J. W. Hall and H. F. Rase, Dislocations and catalysis, *Nature* **4893**, 858 (1963).
99. H. M. C. Sosnovsky, The catalytic activity of silver crystals of various orientations after bombardment with positive ions, *J. Phys. Chem. Solids* **10**, 304–310 (1959).
100. I. Matsuura and G. C. A. Schuit, Adsorption and reaction of adsorbed species on Bi_2MoO_6 catalysts, *J. Catal.* **25**, 314–325 (1972).
101. K. Aykan, A. W. Sleight, and D. B. Rogers, Defect control in oxidation catalysts, *J. Catal.* **29**, 185–187 (1973).
102. R. van Hardeveld and A. Van Montfoort, Infrared spectra of nitrogen adsorbed on nickel-on-aerosil catalysts. Effects of intermolecular interaction and isotopic substitution, *Surface Sci.* **17**, 90–124 (1969).
103. M. Boudart, Four decades of active centers, *Am. Scientist* **57**, 1, 97–111 (1969).
104. R. J. Kokes, in *Experimental Methods in Catalytic Research* (R. B. Anderson, ed.), pp. 436–476, Academic Press, New York (1968).
105. R. J. H. Voorhoeve, Electron spin resonance study of active centers in nickel–tungsten sulfide hydrogenation catalysts, *J. Catal.* **23**, 236–242 (1971).
106. R. J. H. Voorhoeve and H. B. M. Wolters, Tungsten sulfides obtained by decomposition of ammonium tetrathiotungstate, *Z. Anorg. Allgem. Chem.* **376**, 165–179 1970; **380**, 326 (1971).
107. R. J. H. Voorhoeve and J. C. M. Stuiver, The mechanism of the hydrogenation of cyclohexene and benzene on nickel–tungsten sulfide catalysts, *J. Catal.* **23**, 243–252 (1971).
108. A. L. Farragher and P. Cossee, Catalytic chemistry of molybdenum and tungsten sulfides and related ternary compounds, in *Proc. Fifth Internat. Congr. Catal.* (J. W. Hightower, ed.), pp. 1301–1318, North-Holland, Amsterdam (1973).
109. A. Aoshima and H. Wise, Hydrodesulfurization activity and electronic properties of molybdenum sulfide catalyst, *J. Catal.* **34**, 145–151 (1974).
110. G. C. A. Schuit, Structure of hydrodesulfurization catalysts, *Ann. N.Y. Acad. Sci.* (1976).
111. V. H. J. DeBeer, Some structural aspects of the CoO–MoO_3–γ-Al_2O_3 hydrodesulfurization catalyst, Thesis, Eindhoven (Netherlands), 1975.
112. J. H. Lunsford and T. W. Leland, Effects of neutron and ultraviolet irradiation on the catalytic activity of magnesium oxide, *J. Phys. Chem.* **66**, 2591–7 (1962).
113. C. G. Harkins, W. W. Shang, and T. W. Leland, Relation of the catalytic activity of MgO to its electron energy states, *J. Phys. Chem.* **73**, 130–141 (1969).
114. J. H. Lunsford, A study of irradiation-induced active sites on magnesium oxide using electron paramagnetic resonance, *J. Phys. Chem.* **68**, 2312–2316 (1964).
115. M. Boudart, A. Delbouille, E. G. Derouane, V. Indovina, and A. B. Walters, Activation of hydrogen at 78°K on paramagnetic centers of magnesium oxide, *J. Am. Chem. Soc.* **94**, 6622–30 (1972).
116. R. P. Eischens, W. A. Pliskin, and M. J. D. Low, The infrared spectrum of hydrogen chemisorbed on ZnO, *J. Catal.* **1**, 180–191 (1962).

117. R. J. Kokes, A. L. Dent, C. C. Chang, and L. T. Dixon, Infrared studies of isotope effects for hydrogen adsorption on zinc oxide, *J. Am. Chem. Soc.* **94**, 4429–4436 (1972).
118. R. E. Allen, G. P. Alldredge, and F. W. de Wette, Studies of vibrational surface modes. I. General formulation, *Phys. Rev. B* **4**, 1648–1660 (1971).
119. R. E. Allen, G. P. Alldredge, and F. W. de Wette, Studies of vibrational surface modes. II. Monoatomic fcc crystals, *Phys. Rev. B* **4**, 1661–1681 (1971).
120. G. P. Alldredge, R. E. Allen, and F. W. de Wette, Studies of vibrational surface modes. III. Effect of an adsorbed layer, *Phys. Rev. B* **4**, 1682–1697 (1971).
121. T. Wolfram and R. E. De Wames, Surface dynamics of magnetic materials, in *Progress in Surface Science*, Vol. 2, Part 4, pp. 233–330 (1972).
122. H. Suhl, Magnetic effects in surface reactions, in *AIP Conference Proceedings*, No. 18, Part 1, pp. 33–47 (1974).
123. P. Kumar, Magnetic phase transition at a surface: mean field theory, *Phys. Rev. B* **10**, 2928–2933 (1974).
124. P. Kumar and K. Maki, Surface spin fluctuations in paramagnetic phase, unpublished (1975).
125. K. L. Kliewer and R. Fuchs, Theory of dynamical properties of dielectric surfaces, *Advan. Chem. Phys.* **27**, 355–541 (1974).
126. J. A. Appelbaum and D. R. Hamann, Surface states and surface bonds of Si(111), *Phys. Rev. Lett.* **31**, 106–9 (1973).
127. J. A. Appelbaum and D. R. Hamann, Surface potential, charge density, and ionization potential for Si(111)—a self-consistent calculation, *Phys. Rev. Lett.* **32**, 225–228 (1974).
128. J. A. Appelbaum and D. R. Hamann, Electronic structure of Si and Ge surfaces, in *Proc. 12th International Conference on the Physics of Semiconductors*, Stuttgart, Germany, July 15–19 (1974).
129. J. A. Appelbaum and D. R. Hamann, Self-consistent quantum theory of chemisorption: H on Si(111), *Phys. Rev. Lett.* **34**, 806–809 (1975).
130. P. W. Anderson, Localized magnetic states in metals, *Phys. Rev.* **124**, 41–53 (1961).
131. D. Newns, Self-consistent model of hydrogen chemisorption, *Phys. Rev.* **178**, 1123–1135 (1969).
132. J. R. Smith, S. C. Ying, and W. Kohn, Charge densities and binding energies in hydrogen chemisorption, *Phys. Rev. Letters* **30**, 610–613 (1973).
133. J. R. Schrieffer and R. Gomer, Induced covalent bond mechanism of chemisorption, *Surface Sci.* **25**, 315–320 (1971).
134. T. B. Grimley, Chemisorption of some small molecules on transition metals, in *Molecular Processes on Solid Surfaces* (E. Drauglis, R. Gretz, and R. Jaffee, eds.), McGraw-Hill, New York (1969), pp. 299–316.
135. J. R. Schrieffer, Theory of chemisorption, *J. Vac. Sci. Technol.* **9**, 561–568 (1972).
136. J. R. Schrieffer and P. Soven, Surface physics: Theory of the electronic structure, *Physics Today* **1975** (April), 24–30.
137. A. Madhukar, Chemisorption on transition-metal surfaces: Electronic structure, *Phys. Rev. B* **8**, 4458–4463 (1973).
138. R. H. Paulson and J. R. Schrieffer, Induced covalent bond theory of chemisorption of hydrogen on a metal surface, *Surface Sci.* **48**, 329–352 (1975).
139. B. J. Thorpe, Chemisorption theory and the surface molecule, *Surface Sci.* **33**, 306–325 (1972).

140. T. L. Einstein, Short-chain model of chemisorption: Exact and approximate results, *Phys. Rev. B* **11**, 577–587 (1975).
141. A. P. Mortola, C. Geller, C. Melius, J. W. Moskowitz, and M. B. Bailee, A Theoretical model for chemisorption, *Abstracts ACS Mexico City Meeting*, (November 1975).
142. A. Van der Avoird, Some model calculations for adsorption on transition metals, *Surface Sci.* **18**, 159–177 (1969).
143. K. H. Johnson, J. G. Norman, Jr., and J. W. D. Connolly, in *Computational Methods for Large Molecules and Localized States in Solids* (F. Herman, A. D. McLean, and R. K. Nesbet, eds.), pp. 161–201, Plenum, New York (1973).
144. S. J. Niemczyk, A SCF-Xα-SW investigation of chemisorption bonding of chalcogens on nickel (001), *J. Vac. Sci. Technol.* **12**, 246–248 (1975).
145. I. P. Batra and O. Robaux, Electronic energy level structure calculations of chemisorbed CO on Ni(100), *J. Vac. Sci. Technol.* **12**, 242–245 (1975).
146. I. P. Batra and P. S. Bagus, Interpretation of the photoemission spectrum of chemisorbed carbon monoxide on Ni(100), *Solid State Commun.* **16**, 1097–1100 (1975).
147. J. T. Waber, H. Adachi, F. W. Averill, and D. E. Ellis, Molecular cluster study of the approach of CO to a Ni(100) surface, *Japan J. Appl. Phys.* (Suppl. 2, Pt. 2) **1974**, 695–697.
148. D. E. Eastman and J. K. Cashion, Photoemission energy-level measurements of chemisorbed CO and O on Ni, *Phys. Rev. Lett.* **27**, 1520–1523 (1971).
149. W. G. Klemperer and K. H. Johnson, *J. Chem. Phys.* (to be published).
150. W. H. Weinberg, The bond-energy bond-order (BEBO) model of chemisorption, *J. Vac. Sci. Technol.* **10**, 89–94 (1973).
151. W. H. Weinberg, H. A. Deans, and R. P. Merrill, The structure and chemistry of ethylene adsorbed on platinum (111), *Surface Sci.* **41**, 312–336 (1974).
152. R. Hoffmann, An extended Hückel theory. I. Hydrocarbons, *J. Chem. Phys.* **39**, 1397–1412 (1963).
153. C. J. Ballhausen and H. B. Gray, The electronic structure of the vanadyl ion, *Inorg. Chem.* **1**, 111–122 (1962).
154. R. F. Fenske, K. G. Caulton, D. D. Radtke, and C. C. Sweeny, A method for molecular orbital calculations for metal complexes, *Inorg. Chem.* **5**, 951–964 (1966).
155. R. Hoffman and R. B. Woodward, Selection Rules for Concerted Cycloaddition Reactions, *J. Amer. Chem. Soc.* **87**, 2046–2048 (1965).
156. F. D. Mango and J. H. Schachtschneider, Orbital symmetry restraints to transition metal catalyzed [2 + 2] cycloaddition reactions, *J. Am. Chem. Soc.* **93**, 1123–1130 (1971).
157. H. E. Simmons and J. F. Bunnett (eds.), *Orbital Symmetry Papers*, American Chemical Society, Washington, D.C. (1974).
158. J. Halpern, Catalysis of the rearrangements of strained hydrocarbons by transition metal compounds, *Proc. 14th Internat. Conference on Coordination Chemistry, Toronto*, pp. 698–703 (1972).
159. R. B. Woodward and R. Hoffman, Stereochemistry of electrocyclic reactions, *J. Am. Chem. Soc.* **87**, 395–397 (1965).

160. R. G. Pearson, Symmetry rules for chemical reactions, *Accts. Chem. Res.* **4**, 152–160 (1971).
161. V. I. Labunskaya, A. D. Shebaldova, and M. L. Khidekal', Catalysis of symmetry-disallowed reactions, *Russ. Chem. Rev.* **43**, 1–16 (1974).
162. L. Kleinman, Orbital-symmetry rules for chemisorption, *Phys. Rev. B* **9**, 1989–1992 (1974).
163. A. B. Anderson and R. Hoffmann, Molecular orbital studies of dissociative chemisorption of first period diatomic molecules and ethylene on (100) W and Ni surfaces, *J. Chem. Phys.* **61**, 4545–4559 (1974).
164. D. Menzel, Investigations of adsorption on metal surfaces by photoelectron spectroscopy, combined with other methods, *J. Vac. Sci. Technol.* **12**, 313–323 (1975).
165. L. Hedin, in *Electrons in Crystalline Solids. Proceedings of the Seventh International Course at Trieste, 1972*, pp. 665–731, International Atomic Energy Agency, Vienna (1973).
166. R. P. Eischens, W. A. Pliskin, and S. A. Frances, Infrared spectra of chemisorbed carbon monoxide, *J. Chem. Phys.* **22**, 1786–1787 (1954).
167. Extensive references to the work of A. Terenin are contained in Ref. 168.
168. L. H. Little, *Infrared Spectra of Adsorbed Species*, Academic Press, London (1966).
169. M. L. Hair, *Infrared Spectroscopy in Surface Chemistry*, Marcel Dekker, New York (1967).
170. A. C. Yang and C. W. Garland, Infrared studies of carbon monoxide chemisorbed on rhodium, *J. Phys. Chem.* **61**, 1504–1512 (1957).
171. L. F. Dahl, C. Martell, and D. L. Wampler, Structure of and metal–metal bonding in $Rh(CO)_2Cl$, *J. Amer. Chem. Soc.* **83**, 1761–1762 (1961).
172. T. L. Brown and D. J. Darensbourg, Intensities of CO stretching of adsorbed CO and metal carbonyls, *Inorg. Chem.* **6**, 971–977 (1967).
173. J. T. Yates, Jr., R. G. Greenler, I. Ratajczkowa, and D. A. King, Reflection-absorption infrared spectrum of α-CO chemisorbed on polycrystalline tungsten, *Surface Sci.* **36**, 739–755 (1973).
174. J. Pritchard, T. Catterick, and R. K. Gupta, Infrared spectroscopy of chemisorbed carbon monoxide on copper, to be published.
175. G. Blyholder, Infrared spectrum of CO chemisorbed on iron, *J. Chem. Phys.* **36**, 2036–2039 (1962).
176. D. E. Eastman and J. E. Demuth, Photoemission studies of inorganic and organic adsorbates on Ni(111) and surface reactions, *Japan J. Appl. Phys.* (Suppl. 2, Pt. 2) **1974**, 827–836.
177. G. Blyholder, CNDO model and interpretation of the photoelectron spectrum of CO chemisorbed on Ni, *J. Vac. Sci. Technol.* **11**, 865–868 (1974).
178. T. Gustafsson, E. W. Plummer, D. E. Eastman, and J. L. Freeouf, Identification of the energy levels of molecularly adsorbed CO on Ni and Pd by means of $h\omega$ dependent photoemission, *Bull. Am. Phys. Soc.* **1975** (March), 304.
179. J. Fuggle, T. E. Madey, M. Steinkilberg, and D. Menzel, X-Ray photoelectron spectroscopy (XPS) of adsorbate valence bands, *Phys. Letters* **51A**, 163 (1975).
180. K. Yu, I. Lindau, P. Pianetta, and W. E. Spicer, Ultraviolet photoemission studies of O_2, CO, C_2H_2 and C_2H_4 chemisorbed on copper, *Bull. Am. Phys. Soc.* **1975** (March), 359.

181. G. A. Somorjai and F. J. Szalkowski, Simple rules to predict the structure of adsorbed gases on crystal surfaces, *J. Chem. Phys.* **54**, 389–399 (1971).
182. R. J. H. Voorhoeve, Molecular beam deposition of solids on surfaces: ultra-thin films, Chapter 4, this Volume of the Treatise.
183. J. J. Lander, in *Progress in Solid State Chemistry*, Volume 2, 26 (H. Reiss, ed.), Pergamon, Oxford (1965).
184. D. Haneman, Surface structures and properties of diamond-structure semiconductors, *Phys. Rev.* **121**, 1093–1100 (1961).
185. E. Tosatti and P. W. Anderson, Two-dimensional excitonic insulators: Si and Ge(111) surfaces, *Solid State Commun.* **14**, 773–777 (1974).
186. E. Tosatti and P. W. Anderson, Charge and spin density waves on semiconductor surfaces, *Japan J. Appl. Phys.* (Suppl. 2, Pt. 2) **1974**, 381–388.
187. J. Koutecky, A contribution to the molecular orbital theory of chemisorption, *Trans. Faraday Soc.* **54**, 1038–1052 (1958).
188. T. B. Grimley, The indirect interaction between atoms or molecules adsorbed on metals, *Proc. Phys. Soc.* **90**, 751–764 (1967).
189. T. B. Grimley, The electron density in a metal near a chemisorbed atom or molecule, *Proc. Phys. Soc.* **92**, 776–782 (1967).
190. T. B. Grimley and S. M. Walker, Interactions between adatoms on metals and their effects on the heat of adsorption at low surface coverage, *Surface Sci.* **14**, 395–406 (1969).
191. T. L. Einstein and J. R. Schrieffer, Indirect interactions between adatoms on a tight-binding solid, *Phys. Rev. B* **7**, 3629–3648 (1973).
192. J. T. Yates, Jr. and T. E. Madey, Interactions between chemisorbed species: H_2 and CO on (100) tungsten, *J. Chem. Phys.* **54**, 4969–4978 (1971).
193. M. M. Siddiqui and F. C. Tompkins, Surface potential of mixed adsorbates on metal films, *Proc. Roy. Soc.* (*London*) *A* **268**, 452–473 (1962).
194. D. O. Hayward and B. M. W. Trapnell, *Chemisorption*, Butterworths, Washington (1964).
195. A. Clark, *The Chemisorptive Bond*, Academic Press, New York and London (1974).
196. J. R. Anderson and B. G. Baker, Catalytic reactions on metal films, in *Chemisorption and Reactions on Metallic Films*, Vol. 2 (J. R. Anderson, ed.), Academic Press, London and New York (1971).
197. E. G. Allison and G. C. Bond, The structure and catalytic properties of Pd–Ag and Pd–Au alloys, *Catal. Rev.* **7**, 233–289 (1972).
198. R. L. Moss and L. Whalley, Adsorption and catalysis on evaporated alloy films, *Advan. Catal.* **22**, 115–189 (1972).
199. N. F. Mott and H. Jones, *The Theory of the Properties of Metals and Alloys*, Clarendon Press, Oxford (1936).
200. A. Couper and D. D. Eley, The parahydrogen conversion on palladium gold alloys, *Disc. Faraday Soc.* **8**, 172–184 (1950).
201. S. Hufner, G. K. Wertheim, and J. H. Wernick, X-ray photoelectron spectra of the valence bonds of some transition metals and alloys, *Phys. Rev. B* **8**, 4511–4524 (1973).
202. W. E. Spicer, in *Band Structure Spectroscopy of Metals and Alloys* (D. J. Fabian and L. M. Watson, eds.), pp. 7–53, Academic, London (1973).
203. W. M. H. Sachtler and R. Jongepier, The surface of copper–nickel alloy films, *J. Catalysis* **4**, 665–671 (1965).

204. P. van der Plank and W. M. H. Sachtler, Interaction of benzene and protium and deuterium on copper–nickel films with known surface composition, *J. Catalysis* **12**, 35–44 (1968).
205. M. Ono, Y. Takasu, K. Nakayama, and T. Yamashina, Auger spectroscopy study on Cu–Ni alloy surfaces related to catalysis, *Surface Sci.* **26**, 313 (1971).
206. K. Nagayama, M. Ono, and H. Shimizu, Auger spectroscopy study on the surface composition of copper–nickel alloys after annealing and sputtering, *J. Vac. Sci. Technol.* **9**, 749–751 (1972).
207. C. R. Helms, Observation of the segregation of Cu to the surface of a clean, annealed 50% Cu/50% Ni alloy by Auger electron spectroscopy, *J. Catalysis* **36**, 114–117 (1975).
208. K. Y. Yu, C. R. Helms, and W. Spicer, UPS Measurements of the surface electronic structure and surface composition of the Cu–Ni alloys, *Phys. Rev.*, to be published.
209. F. L. Williams and D. Nason, Binary alloy surface compositions from bulk alloy thermodynamic data, *Surface Sci.* **45**, 377–408 (1974).
210. R. A. Van Santen and W. M. H. Sachtler, A theory of surface enrichment in ordered alloys, *J. Catalysis* **33**, 202–209 (1974).
211. Y. Soma-Noto and W. M. H. Sachtler, Infrared spectra of CO adsorbed on supported Pd and Pd–Ag alloys, *J. Catalysis* **32**, 315–324 (1974).
212. Y. Soma-Noto and W. M. H. Sachtler, Infrared spectra of CO adsorbed on silica-supported Ni–Cu alloys, *J. Catalysis* **34**, 162–165 (1974).
213. F. L. Williams and M. Boudart, Surface composition of nickel–gold alloys, *J. Catalysis* **30**, 438–443 (1973).
214. J. H. Sinfelt, Supported 'bimetallic cluster' catalysts, *J. Catalysis* **29**, 308–315 (1973).
215. E. Ruckenstein, Phase stability of supported bimetallic catalysts, *J. Catalysis* **35**, 441 (1974).
216. R. B. Levy and M. Boudart, Platinum-like behavior of tungsten carbide in surface catalysis, *Science* **181**, 547–549 (1973).
217. L. H. Bennett, J. R. Cuthill, A. J. McAlister, N. E. Erickson, and R. E. Watson, Electronic structure and catalytic behavior of tungsten carbide, *Science* **184**, 563–565 (1974).
218. J. E. Houston, G. E. Laramore, and R. L. Park, Surface electronic properties of tungsten, tungsten carbide, and platinum, *Science* **185**, 258–259 (1974).
219. L. Fiermans, R. Hoogewijs, and J. Vennik, Electron spectroscopy of transition metal oxide surfaces, *Surface Sci.* **47**, 1–40 (1975).
220. G. Parravano, Ferroelectric transitions and heterogeneous catalysis, *J. Chem. Phys.* **20**, 342–343 (1952).
221. G. Parravano, Catalytic activity of lanthanum and strontium manganite, *J. Am. Chem. Soc.* **75**, 1497–8 (1953).
222. F. F. Vol'kenshtein, *The Electronic Theory of Catalysis on Semiconductors*. Pergamon/Macmillan, New York (1963).
223. V. J. Lee, Electrons and holes as energy-transport agents in catalysis on semiconductors—Part I, *J. Catalysis* **17**, 178–189 (1970).
224. V. J. Lee, Catalysis on wide-band-gap semiconductors, *J. Chem. Phys.* **55**, 2905–2913 (1971).
225. O. V. Krylov, *Catalysis by Non-Metals*. Academic Press, New York (1970).

226. A. Many, Y. Goldstein, and N. B. Grover, *Semiconductor Surfaces*, Chapter 4, North-Holland, Amsterdam (1965).
227. P. C. Gravelle, G. El Shobaky, and S. J. Teichner, Determination a l'aide du microcalorimetre calvet du mechanisme de l'oxydation catalytique de l'oxyde de carbone au contact de l'oxyde de nickel VII. Oxyde de nickel contenant des ions lithium, *J. Chim. Phys.* **66**, 1953–1965 (1969).
228. G. El Shobaky, P. C. Gravelle, and T. J. Teichner, Influence of the surface structure of a nickel oxide catalyst on the mechanism of the room temperature oxidation of carbon monoxide, *J. Catal.* **14**, 4–22 (1969).
229. J. Deren, Z. Guzik, and J. Sloczynski, Catalytic oxidation of carbon monoxide on monocrystalline nickel oxide catalysts, *Bull. Acad. Pol. Sci., Ser. Sci. Chim.* **20**, 361–368 (1972).
230. D. Adler, The imperfect solid—transport properties, Vol. 2, pp. 237–332 of this Treatise.
231. C. Wagner, Reduction of the rate of carbon monoxide combustion in nickel oxide (NiO) through catalyst doping with gallium oxide (Ga_2O_3), *Ber. Bunsenges. Phys. Chem.* **74**, 1270–3 (1970).
232. J. Deren and A. Kowalska, The changes of adsorptive properties of nickel oxide in the course of adsorption-desorption cycles, *Bull. Acad. Pol. Sci., Ser. Sci. Chem.* **21**, 131–136 (1973).
233. F. Morin, in *Semiconductors* (N. B. Hannay, ed.), Chapter 14, pp. 600–633, Reinhold, New York (1959).
234. J. Bardeen, Surface states and rectification at a metal semiconductor contact, *Phys. Rev.* **71**, 717–727 (1947).
235. T. J. Gray and N. Lowery, Surface electronic structure of oxides as established by thermally stimulated electron current measurements, *Disc. Faraday Soc.* **52**, 132–139 (1971).
236. A. Cimino, E. Molinari, F. Cramarossa, and G. Ghersini, Hydrogen chemisorption and electrical conductivity of zinc oxide semiconductors, *J. Catal.* **1**, 275–292 (1962).
237. Ph. Coussel and S. J. Teichner, Electron localization and oxygen transfer reactions on zinc oxide, *Catal. Rev.* **6**, 133–260 (1972).
238. E. Arijs and F. Cardon, The influence of surface donor states on the chemisorption kinetics of oxygen at the surface of ZnO single crystals, *J. Solid State Chem.* **6**, 310–326 (1973).
239. R. J. Kokes and A. L. Dent, Hydrogenation and isomerization over zinc oxide, *Advan. Catal.* **22**, 1–50 (1972).
240. E. R. S. Winter, Adsorption upon pure and lithium-doped nickel oxide, *J. Catal.* **6**, 35–49 (1966).
241. L. A. Peterman, in *Adsorption-Desorption Phenomena* (F. Ricca, ed.), pp. 227–243, Academic, London (1972).
242. Y. Morooka and A. Ozaki, Regularities in catalytic properties of metal oxides in propylene oxidation, *J. Catal.* **5**, 116–124 (1966).
243. Y. Morooka, Y. Morikawa, and A. Ozaki, Regularity in the catalytic properties of metal oxides in hydrocarbon oxidation, *J. Catal.* **7**, 23–32 (1967).
244. W. M. H. Sachtler, G. J. H. Dorgelo, J. Fahrenfort, and R. J. H. Voorhoeve, Correlations between catalytic and thermodynamic parameters of transition metal oxides, *Rec. Trav. Chim.* **89**, 460–480 (1970).

245. R. J. H. Voorhoeve, J. P. Remeika, and L. E. Trimble, Nitric oxide and perovskite-type catalysts: Solid state and catalytic chemistry, in *Proc. Symp. Chemistry of Nitrogen Oxides* (R. L. Klimisch and J. G. Larson, eds.), pp. 215–233, Plenum, New York (1975).
246. F. Basolo and R. G. Pearson, *Mechanism of Inorganic Reactions*. Wiley, New York (1967).
247. A. Cimino, Catalytic activity of transition metal ions in an oxide matrix, *Chim. Ind. (Milan)* **56**(1), 27–38 (1974).
248. C. C. Chao and J. H. Lunsford, An infrared and electron paramagnetic resonance study of some silver–nitric oxide complexes in Y type zeolites, *J. Phys. Chem.* **78**, 1174–1177 (1974).
249. K. Klier, R. Kellerman, and P. J. Hutta, Spectra of synthetic zeolites containing transition metal ions. V. π Complexes of olefins and acetylene with Co(II) A molecular sieve, *J. Chem. Phys.* **61**, 4224–4234 (1974).
250. P. A. Batist, P. C. van der Heyden, and G. C. A. Schuit, Isomerization of butenes on bismuth molybdate—recirculating and pulse reactions of butenes on koechlinite, *J. Catal.* **22**, 411–418 (1971).
251. I. Matsuura and G. C. A. Schuit, Adsorption equilibria and rates of reactions of adsorbed compounds on reduced and oxidized Bi–Mo catalysts, *J. Catal.* **20**, 19–39 (1971).
252. A. W. Sleight and W. J. Linn, Olefin oxidation over oxide catalysts with the scheelite structure, *Ann. New York Acad. Sci.* (1976).
253. K. Aykan, D. Halvorson, A. W. Sleight, and D. B. Rogers, Olefin oxidation and ammoxidation on studies over molybdate, tungstate and vanadate catalysts having point defects, *J. Catal.* **35**, 401–406 (1974).
254. A. W. Sleight, K. Aykan, and D. B. Rogers, New nonstoichiometric molybdate, tungstate and vanadate catalysts with the scheelite-type structure, *J. Solid State Chem.* **13**, 231–236 (1975).
255. R. J. H. Voorhoeve, J. P. Remeika, L. E. Trimble, A. S. Cooper, F. J. DiSalvo, and P. K. Gallagher, Perovskite-like $La_{1-x}K_xMnO_3$ and related compounds: Solid state chemistry and the catalysis of the reduction of NO by CO and H_2, *J. Solid State Chem.* **14**, 395–406 (1975).
256. H. C. Yao and M. Shelef, Nitric oxide and carbon monoxide chemisorption on cobalt-containing spinels, *J. Phys. Chem.* **78**, 2490–2496 (1974).
257. M. Boudart, A. Aldag, J. E. Benson, N. A. Dougharty, and C. G. Harkins, On the specific activity of platinum catalysts, *J. Catal.* **6**, 92–99 (1966).
258. G. A. Somorjai, The mechanism of hydrocarbon catalysis on platinum single crystal surfaces, Battelle Conf. on The Physical Basis for Heterogenous Catalysis, Gstaad, Switzerland, Sept. 1974; also see Ref. 83.
259. H. Kral, Freie und aktive Oberfläche von Pd/C-Katalysatoren, *Chemiker-Zeitung, Chem. Apparatur* **91**, 41–47 (1967).
260. J. T. Yates, Jr., T. E. Madey, and M. J. Dresser, Adsorption and decomposition of formaldehyde on tungsten (100) and (111) crystal planes, *J. Catal.* **30**, 260–275 (1973).
261. M. Boudart, Chemisorption during catalytic reaction on metal surfaces, *J. Vac. Sci. Technol.* **12**, 329–332 (1975).
262. S. L. Bernasek, W. J. Siekhaus, and G. A. Somorjai, Molecular-beam study of hydrogen–deuterium exchange on low- and high-Miller-index platinum single-crystal surfaces, *Phys. Rev. Letters* **30**, 1202–1204 (1973).

263. G. A. Somorjai and S. B. Brumbach, The interaction of molecular beams with solid surfaces, *CRC Critical Reviews in Solid State Sciences*, pp. 429–453 (May 1974).
264. R. R. Rye and K. E. Lu, Equilibrium of H_2 and D_2 on single crystal surfaces of platinum, *J. Vac. Sci. Technol.* **12**, 334–337 (1975).
265. R. W. Joyner, B. Lang, and G. A. Somorjai, Low pressure studies of dehydrocyclization of *n*-heptane on platinum crystal surfaces using mass spectrometry, Auger electron spectroscopy, and low energy electron diffraction, *J. Catal.* **27**, 405–415 (1972).
266. G. A. Somorjai, private communication.
267. T. E. Whyte, Jr., Metal particle size determination of supported metal catalysts, *Catal. Rev.* **8**, 117–134 (1973).
268. J. G. Allpress and J. V. Sanders, The structure and orientation of crystals in deposits of metals on mica, *Surface Sci.* **7**, 1–25 (1967).
269. B. G. Bagley, Five-fold pseudosymmetry, *Nature* **225**, 1040–1041 (1970).
270. M. R. Hoare and P. Pal, Statistics and stability of small assembles of atoms, *J. Crystal Growth* **17**, 77–96 (1972).
271. J. J. Burton, Structure and properties of microcrystalline catalysts, *Catal. Rev.—Sci. Eng.* **9**, 209–222 (1974).
272. J. L. Carter and J. H. Sinfelt, The paramagnetic susceptibility of supported nickel, *J. Catal.* **10**, 134–139 (1968).
273. R. L. Burwell, Jr., The use of stereochemistry in heterogeneous catalysis, *Intra-Science Chem. Rept.* **6**, 135–149 (1973).
274. S. Siegel, Stereochemistry and the mechanism of hydrogenation of unsaturated hydrocarbons, *Adv. Catal.* **16**, 123–177 (1966).
275. R. L. Burwell, Jr., Deuterium as a tracer in reactions of hydrocarbons on metallic catalysts, *Accounts Chem. Res.* **2**, 289–296 (1969).
276. R. L. Burwell, Jr., Stereochemistry and heterogeneous catalysis, *Chem. Rev.* **57**, 895–934 (1957).
277. A. T. Bloomquist, L. H. Liu, and J. C. Bohrer, Many membered carbon rings. VI. Unsaturated nine-membered cyclic hydrocarbons, *J. Amer. Chem. Soc.* **74**, 3643–3647 (1952).
278. E. McMahon and J. K. A. Clarke, The exchange of norbornane with deuterium on a palladium surface, *Tetrahedron Letters* **18**, 1413–1414 (1971).
279. K. Schrage and R. L. Burwell, Jr., The mechanism of the isotopic exchange between deuterium and cycloalkanes on palladium catalysts, *J. Amer. Chem. Soc.* **88**, 4555–4560 (1966).
280. *Nobel Lectures, Chemistry*, 1963–70, Elsevier Publishing Co., (1972), pp. 1–61.
281. P. Cossee and E. J. Arlman, Ziegler–Natta catalysis, I, II, and III, *J. Catal.* **3**, 80–104 (1964).
282. L. A. M. Rodriquez and H. M. Van Looy, Studies on Ziegler–Natta catalysts, Part V. Stereospecificity of the active center, *J. Polymer Sci. A-1* **4**, 1971–1992 (1966).
283. B. W. Wojceichowski, A theoretical treatment of catalyst decay, *Can. J. Chem. Eng.* **46**, 48–52 (1968); The kinetic foundations and the practical application of the time on stream theory of catalyst decay, *Catal. Rev.* **9**, 79–113 (1974).
284. G. A. Mills and F. W. Steffgen, Catalytic methanation, *Catal. Rev.* **8**(2), 159–210 (1973).

285. M. M. Bhasin, Auger electron spectroscopic study of the surface poisoning of copper catalysts, *J. Catal.* **34**, 356–359 (1974).
286. H. P. Bonzel and R. Ku, Adsorbate interactions on a Pt(110) surface. II. Effect of sulphur on the catalytic CO oxidation, *J. Chem. Phys.* **59**, 1641–1651 (1973).
287. L. L. Hegedus and E. E. Petersen, Experimental study of the poisoning of a single catalyst pellet in a diffusion reactor, *Chem. Eng. Sci.* **28**, 345–356 (1973).
288. L. D. Schmidt and D. Luss, Physical and chemical characterization of platinum–rhodium gauze catalysts, *J. Catal.* **22**, 269–279 (1971).
289. G. A. Somorjai, On the mechanism of sulphur poisoning of platinum catalysts, *J. Catal.* **27**, 453–456 (1972).
290. P. H. Emmett and S. Brunauer, Accumulation of alkali promotors on surfaces of iron synthetic ammonia catalysts, *J. Am. Chem. Soc.* **59**, 310–315 (1937).
291. V. Solbakken, A. Solbakken, and P. H. Emmett, The exchange of H_2 ^{18}O with the oxygen of promoters on the surface of iron catalysts, *J. Catal.* **15**, 90–98 (1969).
292. H. Topsoe, J. A. Dumesic, and M. Boudart, Alumina as a textural promoter of iron synthetic ammonia catalysts, *J. Catal.* **28**, 477–488 (1973).
293. P. A. Kilty and W. M. H. Sachtler, The mechanism of the selective oxidation of ethylene to ethylene oxide, *Catal. Rev.—Sci. Eng.* **10**, 1–16 (1974).
294. P. Forsalti, E. Martinez, G. C. Kuczynski, and J. J. Carberry, Influence of γ-irradiation upon catalytic selectivity. II. The role of Ca in the Ag catalyzed oxidation of ethylene, *J. Catal.* **28**, 455–458 (1973).
295. J. McAllister and R. S. Hansen, Catalytic decomposition of ammonia on tungsten (100), (110), and (111) crystal faces, *J. Chem. Phys.* **59**, 414–422 (1973).
296. I. Langmuir, The mechanism of the catalytic action of platinum in the reactions $2CO + O_2 = 2CO_2$ and $2H_2 + O_2 = 2H_2O$, *Trans. Faraday Soc.* **17**, 621–654, 672–673 (1922).
297. R. L. Palmer and J. N. Smith, Molecular beam study of CO oxidation on a (111) Pt surface, *J. Chem. Phys.* **60**, 1453–1463 (1974).
298. H. P. Bonzel and R. Ku, Mechanisms of the catalytic carbon monoxide oxidation on Pt(110), *Surface Sci.* **33**, 91–106 (1972).
299. G. Ertl and J. Koch, Adsorption studies with a Pd(111) surface, in *Adsorption-Desorption Phenomena* (F. Ricca, ed.), Adademic Press, London and New York (1972), pp. 345–357.
300. T. Matsushima and J. M. White, On the mechanism and kinetics of the CO oxidation reaction on polycrystalline Pd. I. The reaction paths, to be published.
301. P. Mars, J. J. F. Scholten, and P. Zwietering, The catalytic decomposition of formic acid, *Advan. Catal.* **14**, 35–113 (1963).
302. S. J. Thomson and G. Webb, *Heterogeneous Catalysis*, Oliver and Boyd, Edinburgh and London (1968), pp. 184–188.
303. J. McCarty, J. Falconer, and R. J. Madix, Decomposition of formic acid on Ni(110), *J. Catal.* **30**, 235–249 (1973).
304. J. L. Falconer, J. G. McCarty, and R. J. Madix, Surface explosion: HCOOH on Ni(110), *Surface Sci.* **46**, 473–504 (1974).
305. J. McCarty and R. J. Madix, A study of the kinetics and mechanism of the decomposition of formic acid on carburized and graphetized Ni(110) using AES, LEED and flash desorption, *Surface Sci.* submitted for publication.
306. T. A. Dorling and R. L. Moss, The structure and activity of supported metal catalysts, *J. Catal.* **5**, 111–115 (1966).

307. P. C. Aben, J. C. Platteeuw, and B. Stouthamer, The hydrogenation of benzene over supported platinum, palladium, and nickel catalysts, *Rec. Trav. Chim.* **89**, 449–459 (1970).
308. V. Nikolajenko, V. Bosacek, and Vl. Dames, Investigation of properties of the metallic nickel surface in mixed Ni–MgO catalysts, *J. Catal.* **2**, 127–130 (1963).
309. F. M. Dautzenberg and J. C. Platteeuw, Isomerization and dehydrocyclization of hexanes over monofunctional supported platinum catalysts, *J. Catal.* **19**, 41–48 (1970).
310. O. M. Poltorak and V. S. Boronin, Chemisorption and catalysis on platinized silica gels. II. Specific catalytic activity, *Zh. Fiz. Khim.* **39**, 2491–2498 (1965).
311. V. S. Chesalova and G. K. Boreskov, The specific catalytic activity of metals. I. Oxidation of sulfur dioxide on platinum catalysts, *Zh. Fiz. Khim.* **30**, 2560 (1956).
312. D. J. C. Yates, W. F. Taylor, and J. H. Sinfelt, Catalysis over supported metals, I. Kinetics of ethane hydrogenolysis over nickel surfaces of known area, *J. Amer. Chem. Soc.* **86**, 2996–3001 (1964).
313. G. K. Boreskov, M. G. Slin'ko, and V. S. Chesalova, The specific catalytic activity of platinum. II. The reaction between hydrogen and oxygen, *Zh. Fiz. Khim.* **30**, 2787–2797 (1956).

UNCLASSIFIED

SECURITY CLASSIFICATION OF THIS PAGE (When Data Entered)

REPORT DOCUMENTATION PAGE

READ INSTRUCTIONS BEFORE COMPLETING FORM

1. REPORT NUMBER: Technical Report #5
2. GOVT ACCESSION NO. (14) TR-5
3. RECIPIENT'S CATALOG NUMBER (9)
4. TITLE (and Subtitle): Catalysis by Solid Surfaces. (6)
5. TYPE OF REPORT & PERIOD COVERED: Interim Technical Report,
6. PERFORMING ORG. REPORT NUMBER
7. AUTHOR(s): (10) T. E. Madey, J. T. Yates, Jr., D. R. Sandstrom R. J. H. Voorhoeve
8. CONTRACT OR GRANT NUMBER(s): (15) ~~N00014~~ NAonr-18-76
9. PERFORMING ORGANIZATION NAME AND ADDRESS: Surface Processes and Catalysis Section, National Bureau of Standards, Washington, DC 20234
10. PROGRAM ELEMENT, PROJECT, TASK AREA & WORK UNIT NUMBERS: ~~61153N~~, RR 013-08; RR 013-08-01, NR 056-573
11. CONTROLLING OFFICE NAME AND ADDRESS: Office of Naval Research, Chemistry Program Office (Code 472), Rm 624, 800 N. Quincy St., Arlington, VA 22217
12. REPORT DATE: October 6, 1976
13. NUMBER OF PAGES: 124
14. MONITORING AGENCY NAME & ADDRESS (if different from Controlling Office): (11) 1976 (12) 126p.
15. SECURITY CLASS. (of this report): Unclassified
15a. DECLASSIFICATION/DOWNGRADING SCHEDULE

16. DISTRIBUTION STATEMENT (of this Report)

Approved for public release; distribution unlimited.

(16) RR013-08, NR-056-573 (17) RR013-08-01

17. DISTRIBUTION STATEMENT (of the abstract entered in Block 20, if different from Report)

Approved for public release; distribution unlimited.

18. SUPPLEMENTARY NOTES

Reprinted from Treatise on Solid State Chemistry, Vol. 6B, Surfaces II, Ed. by N. B. Hannay (Plenum, New York, 1976).

19. KEY WORDS (Continue on reverse side if necessary and identify by block number)

Heterogeneous catalysis, d electrons, surface area, dispersion of catalysts, catalytic activity, chemisorption theory, active site, alloy catalysts, catalytic particles, promoters, poisons.

20. ABSTRACT (Continue on reverse side if necessary and identify by block number)

This chapter gives an overview of current concepts in catalysis of predominantly simple reactions. Catalysts covered are metals, semiconducting oxides, and sulfides. The emphasis is on the connections between solid-state chemistry/physics, spectroscopy, and surface physics in ultrahigh vacuum on the one hand and catalysis on the other hand. For physicists and materials scientists of various plumage, the chapter is expected to serve as a concise (but not oversimplified) primer.

DD FORM 1 JAN 73 1473 EDITION OF 1 NOV 65 IS OBSOLETE S/N 0102-014-6601 USCOMM-NBS DC

UNCLASSIFIED 240 800

SECURITY CLASSIFICATION OF THIS PAGE (When Data Entered)

LB